THESIS

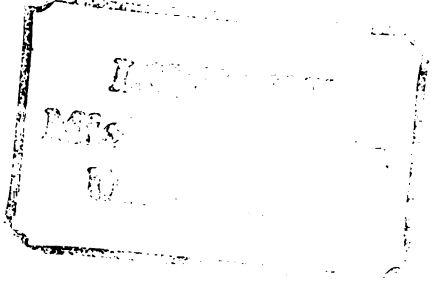

This is to certify that the

thesis entitled

A NEW APPROACH TO MEASURE THE
UNDRAINED SHEAR STRENGTH OF MUDS

presented by

Paul Tarvin

has been accepted towards fulfillment
of the requirements for

Master of Science degree in Civil Engineering

Luis E. Vallejo
Major professor

Date May 18, 1982

O-7639

A NEW APPROACH TO MEASURE THE UNDRAINED SHEAR STRENGTH OF MUDS

by

Paul Tarvin

A THESIS

Submitted to
Michigan State University
in partial fulfillment of the requirements
for the degree of

MASTER OF SCIENCE

Department of Civil and Sanitary Engineering

1982

ABSTRACT

A NEW APPROACH TO MEASURE THE
UNDRAINED SHEAR STRENGTH OF MUDS

by

Paul Tarvin

Mudflows are powerful agents of degradation of natural slopes and are reported to cause during their travel loss of life and destruction of civil engineering structures such as offshore platforms, pipelines, and communication cables.

Mudflows are reported to behave as purely cohesive materials. Therefore, their stability is often analyzed in terms of their undrained shear strength. A new approach to measure the undrained shear strength of muds, called the "cylinder strength meter test," is introduced. The new approach uses a cylinder as a measuring device and the theory developed by Sokolovskii to calculate the indentation pressures developed in a Tresca plastic when a cylinder penetrates it. The implementation of the new approach is carried out in the laboratory by measuring the undrained shear strength of artificially prepared muds. A review of other methods developed to measure the undrained shear strength of muds is also presented. Advantages of using the new approach rather than preexisting ones is also discussed.

ACKNOWLEDGMENTS

The writer would like to express his utmost gratitude and appreciation to his advisor and friend, Dr. Luis E. Vallejo, Assistant Professor of Civil Engineering, for his invaluable help and guidance throughout the author's master studies. Thanks are also in order for the other members of the writer's committee: Dr. O. B. Andersland, Professor of Civil Engineering, and Dr. R. J. B. Bouwmeester, Assistant Professor of Civil Engineering. The author would also like to thank Dr. W. Taylor, Professor and Chairman of the Civil Engineering Department, for use of the facilities and equipment during the writer's research. The writer would also like to express his appreciation to Ms. Vicki Brannan for the preparation of this manuscript. Special gratitude is also expressed to the writer's family for their patience, help and encouragement.

TABLE OF CONTENTS

LIST OF TABLES

LIST OF FIGURES

LIST OF SYMBOLS

A = cross-sectional area

b = slice width

c = concentration of clay or rock pieces per unit volume of mudflow structure

C = grain concentration ratio

c' = cohesion, effective stress basis

c_u = undrained shear strength

d = diameter of cylinder (pipe)

d_v = diameter of the vane

D = depth of failure zone

F = flotation force

F.S. = factor of safety

g = acceleration due to gravity

h = depth of penetration

h = thickness of mudflow

H = height of vane blade

k = yield strength of Tresca plastic

L = length of failure zone

L = length of the cylinder (pipe)

m = height of piezometric head

M = total resisting moment at failure

M_E = resisting moment from the ends of the cylinder

M_s = resisting moment from the circumference of the cylinder

N = total normal force on slice

N_c = bearing capacity factor

P_b = buoyancy force

P_s = strength of the plastic

q_c = measured cone resistance

R = radius

R = soil resistance

R_y = soil resistance at zero displacement rate

s = shear strength

S = radius of projected circle

S_H = shear strength in the horizontal direction

S_u = undrained shear strength from the vane test

S_v = shear strength in the vertical direction

s/t = average rate of displacement

T = shear force at base of slice

T = upward force on pipe

T_o = tension force

T_1, T_2, T_3 = applied forces on pipe

V_i = volume fraction

W = weight of the cylinder (pipe)

W_i = weight fraction of individual constituent

y = radius minus depth of imbedment

z = thickness of slice

α = inclination of surface of mudflow to horizontal

α = angle between point of contact and vertical

β = angle from the horizontal

γ = total unit weight

γ_c = unit weight of cylinder

γ_f = unit weight of muddy matrix

γ_{MIX} = unit weight of soil mixture

γ_s = bulk unit weight of hard clay fragments or rock pieces

γ_w = unit weight of water

ϕ = angle of internal friction

ϕ' = friction angle based on effective stresses

ρ_c = density of composite material

ρ_d = density of soil slurry

ρ_i = density of individual constituent

ρ_s = unit weight of sphere

σ = normal stress

σ' = effective stress

σ_o = in-situ vertical total stress at cone level

σ_1, σ_3 = principle stresses

τ = shear stress

The Greek Alphabet

α	ALPHA	μ	MU
β	BETA	ν	NU
γ	GAMMA	ρ	RHO
δ	DELTA	σ	SIGMA
ε	EPSILON	τ	TAU
ξ	XI	ϕ	PHI
η	ETA	χ	CHI
θ	THETA	ψ	PSI
λ	LAMDA	ω	OMEGA

I. INTRODUCTION

Subaerial mudflows are a serious and dangerous threat to both life and property; they should, therefore, be dealt with in the utmost care. This also applies to submarine mudflows, especially with the marked increase in the use of underwater pipelines.

The damage caused by mudflows can be substantial, and these damages are not limited by geographical or geopolitical boundaries. "Rapid earth flows have caused loss of life and immense destruction of property in Scandanavia, the St. Lawrence River Valley in Canada, and Alaska during the 1964 earthquake" (Varnes, 1978). More recently, the mudslides which occured in the San Francisco Bay area in January of 1982 provide an excellent, if not unfortunate, example of the damage a mudslide can afflict. These landslides produced a damage total well in excess of $300 million, and the deathtoll stood at 29 (Beck and Gary, 1982).

As can be seen, tremendous loss of life can be a consequence of an uncontrollable mudflow. Japan is also an area highly susceptible to earth flows due to the large number of earthquakes which occur in this region. These flows, in addition to causing a great amount of damage, are also responsible for a significant amount of lives lost (see Table 1).

In addition to the great havoc caused by earthflows which occur on land, submarine mudflows wreak their fair share of damage and destruction. This has been expecially true during the last 20-30 years, as offshore pipelines, communication cables, and drilling platforms have come into increased usage. In the Gulf of Mexico alone "pipeline mileage has increased at a rate of several hundred miles per year...Worldwide, over 12,000 miles of offshore pipeline are in place" (Demars, et al, 1977).

TABLE 1. Deaths and Damages Due to Recent Slope Failures in Japan (Schuster, 1978).

Year	Houses Damaged	Deaths	
		Number	Percent[a]
1969	521	82	50
1970	38	27	26
1971	5205	171	54
1972	1564	239	44

[a] Of deaths due to slope failure in relation to deaths due to all other natural disasters.

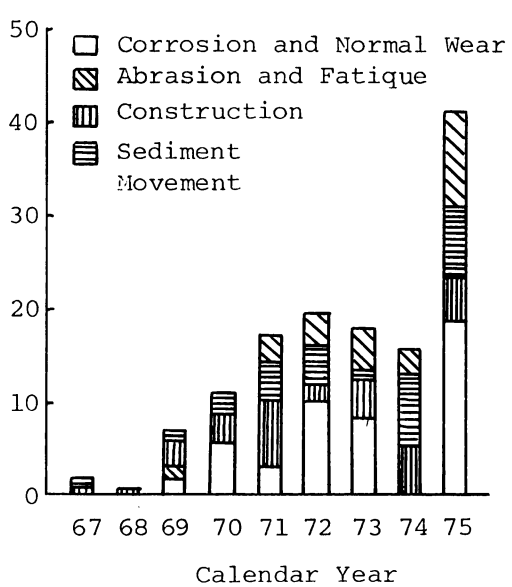

FIGURE 1: Histogram of Pipeline Failures (Demars, et al, 1977).

TABLE 2. Pipeline Failures in Mississippi Delta Area (Demars, et al, 1977).

	1958-1965 (Excluding Hurricanes)	Carla (1961)	Hilda (1964)	Betsy (1965)	Total	
Corrosion	79				79	
Anchor or Spud	23				23	
Leak in Clamp	19		1	1	21	Due to Soil Motion or Currents
Rubbing	21	1	2	1	25	
Line Goes Into Mud	10	5	5	5	25	
Line in Tension	2	5	5	0	12	
Riser Pulled	4	4	6	1	15	
Breaks Above MGL	0	4	4	14	22	
Unknown Mechanical Break	22	11	6	10	49	
	180	30	29	32	271	

In addition, the gas and oil industry has placed over 500 major and minor structures in the offshore Mississippi Delta area since the late 1950's (Bea and Audibert, 1980).

Generally these structures have faired quite well considering the wide variety of forces to which they are subjected. However, some failures have inevitably occurred. These failures, and pipeline failures in particular, "are divided into four categories for analyses purposes including: (1) corrosion and normal wear, (3) abrasion and fatigue, (3) construction-related mishaps, and (4) sediment movement. Sediment instabilities may be directly or indirectly related to three of the four failure categories (see Table 2 and Fig. 1)" (Demars, et al, 1977).

Pipeline failures attributed to abrasion and fatigue may be related to soil movement in that the supporting soil beneath the pipeline may oscillate due to wave action causing flexural stresses in the pipe; or, sediment movement may completely bury a portion of the pipe, again causing large bending stresses in the pipe.

A number of studies have been performed (Gade, 1958), (Henkel, 1970), (Wright and Dunham, 1972), and (Wright, 1976) analyzing the effect of wave loading on the soft sediments. "These analyses show that wave excitation of soft cohesive sediments may lead to sediment oscillation, progressive downslope displacement when combined with gravity forces and possibly large-scale plastic displacements or slumps. Laboratory and field measurements have confirmed the coupling of sediment displacement to wave forces and the role of wave forces in the generation of submarine slides...It is probable that sediment oscillations will have a greater effect on local pipe bending stresses than wave forces on unburied pipe" (Demars, et al, 1977).

Construction related mishaps causing pipeline failure may also be sometimes attributed to soil or sediment movement. Jack-up drilling in the vicinity of a pipeline may cause a soil movement eventually resulting in the failure of the pipeline due to excessive bending stresses or burying of the pipe. Or barge anchor damage encountered during a storm may indirectly be caused by soil movement; if wave action caused sediment oscillations or flows to occur where an anchor happened to be located, the anchor may work itself loose and impact with the pipeline causing damage or failure.

Mass downslope movement is probably the most obvious cause of failure. The forces induced by this type of movement can be estimated using slope stability analyses. However, as Demars, et al, (1977), point out, "the basic problem with these analyses is that all stability parameters are not well defined including applied loads, slope angle, and soil strength and density." This is echoed by Bea and Audibert (1980): "mudslide forces and soil deformation are still not known with precision...The foundation support conditions (vertical and lateral soil movements below the soils which translate significantly) remain unknown, and these can be as important to the design of the foundation as the forces themselves."

One of the most important parameters needed for a stability analyses of a mud is the undrained shear strength of the sediment, c_u. In-situ and laboratory measurements of c_u of very soft sediments is very difficult to assess with the methods generally used to date, such as the vane shear test and the cone penetrometer test, which will be discussed momentarily. Therefore, a more reliable method is needed, and the author would like to propose a new approach to measure the undrained shear strength of a mud to aid in more accurate stability analyses.

II. MUDFLOW STRUCTURE AND DEVELOPMENT

Before a stability analysis can begin, the engineer must know what type of material he is dealing with. This holds true in calculating stability analyses with mudflows.

Mudflows, also known as earth flows, are defined according to Varnes (1978) as having "material that is wet enough to flow rapidly and that contains at least 50 percent sand-, silt-, and clay-sized particles... Once in motion, a small stream of water heavily laden with soil has transporting power that is disproportionate to its size, and, as more material is added to the stream by caving of its banks, its size and power increase. These flows commonly follow preexisting drainageways, and they are often of high density, perhaps 60 to 70 percent solids by weight, so that boulders as big as automobiles may be rolled along."

This wet material is formed by "the mixing of water, usually from rainfall, and the smaller sized pieces of soft rock or clay forming the weathered surface of natural slopes" (Vallejo, 1981a). Or, in the case of submarine flows, the material is usually at or above its liquid limit (Bea and Audibert, 1980).

Mudflow development usually occurs in two phases, (1) the initial sliding phase, and (2) the streaming or flowing stage (Vallejo, 1981a). The initial stage is characterized by failure along one or a few failure planes, and little deformation takes place in the soil mass, similar to a block glide. In the flowing stage, a vast number of failure planes are mobilized within the mass, and the former state is indistinguishable.

These flows can take on various shapes and forms, but the most common is that shown in Figures 2 and 3. The flow consists of the "head," or upper part of the slide material, located in the source area

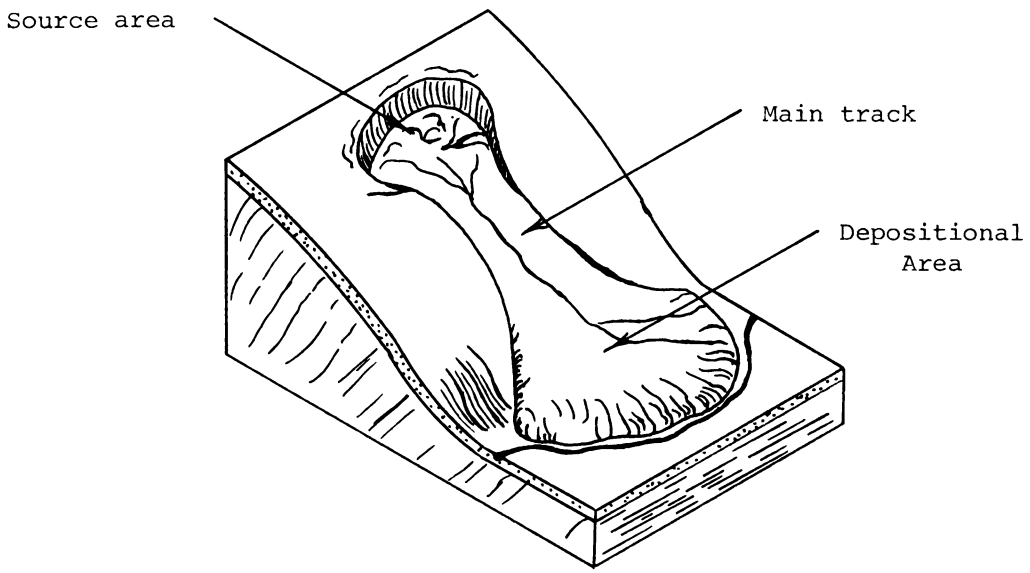

FIGURE 2: Typical Mud (Earth) Flow (Varnes, 1978).

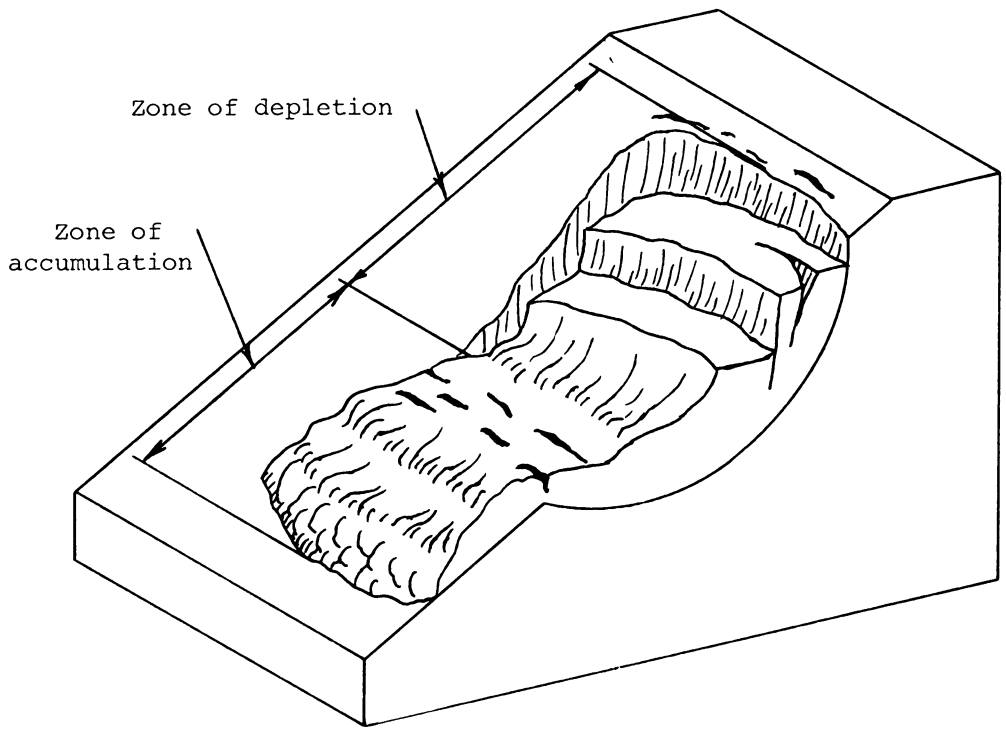

FIGURE 3: Cross Section of Mud (Earth) Flow (Varnes, 1978).

of Figure 2. The head is in contact with the relatively undisturbed material above it, this area being called the "main scarp." Below the head is an area described as the "main body" or "main track." This is also considered part of the flow, and its width is usually somewhat less than the head or toe (base) areas, so that the flow takes on a peculiar bone-shaped appearance. The toe, or depositional area, contains the material that has slid down from its original position on the slope. So the three basic constituents of a flow are the head, or upper portion; the main body; and the toe, or lower portion of the flow.

The initial sliding stage usually takes place by a shallow translational or rotational slide (Vallejo, 1981a). Shallow failures are classified as those failures which have a ratio of depth, D, to length, L, less than 0.10 (see Figure 4, Skempton and Hutchinson, 1969). The cause of the initial slide is usually due to (a) dynamic loads such as earthquakes, (b) by an increase in pore water pressures within the slope due to excessive rainfall, (c) by rainfall impact and remoulding, and (d) by thawing (Vallejo, 1981a).

The excess water present in the soil mass may eventually turn the smaller sized particles into a liquid-like slurry, which then continues to move and evolves into a true flow, the second phase of a mudflow. This liquid-like slurry has enough power and speed to transport much larger particles, as mentioned previously. This is possible due to the buoyancy effect of the liquid portion of the mass, and also due to the cohesive strength of the clay-sized particles.

The second phase of a mudflow also forms its own peculiar profile. As can be seen from Figure 5, "mudflows in the advancing front form sharp breakes in slope. This frontal bulbous ridge section is called

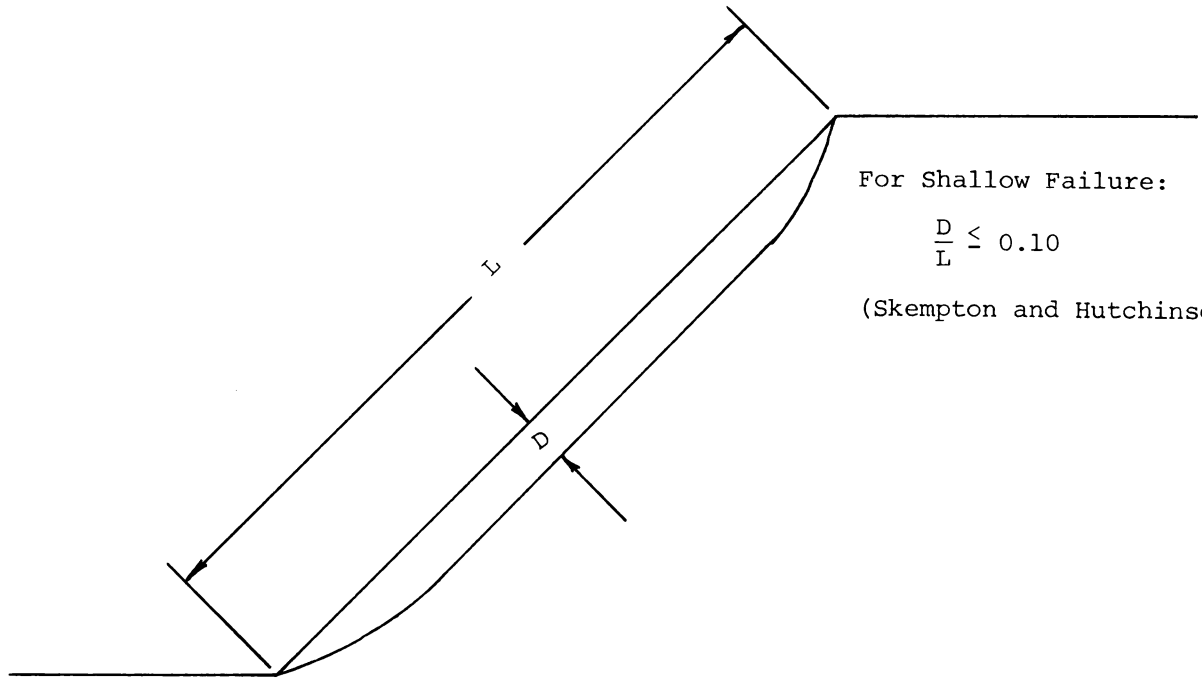

For Shallow Failure:

$$\frac{D}{L} \leq 0.10$$

(Skempton and Hutchinson, 1969)

FIGURE 4: Parameters to Classify Shallow Failure.

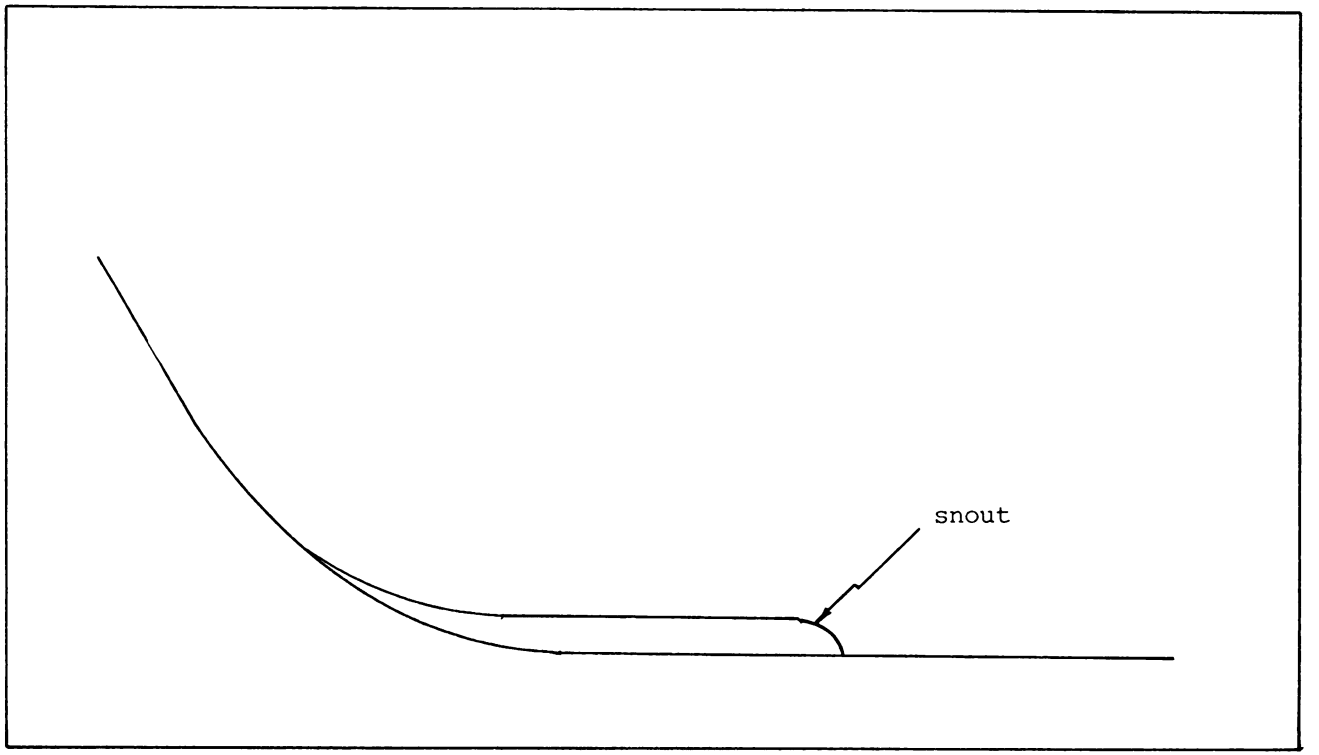

FIGURE 5: Mud Flow Profile at Beltinge, England (Hutchinson, 1970).

the snout (Johnson, 1970). Behind it the longitudinal profile of the mudflow is nearly straight and has a free surface with an inclination α with respect to the horizontal" (Vallejo, 1981a).

Knowing the shape of the final failure profile, the engineer can then decide what type of stability analysis to perform. In the case of mudflows, this stability analysis is closely approximated by the infinite slope type analysis.

III. STABILITY ANALYSIS OF MUDFLOWS

Since it is very difficult to obtain good undisturbed samples of soft clays and muds, it is important that accurate measurements of their shear strength be made by in-situ testing methods. "In soft clays even the most perfect sampling methods will lead to some reduction in undrained strength, due to the changes in total stresses inevitably associated with removing the sample from the ground. Mechanical disturbance... must be a further source of strength reduction in soft clays...Difficulties associated with sampling, and the necessarily rather small size of sample used in laboratory testing, can to some extent be overcome by measuring the shear strength of clays in-situ" (Skempton and Hutchinson, 1969).

The vane shear test device as well as the cone penetrometer test device are used to measure the undrained shear strengths of muds assuming that they behave as $\phi = 0$ soils. (Kraft, et al, 1976; Hirst, et al, 1976).

This type of total stress analysis is valid if the mud is totally saturated and no change in water content occurs. Since most muds, and particularly offshore muds encountered in the Gulf of Mexico, are above their liquid limits, these muds can be assumed to be saturated. Also, the failure of a mud generally happens very quickly, so that no change in water content occurs and the $\phi = 0$ analysis is valid. "Saturated clays, including the full range from very soft to very stiff, when tested under conditions of no water content change behave with respect to the applied stresses at failure as purely cohesive materials with an angle of shearing resistance (ϕ) equal to zero. Consequently the criterion of failure can be written in the form

$$1/2\ (\sigma_1 - \sigma_3) = c_u \qquad (1)$$

where c_u is the cohesion or shear strength of the clay. That is to say the shear strength is equal to one half the compression strength...The $\phi = 0$ analysis can therefore be applied to saturated clays in order to estimate stability in those cases where the clay is stressed under conditions of no water content change" (Skempton and Golder, 1948).

Since failure of a mudflow in the first phase occurs as a shallow failure, and the mass remains relatively intact, an infinite slope stability analysis is performed. In this type of analysis, the failure surface is assumed to be a plane parallel to the ground surface and the end effects are neglected. The forces acting in this type of failure are shown in Figure 6. For this case the internal forces on the sides of any slice are equal and opposite since there is no internal distortion and end effects are neglected, and these forces cancel out. In other words, $P_L = P_R$. It can then be shown from statics that the normal stress, σ, is equal to:

$$\sigma = \frac{N}{A} = \frac{z\ \gamma\ b\ \cos\ \beta}{b/\cos\ \beta} = \gamma\ z\ \cos^2\ \beta \qquad (2)$$

where N = the total normal force on the slice,

A = the cross-sectional area,

Z = thickness of the slice,

γ = total unit weight of the soil,

b = width of the slice,

β = the angle from the horizontal.

It can also be shown that the shear stress, τ, is equal to:

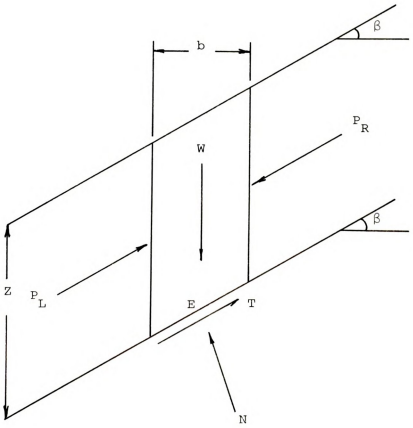

FIGURE 6: Forces Acting in the Infinite Slope Analysis (Skempton and Hutchinson, 1969).

$$\tau = \frac{T}{A} = \frac{z\ \gamma\ b\ \sin\ \beta}{b/\cos\ \beta} = z\ \gamma\ \cos\ \beta\ \sin\ \beta \qquad (3)$$

where the symbols are the same as used in equation (2), and T is the shear force acting at the base of the slice.

If additional consideration is given to the presence of a water table in the slope, the effective stresses can then be calculated. The effective stress becomes:

$$\sigma' = (\gamma - m\ \gamma_w)\ z\ \cos^2\ \beta \qquad (4)$$

where the symbols are again the same as in equation (2), m is the pore water pressure ratio, and γ_w is the unit weight of water. For cohesive soils, the shear strength, s, is given by:

$$s = c' + \sigma'\ \tan\ \phi' \qquad (5a)$$

which becomes

$$s = c' + (\gamma - m\ \gamma_w)\ z\ \cos^2\ \beta\ \tan\ \phi' \qquad (5b)$$

The factor of safety is defined as the shear strength divided by the shear stress, so that:

$$F.S. = \frac{s}{\tau} = \frac{c' + (\gamma - m\ \gamma_w)\ z\ \cos^2\ \beta\ \tan\ \phi'}{\gamma\ z\ \sin\ \beta\ \cos\ \beta} \qquad (6)$$

The pore pressures are quite difficult to measure in a submarine mud, therefore a total stress analysis is often performed. In this case, equation (6) can be simplified to:

$$F.S. = \frac{c_u}{\gamma\ z\ \sin\ \beta\ \cos\ \beta} \qquad (7)$$

where c_u is the undrained shear strength.

For this type of analysis it is assumed that $\phi = 0$ and that $c_u = 1/2\ (\sigma_1 - \sigma_3)$. However, there are three important limitations to these assumptions. "(1) For fully saturated clays the angle of shearing resistance is zero only when there is no water content change under the applied stresses. The rate of consolidation of clays is so small that, in most cases, the change in water content is negligible. Therefore the $\phi = 0$ analysis applies almost exactly" (Skempton, 1948). This is particularly true of muds.

The second limitation is that "even in fully saturated clays, tested under conditions of no water content change, the true angle of internal friction ϕ_f of the clay is not zero. Although the clay, at any particular water content, behaves with respect to the applied stresses at failure as if it were a purely cohesive material (when tested under these conditions), its behavior is at all times controlled by the true cohesion and true angle of internal friction and the effective stresses. As shown by Terzaghi (1936) the presence of the true internal friction is apparent from the observation that the shear planes in a compression test specimen are inclined to the horizontal at angles greater than 45° (45° corresponding to the case of true non-frictional materials).

"It therefore follows that whereas the applied stresses at failure are given correctly by the $\phi = 0$ analysis, according to equation (1), the shear surface is controlled by the true angle of friction ϕ_f: an angle which is greater than zero. Thus the $\phi = 0$ analysis will not, in general, lead to a correct prediction of the actual shear surface, nor will the analysis, theoretically, give a correct factor of safety if the values of c_u are applied to an observed shear surface. In practice the

errors arising from this latter point may often, though not always, be small" (Skempton, 1948).

The third limitation is that "clays which are not fully saturated do not give an angle of shearing resistance equal to zero when tested under conditions of no overall water content change" (Skempton, 1948). This, fortunately, would not apply to muds, especially submarine muds, in that they are generally totally saturated; indeed, their water contents are very often above the liquid limit.

The engineering properties of the soil needed in the infinite slope stability analysis are the unit weight of the soil, γ, and the undrained shear strength, c_u. The unit weight of the material may be obtained in the lab using either disturbed or undisturbed soil samples. However, this is not the case for measurement of undrained shear strength. The shear strength must be obtained using an undisturbed sample in order to achieve an accurate estimate, and several methods have been devised to obtain these results.

IV. METHODS OF MEASUREMENT OF THE UNDRAINED SHEAR STRENGTH

There are several test methods employed to measure the undrained shear strength of a soil. However, due to the very soft state and almost viscous behavior that a mud exhibits, some of these test methods are deemed unpractical, and need not be considered. The triaxial, direct shear, and unconfined compression tests would fall into this category, since obtaining undisturbed samples of a mud is nearly impossible, in that they have a tendency to sag under their own weight. Therefore, in-situ test methods have been developed to circumvent this problem.

One of the most common methods of in-situ strength measurement is the vane shear test. "In the vane test, a vane is pushed into the soil specimen, and a torque is applied to the stem to produce shear failure over a cylindrical surface. The shear strength is obtained by equating the torque measured at failure to the moment produced by the shear stresses along the cylindrical surface" (Wu and Sangray, 1978). A typical vane apparatus is shown in Figure 7.

The vane is inserted into the soil in a number of different ways. One method is to insert the vane into the soil from the bottom of a hole previously drilled, which has been bored by augering, washboring, or rotary drilling. In this case the vane must be inserted far enough from the bottom of the drillhole so that disturbance effects from the drilling do not affect the test results.

In some instances the soil may be soft enough for the vane to be pushed into the soil within a protection device without any predrilling. Or, if the soil is very soft, the vane may be pushed into the soil with no protection device whatsoever. Although less force is needed to push the vane into the soil with this method, it has to be done in soils

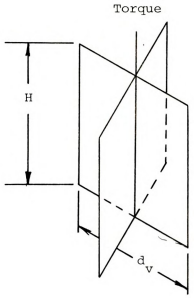

FIGURE 7: Typical Vane Apparatus (Wu and Sangrey, 1978).

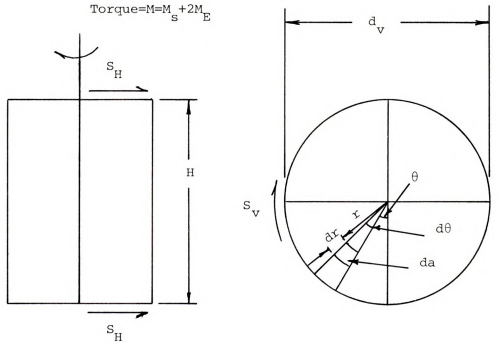

a) Side View b) End View

FIGURE 8: Basis of Evaluation of Shear Strength in the Vane Test.

free from stones or stiffer soil layers.

Once the vane is inserted into the soil, regardless of the method used, a torque is applied to the vane transmitted through an extension rod connecting the vane to the surface. Friction between the extension rod and soil, and between extension rod and any connections, is generally accounted for in the evaluation of the data. The torque is most commonly measured by moment spring instruments at the surface.

Computations of the shear strength are based on the following, with reference to Figure 8. The assumption is made that there is no progressive failure on the end surfaces. Then:

$$M_s = \pi\, d_v\, H\, S_v\, \frac{d_v}{2} = \frac{\pi}{2}\, H\, d_v^2\, S_v \tag{8}$$

$$dM_E = da\; S_H r \tag{9a}$$

$$da = rdrd\theta \tag{9b}$$

$$M_E = \int\int dM_E = \int\int S_H\, r^2\, d\theta dr$$

$$= S_H \int_0^{d_v/2} r^2\, dr \int_0^{2\pi} d\theta = 2\pi\, S_H \left[\frac{r^3}{3}\right]\Bigg|_0^{d_v/2} \tag{10}$$

$$= \frac{\pi}{12}\, d_v^3\, S_H$$

$$M = M_s + 2M_E = \frac{\pi}{2}\, H\, d_v^2\, S_v + \frac{\pi}{6}\, d_v^3\, S_H \tag{11}$$

Assuming that $H = 2\, d_v$, which is generally the case,

$$M = \pi\, d_v^3\, S_v + \frac{\pi}{6}\, d_v^3\, S_H = \pi\, d_v^3 \left[S_v + \frac{S_H}{6}\right] \tag{12}$$

Also assuming the undrained shear strengths are the same in both the

horizontal and vertical directions ($S_v = S_H$), then:

$$M = \pi S_u d_v^3 \, 7/6 \tag{13a}$$

or

$$S_u = \frac{6}{7} \frac{M}{\pi d_v^3} \tag{13b}$$

where H = height of the vane,

d_v = diameter of the vane,

S_v = shear strength in the vertical direction,

S_H = shear strength in the horizontal direction,

S_u = undrained shear strength from the vane test,

M_s = resisting moment from the circumference of the cylinder,

M_E = resisting moment from the ends of the cylinder,

$M = M_s + 2 M_E$ = total resisting moment at failure,

for equations 8 through 13b.

Despite its popularity, there are several drawbacks to this test method. The vane shear test works on the assumption that the failure surface for mud strength determination is that of a cylinder with dimensions equal to or slightly greater than those of the vane blades (Kraft Jr., et al, 1976; Ladd, et al, 1977). However, due to the fluidity of the muds, the failure surface induced by the vane cannot rigorously be repsresented as that of a cylinder (Johnson, 1965). Also, it has been found by Krone (1963, 1976) that during the rotation of a vane-like apparatus in muds, collisions and adhesion between the particles of clay take place which causes the formation of different orders of aggregation among the particles with a resulting decrease of the mud's undrained

shear strength (see Table 3).

The above two important shortcomings of the vane shear test when applied to muds, therefore, reduces its reliability when used to measure the undrained shear strength of them.

Another way to obtain the undrained shear strength of muds is by the use of quasistatic cone penetrometers (Hirst, et al, 1972; Rodine, 1975). The test involves the measurement of the resistance offered by a mud sample to its penetration by a cone. This resistance is then correlated to the undrained shear strength of the mud by the use of the following bearing capacity equation (Hirst, et al, 1972; Ladd, et al, 1977).

$$q_c = c_u N_c + \sigma_o \tag{14}$$

where q_c = measured cone resistance,

N_c = bearing capacity factor,

σ_o = in-situ vertical total stress at cone level (for measurement at shallow depths this vertical stress can be taken equal to zero),

c_u = undrained shear strength of the mud.

In order to obtain the values of c_u from equation (14), the value of the bearing capacity factor N_c needs to be known. Various theoretical solutions for the calculation of N_c for cohesive soils ($\phi = 0$) have been developed on the basis of bearing capacity theories (Meyerhof, 1951; Rodine, 1975). However, there is no general agreement of what values to choose for the bearing capacity factor N_c (see Table 4). The value of N_c has been found to be related to the type of soil tested and the type of cone used (Ladd, et al, 1977).

Since the results of c_u obtained from the cone penetrometer test are related to the value of the bearing capacity factor N_c, and since

TABLE 3. Orders of Particle Aggregation and Changes in the Shear Strength Induced When a Vane-Like Test Device Acts on a Sample of Soft Sediment (Mud) (data from Krone, 1963).

Sediment Sample	Order of Aggregation	Unit Weight grm/cm^3	Shear Strength dyn/cm^2
San Francisco Bay	0	1.269	22
	1	1.179	3.9
	2	1.137	1.4
	3	1.113	1.4
	4	1.098	0.82
	5	1.087	0.36
	6	1.079	0.20

TABLE 4. N_c Values for $\phi = 0$ Soils.

Type of Soil	N_c	Reference
Young, non-fissured not highly sensitive clays	10 - 16	Schmertmann (1975)
Soft clays	5 - 70	Amar, et al (1975)
Normally consolidated marine clays	17 - 2	Lunne, et al (1976)
Varved clay	13	Lunne, et al (1976)

this parameter does not have a fixed value, but has a wide range of values as Table 4 shows, Ladd, et al (1977) states that the cone penetrometer test can only be used as a "useful strength index test."

Several other experimental methods have been developed to measure the undrained shear strength. One of these devices is the so-called "sphere strength-meter," developed by A. M. Johnson at Stanford (1970). "Strength measurements were made by lowering weighted wooden spheres into a slurry sample, measuring the depth of penetration of the sphere into the slurry, and calculating the strength of the slurry required to support the sphere at that depth" (Hampton, 1970).

Three forces act on the sphere: (1) the weight of the sphere, (2) the buoyance due to the displaced fluid, and (3) the strength of the slurry. The weight of the sphere is known, as well as the buoyancy force, which may be calculated using Archimedes' Principle. The remaining unknown is the strength of the material; using some simplifying assumptions from plasticity theory, this too may be calculated.

As Hampton (1970) explains "the strength of a slurry sample (mud) was determined using the following theory. The penetration of the sphere into the slurry is resisted by buoyancy and the strength of the slurry. According to Archimedes' Principle, the upward force due to buoyancy is equal to the weight of the displaced slurry. The upward force due to the strength can be calculated from the theory developed for the indentation pressure of a flat punch on a Tresca Plastic (Levin, 1955).

"If the shape of the sphere is idealized as that of a flat circular punch (see Figure 9), the upward pressure exerted by the slurry on the sphere is

$$5.48\ k \qquad (15)$$

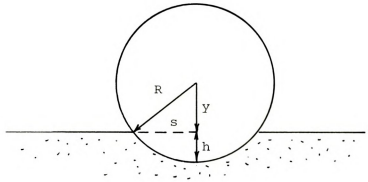

(a)

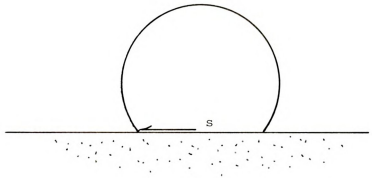

(b)

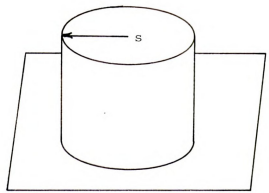

(c)

FIGURE 9: Illustration of Assumptions for Theory of Sphere Strength-Meter (Hampton, 1970).

assuming that the depth of the slurry sample is large (Levin, 1955). The symbol k refers to the yield strength of the plastic (c_u for the case of a mud). The upward force is the pressure times the projected area of the submerged portion of the sphere:

$$5.48\ k\ \pi\ s^2 \tag{16}$$

where s is the radius of the projected circle (Figure 9). For the sphere,

$$S^2 = R^2 - y^2,\ y > 0 \tag{17}$$

Therefore, the upward force is

$$5.48\ k\ \pi\ [R^2 - y^2] \tag{18}$$

"The buoyant force of the slurry is the submerged volume of the sphere multiplied by the density of the slurry, ρ_d, and gravity, g:

$$[h^2/3]\ (3R - h)\ \pi\ \rho_d\ g \tag{19}$$

where h is the depth of penetration of the sphere into the slurry. The downward force of the sphere is equal to the volume of the sphere multiplied by the unit weight of the sphere, ρ_s g,

$$[4/3\ \pi\ R^3]\ \rho_s\ g \tag{20}$$

"Equilibrium of the sphere in the slurry is described by

$$5.48\ k\ \pi\ [R^2 - y^2] = [(4/3\ \pi\ R^3)\ \rho_s - (\tfrac{h^3}{3})(3R - h)\ \pi\ \rho_d]\ g \tag{21}$$

From Figure 9,

$$h = R - y$$

so that equation (21) can be written as

$$c_u = k = \frac{\left[\frac{4}{3} R^3 \rho_s - \frac{1}{3} h^2 \rho_d (3R - h)\right] g}{5.48 \left[2Rh - h^2\right]}, \quad 0 < h < R \qquad (22a)$$

"Equation (22a) is valid for sphere penetrations, h, less than R. If the penetration is greater than R, the projected area is the maximum projected area of the sphere, πR^2, for all depths of penetration, such that $R < h < 2R$. For this situation, equation (22a) alters to

$$c_u = k = \frac{\left[\frac{4}{3} R^3 \rho_s - \frac{1}{3} h^2 \rho_d (3R - h)\right] g}{5.48 R^2}, \quad R < h < 2R." \qquad (22b)$$

The main disadvantage to this method lies in the basic assumption, in that a flat circular punch is approximated by a sphere. It would seem that some shear stresses would be induced where the lower end of the sphere has penetrated the slurry, these stresses being unaccounted for in the analysis.

A different experimental approach was presented by Ghazzaly and Lim (1975), in a paper submitted to the Seventh Annual Offshore Technology Conference held in Houston, Texas, 1975. In this method, a hollow tube of known dimensions and weight is embedded in a liquid clay, and then removed by means of a pulley and winch system (see Figure 10). The resistance of the soil to this pullout is measured, and the strength is calculated from this information.

According to Ghazzaly and Lim (1975), "a body which hangs suspended in a liquid clay, with no movement or corresponding soil resistance, is

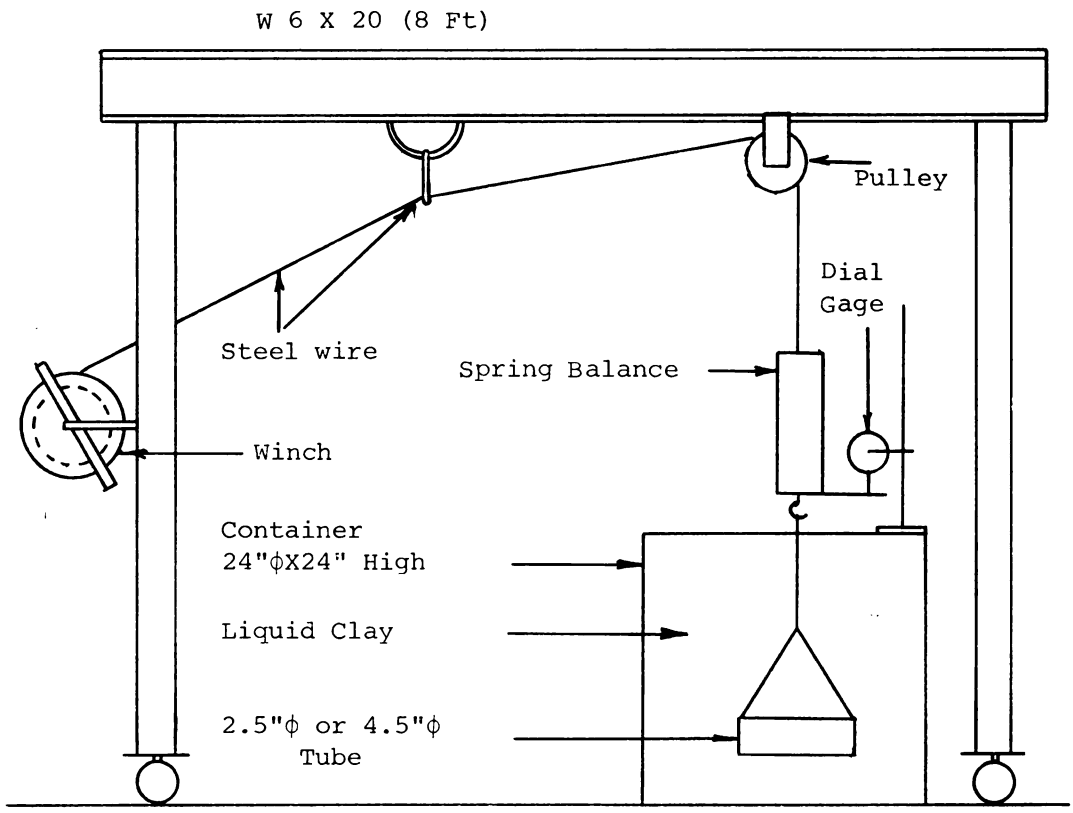

FIGURE 10: Pullout Test Apparatus (Ghazzaly and Lim, 1975).

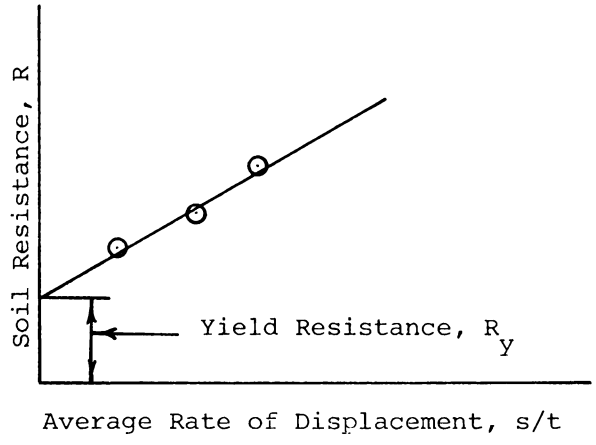

FIGURE 11: Typical Soil Resistance vs. Rate of Displacement Relationship (Ghazzaly and Lim, 1975).

subjected to a tension force, T_o, a flotation force, F, which can be equal to the buoyancy, and the pipe weight, W, such that:

$$T_o = W - F \tag{23}$$

If the body is pulled upward with a force, T, to produce a displacement, s, in a time period, t, and with soil resistance, R, developed, the stability equation is:

$$T = W - F + R \tag{24}$$

Subtracting equation (23) from (24) gives:

$$R = T - T_o \tag{25}$$

Repeating the pullout of the body with larger forces will result in a displacement-time response...from which the average rate of displacement, s/t, for each applied force (T_1, T_2, T_3) can be determined. Extrapolating the curve giving the relationship between soil resistance to pullout, R, in equation (25), and the rate of displacement, at zero displacement rate gives the soil yield resistance, R_y (see Figure 11). Dividing this resistance by the surface area gives the yield strength, τ (or c_u), of the liquid clay. If the surface area of a cylinder is given by

$$\pi\, d\, L \tag{26}$$

where d = diameter of the cylinder

L = length of the cylinder

then the yield strength of the clay will be equal to

$$C_u = \tau = \frac{R_y}{\pi d L} . \qquad (27)$$

The basic flaw in this method is the problems associated with burying the pipe in the first place, as this would cause a definite remoulding of the liquid clay, which would affect the calculated shear strength.

Another experimental method developed by Vallejo (1981a), uses the profile of a mudflow to calculate the undrained shear strength of a mud by geometry and statics. Vallejo (1981a) states that "a liquid-like soil slurry (mud) has cohesive strength, viscosity, and unit weight greater than that of water. The free surface of the mudflow has a slope, α, greater than the slope, β, of the surface on which the mudflow moves. It is assumed that within the mudflow at equilibrium, represented in Figure 12, hydrostatic pressure conditions exist. Following Keulegan (1944) and Nye (1952) for equilibrium conditions when considering the forces acting on section ABCD (Figure 12) of the mudflow which represent hydrostatic pressure differences due to the surface slope and the shear resistance at the bed of the mudflow, the following equation applied:

$$\left(\frac{1}{2}\right)(\gamma_{MIX})(h + dh)^2 - \left(\frac{1}{2}\right)(\gamma_{MIX})(h)^2 + \gamma_{MIX}\, h \sin\beta dx = c_u\, d_x \qquad (28)$$

From further development of equation (28) one can obtain the following equation:

$$\gamma_{MIX}\, h \frac{dh}{dx} dx + \gamma_{MIX}\, h \sin\beta dx = c_u\, d_x \qquad (29)$$

in equations (28) and (29) c_u is the undrained shear strength of the muddy matrix, β is the slope angle of the surface where the mudflow

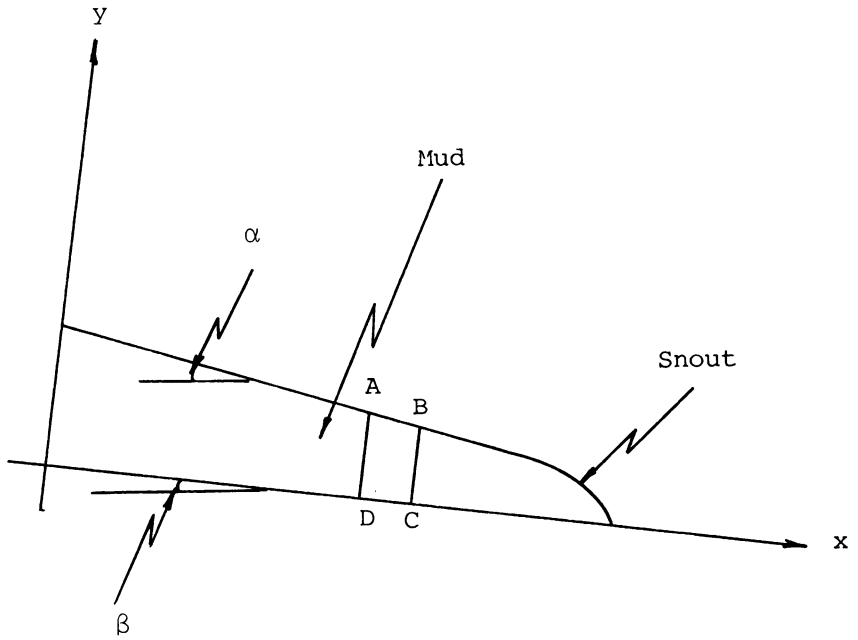

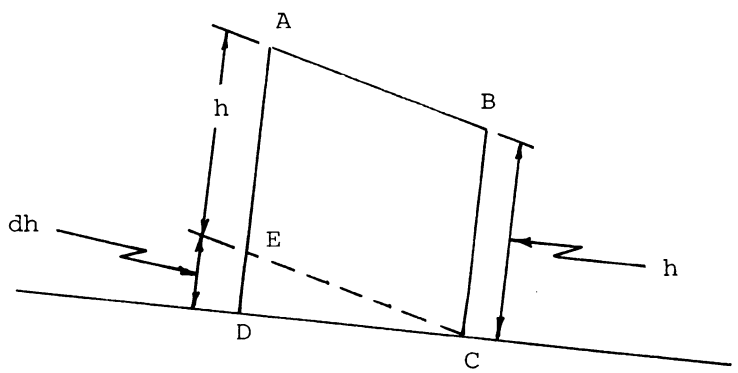

$$DC = dx$$

$$\sphericalangle ECD = \alpha - \beta$$

FIGURE 12: Mudflow Geometry Used in Stability Analysis (Vallejo, 1981a).

moves on, h is the thickness of the mudflow, and γ_{MIX} is the unit weight of the mixture of mud and pieces of hard clay or soft rock forming the mudflow structure, that according to Bagnold (1954) and Vallejo (1979) is equal to

$$\gamma_{MIX} = (1 - c)\ \gamma_f + c\ \gamma_s \tag{30}$$

where γ_f is the unit weight of the muddy matrix, γ_s is the bulk unit weight of the hard clay fragments or rock pieces, and c represents the concentration of clay or rock pieces per unit volume of the mudflow mixture."

Then, for small values of α and β, sin β can be approximated by β, and

$$\frac{dh}{dx} = \alpha - \beta \tag{31}$$

Using these approximations, and substituting equations (30) and (31), equation (29) can be simplified to:

$$[(1 - c)\ \gamma_f + c\ \gamma_s]\ h\ \alpha = c_u \tag{32}$$

In order to apply the method presented by Vallejo (1981a), the profile of the mudflow needs to be known, so from this profile and using equation (32) the undrained shear strength, c_u, of the mud can be calculated.

With the above limitations of each of the test methods brought out, a definite need can be seen for improvement upon these methods to give more accurate estimates of the undrained shear strength of a soft clay (mud), or the development of a totally new method which eliminates or at least reduces the errors involved in the measurement of c_u of muds.

It is this latter approach that the author has taken to improve upon the measurement of c_u in-situ or in the laboratory. This new method is based on the slip-line approach of Plasticity Theory, specifically on an equation developed by Sokolovskii (1955) designed to calculate the indentation pressures developed when a cylinder penetrates a Tresca plastic (mud).

V. THEORETICAL BASIS FOR THE NEW METHOD

Before delving into the mechanics of the method itself, a review of the theory behind the approach is called for. The theory is based on a plasticity analysis made by Sokolovskii (1955) for the case of a smooth circular punch indenting a Tresca plastic. Sokolovskii used a slip line approach to analyze the pressures developed when the smooth punch indented the plastic (see Figure 13a). These stresses are assumed to be constant in the region about the punch. The resisting force, P_s, which is developed by the Tresca plastic is then given as:

$$P_s = 2\,k\,RL\,[(\pi + 2)\,\sin\alpha + 2\,(1 - \cos\alpha - \alpha\sin\alpha)] \qquad (33)$$

where the various parameters are shown in Figure 13b, k is the shear strength of the plastic, and L is the length of the punch.

For our case, the Tresca plastic is represented by the soil slurry (mud), and the circular punch is replaced by a smooth cylinder of known dimensions and unit weight. In this method, the cylinder is slowly lowered into the mud, and then allowed to settle to its equilibrium position. In this state, the downward force due to the weight of the cylinder is resisted by two forces: (1) the buoyancy effect due to the liquid-like state of the slurry, and (2) the shear strength of the soil (mud), which can be calculated by rearranging the equation developed by Sokolovskii (1955).

First, the force acting downward due to the cylinder will be considered. This force is simply the weight of the cylinder. Since the dimensions and unit weight of the cylinder are known, the weight is given by the equation

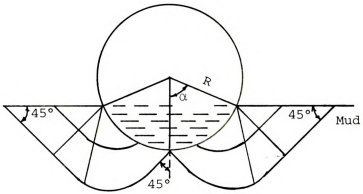

FIGURE 13a: Slip Line Approach Used by Sokolovskii (1955) for the Case of a Smooth Circular Punch.

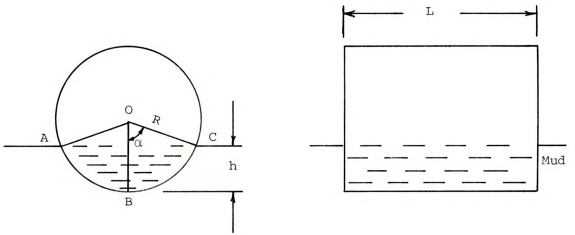

FIGURE 13b: Parameters Used in the Cylinder-Strength Meter Test.

$$W = \pi R^2 L \gamma_c \tag{34}$$

where W = weight of the cylinder,

R = radius of the cylinder,

L = length of the cylinder,

γ_c = unit weight of the cylinder.

The buoyancy force, which acts to oppose the weight acting down, can be calculated using Archimedes' Principle. This buoyancy force is equal to the weight of the displaced mud, which is given by

$$P_b = R^2 L (\alpha - \sin \alpha \cos \alpha) \gamma_f \tag{35}$$

where the parameters are the same as in equation (34), and γ_f is the unit weight of the slurry. The angle α can be calculated from geometry, and is given by

$$\alpha = \cos^{-1} \left(\frac{R-h}{R}\right) = \cos^{-1} \left(1 - \frac{h}{R}\right) \tag{36}$$

where R is again the radius of the cylinder, and h is the depth of imbedment of the cylinder (see Figure 13b).

The remaining force resisting the weight of the cylinder is the strength of the mud, P_s. Since at equilibrium,

$$W = P_s + P_b. \tag{37a}$$

this equation can be rearranged, giving

$$P_s = W - P_b \tag{37b}$$

Then, by substitution and rearrangement of the terms in equation (37b),

the shear strength of the material, k, which is equal to c_u for a soil slurry (mud), is given by

$$c_u = \frac{R\left[\pi \gamma_c - (\alpha - \sin \alpha \cos \alpha)\, \gamma_f\right]}{2\left[(\pi + 2) \sin \alpha + (1 - \cos \alpha - \alpha \sin \alpha)\right]} \tag{38}$$

for the case of a smooth walled cylinder. This equation (38) is valid only for values of α less than 90°.

VI. IMPLEMENTATION OF THE TEST METHOD

Basically, the new test method, herein referred to as the "cylinder strength meter test," consists of lowering a smooth-walled plexiglass cylinder of known dimensions and unit weight, into a soil slurry (mud). When the test device comes in contact with the slurry, it is gently released and allowed to settle under its own weight. The sides of the container in which the test is taking place are lightly jostled to break any surface tension effects which may be present. Once the cylinder strength meter reaches its equilibrium position, where it will settle no further, it is then carefully removed, and the depth of imbedment, h, is measured. Six different test cylinder devices were employed, and their pertinent data is summarized in Table 5.

Three different types of soil slurries were tested. The first was a simple clay-water mixture. Vallejo (1981b) states that "for laboratory investigations on the shear strength of granulo-viscous materials, a fluid phase represented by a mixture of kaolinite clay, calgon (hexamethaphosphate used as a dispersive agent) and water was combined with granular materials (solid phase) in the form of sand...and glass beads. This mixture represents well the structure of a mudflow." The clay-water mixture was tested alone to determine what the shear strength of the so-called fluid phase was. The various constituents were added together one at a time, then carefully mixed both by hand and by an electric mixer. The calgon was added to act as a dispersive agent for the clay particles. The weights of each constituent were recorded, so that calculations of concentrations of each both by weight and by volume could be performed.

The concentrations of each constituent by weight was calculated by

TABLE 5. Summary of Cylinder Data.

Cylinder Number	Diameter (Centimeters)	Length (Centimeters)	Weight (Grams)
1	3.48	7.00	79.3
2	3.48	4.50	50.8
3	3.48	4.00	45.0
4	3.00	5.99	50.1
5	3.00	4.50	37.5
6	3.00	3.48	29.1

NOTE: The average unit weight of the cylinders is equal to 1.19 $\frac{gms}{cm^3}$

taking the weight of each individual material and dividing by the total weight of the slurry. The concentrations by volume were calculated using equations developed by Agarwal and Broutman (1980) for the performance of fiber composites. For our application, the matrix shown in Figure 14 is assumed to be the fluid phase, while the fibers are given by the soil grains. The volume fractions are then given by the equation

$$V_i = \frac{\rho_c}{\rho_i} W_i \tag{39}$$

where V_i = the volume fraction of the constituent in question,

ρ_c = the density of the composite material,

ρ_i = the density of the constituent in question,

w_i = the weight fraction of the constituent in question.

For an arbitrary number of constituents, the density of the composite material is given by

$$\rho_c = \frac{1}{\sum_{i=1}^{m} (W_i/\rho_i)} \tag{40}$$

where W_i = the weight fractions of each of the individual constituents,

ρ_i = the density of each of the individual constituents.

(See Appendix A for an example calculation).

The density of the composite material calculated in this manner was also used as the unit weight of the soil slurry in the modification of Sokolvskii's (1955) equation to calculate c_u (equation (38)).

For the clay-water mixtures, increasing amounts of clay were added

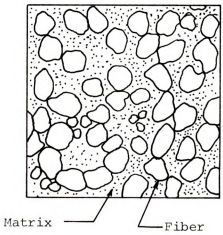

FIGURE 14: Random Distribution of Fibers (Granular Material) in a Fiber-Resin (Mud) (Agarwal and Broutman, 1980).

for each test (one test consisting of one trial each for the six test devices) to determine what effect varying concentrations of clay had on the cylinder strength meter test results. This will be discussed momentarily.

The second type of soil slurry tested was a clay-sand mixture. The sand was added to act as the granular phase explained previously. A granular material is added to the slurry since it has been reported by Hutchinson (1970) that mudflows occurring in the field usually contain varying amounts of clay fragments or rock pieces dispersed in the fluid phase (mud). It is felt that addition of the sand, then, more nearly simulated actual field conditions. The clay-water slurry was made thick enough so that it posessed enough cohesive strength that the sand particles would not settle out of solution (the buoyancy effect also contributed some). The amount of sand in the mixture was varied to test the effect of the concentration of sand on the cylinder strength meter test results.

The third type of soil slurry tested was a clay-glass beads mixture. In this case the sand was substituted for by 5 millimeter diameter glass beads (to simulate rock fragments which may be present in actual mudflows). Again, the clay slurry was made thick enough so that it posessed enough cohesive strength (and buoyancy) to keep the glass beads in dispersion and to prevent them from settling.

A summary of the various materials used in the soil slurries and their densities is given in Table 6.

Once the data was recorded for each of the test cylinders, the value of c_u could be calculated using equation (38). After each test cycle was complete, the final weight of the soil slurry was recorded for comparison with the original weight before the test was begun. A

TABLE 6. Summary of Materials Used and Their Respective Densities.

Material Used	Density (gms/cm^3)
Clay	2.65
Sand	2.70
Glass Beads	1.55
Calgon	2.65

correction was then applied to account for any material which adhered to the test cylinder and subsequently not returned to the slurry, before any new material was added for additional tests.

CLAY-WATER MIXTURES

Figures 15 a-f show a plot of the shear strength of the slurry versus the concentration of clay by volume. At first glance, these plots show a rather random distribution of data points. However, closer examination of the graph shows a rather exagerated axis for the concentration of clay. This shows that all the data points lie between a rather narrow range of concentrations of 38 to 42 percent by volume. This is due to the fact that at concentrations below 38 percent, the cylinder strength meter devices had a tendency to settle past their midpoint; in other words, $h > R$, and therefore $\alpha > 90^{\circ}$. In this instance, the unit weight of the cylinder was too great to measure the shear strength of the slurry below concentrations of 38 percent, and since $\alpha > 90^{\circ}$, Sokolvskii's equation (38) was inapplicable. Use of a cylinder with a lower unit weight would remedy this situation, but was unavailable at the time of testing.

On the other hand, at concentrations of clay greater than 42 percent, the soil slurry became relatively thick, and settlement of the cylinders in the mixture were negligible. Accurate measurements of h were not possible for such small values. Use of a cylinder with a greater density than 1.19 $\frac{gm}{cm^3}$ would rectify this situation, but again, these were unavailable at the time of testing.

It is felt, then, that these plots show an average value for c_u at a clay concentration of approximately 40 percent. A glance at table 6 will show that cylinders 1 through 6 are in relative agreement in

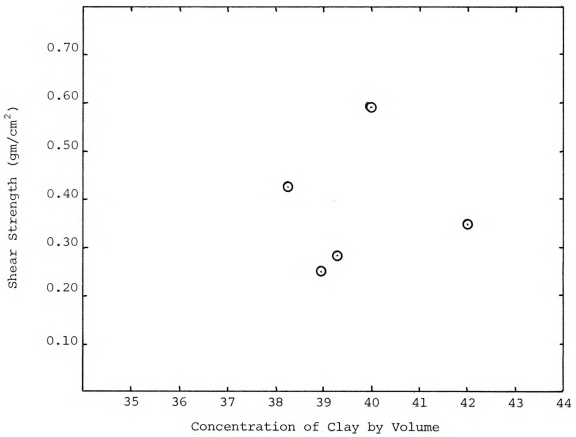

FIGURE 15a: Plot of Shear Strength vs. Concentration of Clay for Cylinder No. 1.

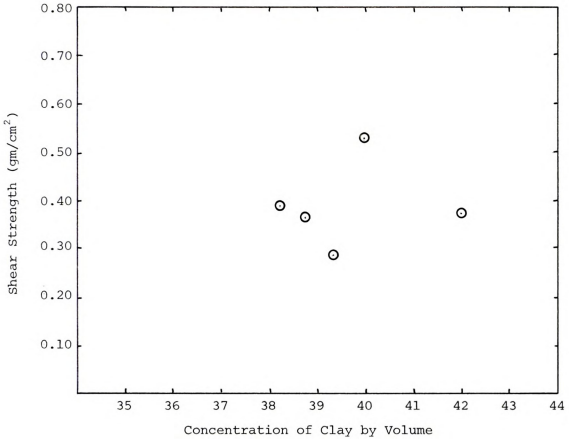

FIGURE 15b: Plot of Shear Strength vs. Concentration of Clay for Cylinder No. 2.

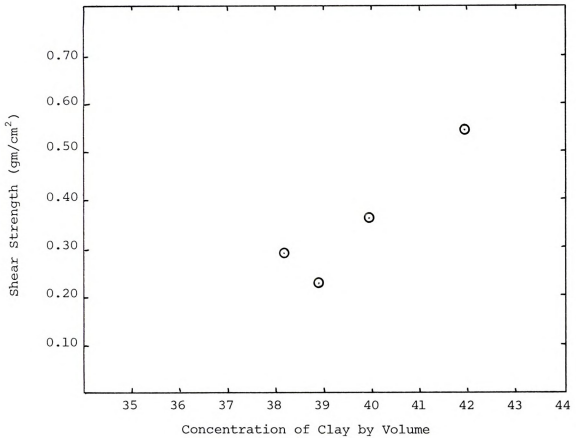

FIGURE 15c: Plot of Shear Strength vs. Concentration of Clay for Cylinder No. 3.

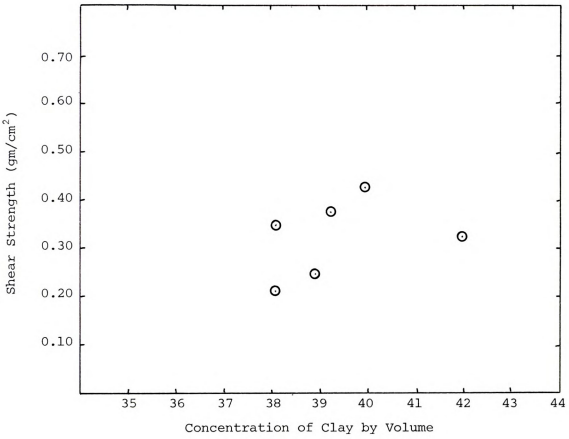

FIGURE 15d: Plot of Shear Strength vs. Concentration of Clay for Cylinder No. 4.

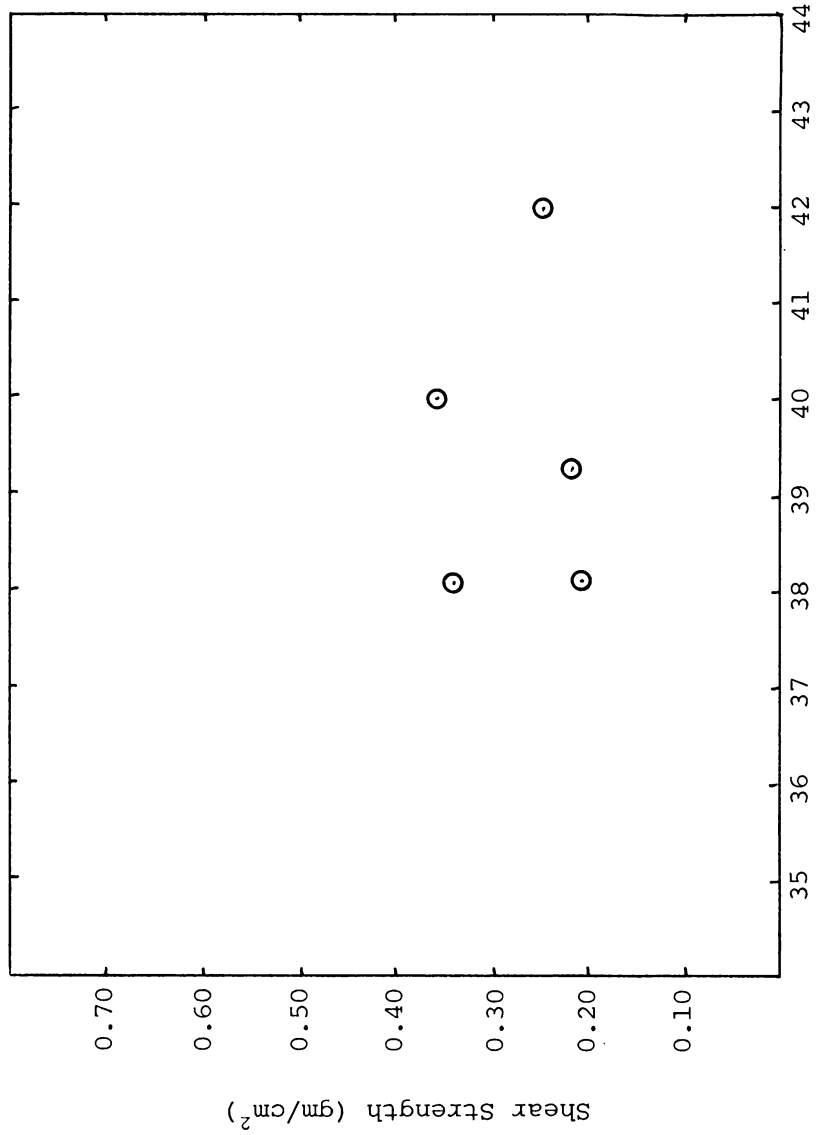

FIGURE 15e: Plot of Shear Strength vs. Concentration of Clay for Cylinder No. 5.

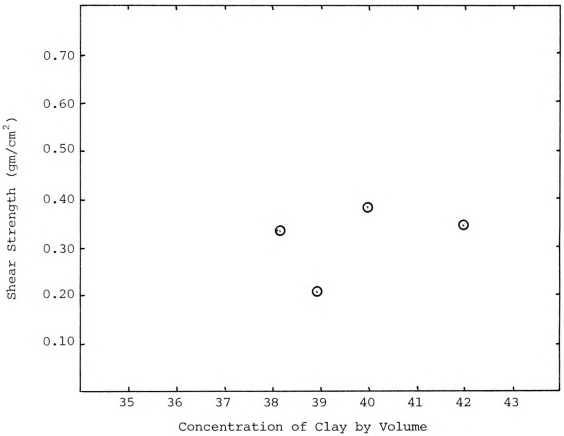

FIGURE 15f: Plot of Shear Strength vs. Concentration of Clay for Cylinder No. 6.

TABLE 7. Average Values of Shear Strength for Figures 15 a-f.

Cylinder Number	Average Value of C_u From Figures 15 a-f
1	0.380 $\frac{gm}{cm^2}$
2	0.388 $\frac{gm}{cm^2}$
3	0.360 $\frac{gm}{cm^2}$
4	0.320 $\frac{gm}{cm^2}$
5	0.274 $\frac{gm}{cm^2}$
6	0.320 $\frac{gm}{cm^2}$

this respect (approximately 0.34 $\frac{gm}{cm^2}$).

As mentioned before, use of a test device with a different density than the one used would enable us to calculate the undrained shear strength of a clay-water slurry at concentrations other than about 40 percent.

Variations in the value of c_u, between the individual cylinders and between the different concentrations, are caused by the following: (1) Sample inhomogeneity; the samples were mixed as well as possible. However, it is very difficult to obtain completely homogeneous samples in the manner in which they were formed. Cylinder placement in different areas of the sample may yield different results. Observation of Table 7 shows that these variations are not great, however. (2) Some evaporation may have taken place during the testing procedure, again resulting in non-homogeneous samples. This is related to cause (1). Also, (3) variations in the measured values of the depth of penetration of the cylinders into the mud may have been caused by operator error. In that this is a new method of testing still under development, it is subject to human error by the operator.

CLAY-SAND MIXTURES

With the addition of sand into the soil slurry, the material becomes more like a mudflow found in the field, in that a greater variety of particle sizes are represented. Figures 16 a through f show plots of shear strength versus concentration of sand by volume.

Analysis of these figures shows that at low concentrations of sand (below 50 percent), the value of c_u remains relatively constant (approximately 0.18 $\frac{gm}{cm^2}$). At concentrations of sand greater than 50 percent, a sharp increase in the value of shear strength is noted. At these larger

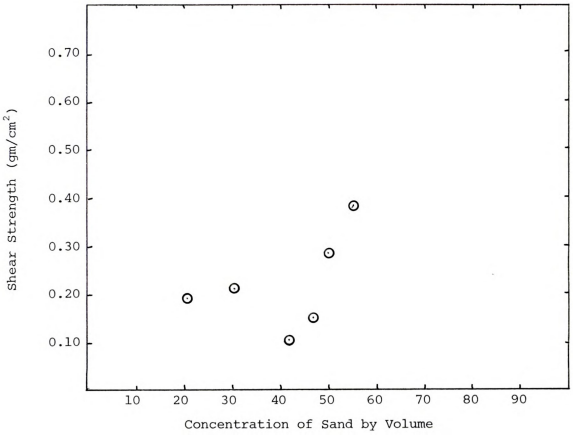

FIGURE 16a: Plot of Shear Strength vs. Concentration of Sand for Cylinder No. 1.

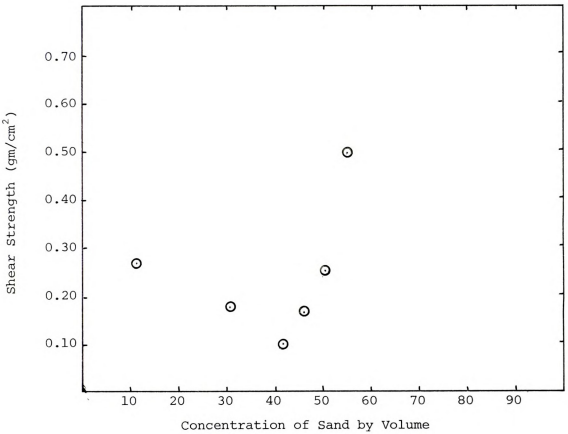

FIGURE 16b: Plot of Shear Strength vs. Concentration of Sand for Cylinder No. 2.

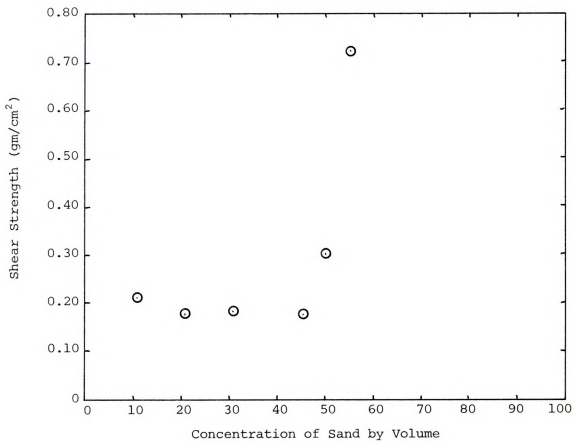

FIGURE 16c: Typical Curve, Plot of Shear Strength vs. Cencentration of Sand by Volume for Cylinder No. 3.

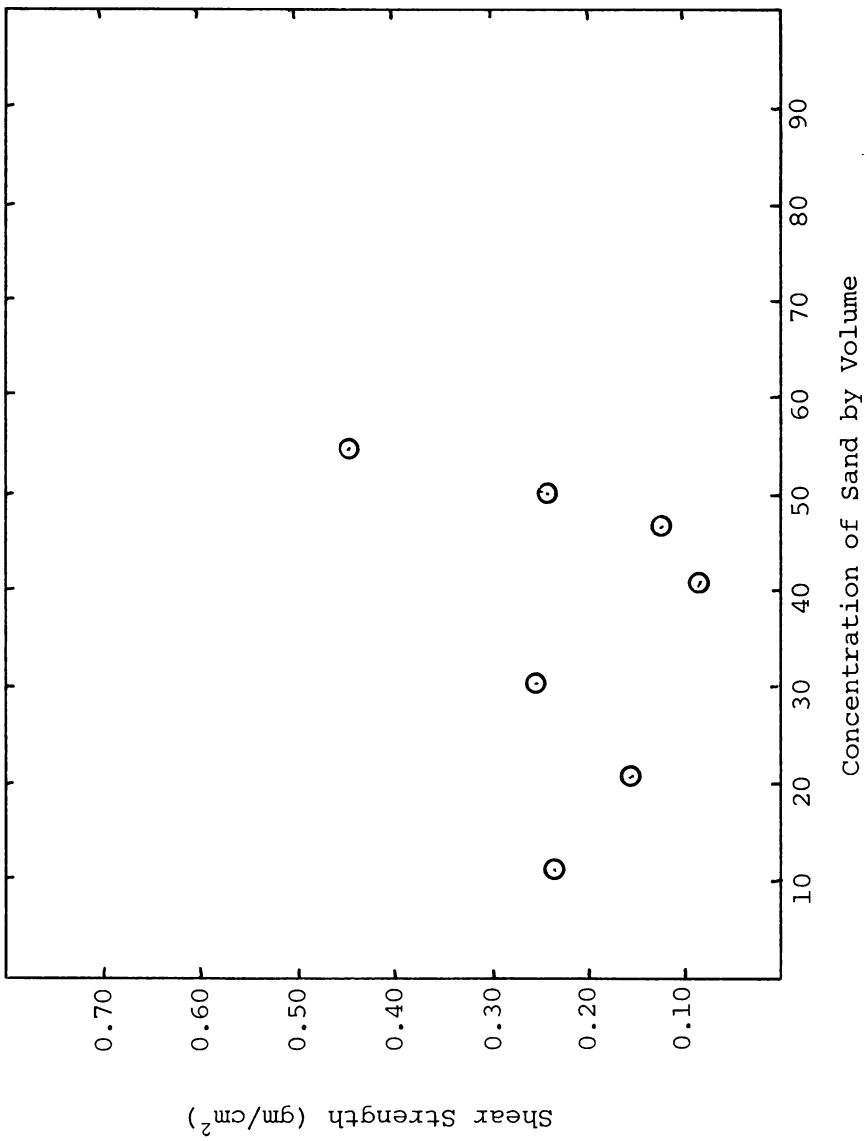

FIGURE 16d: Plot of Shear Strength vs. Concentration of Sand for Cylinder No. 4.

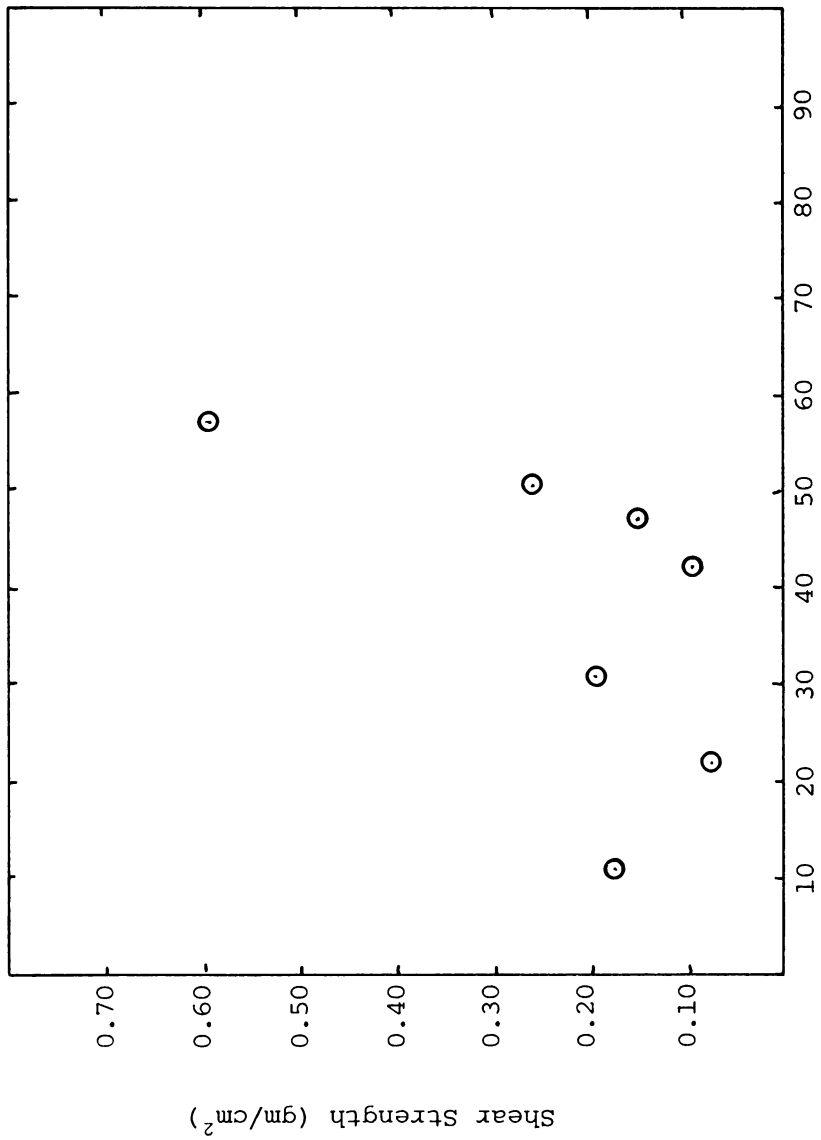

FIGURE 16e: Plot of Shear Strength vs. Concentration of Sand for Cylinder No. 5.

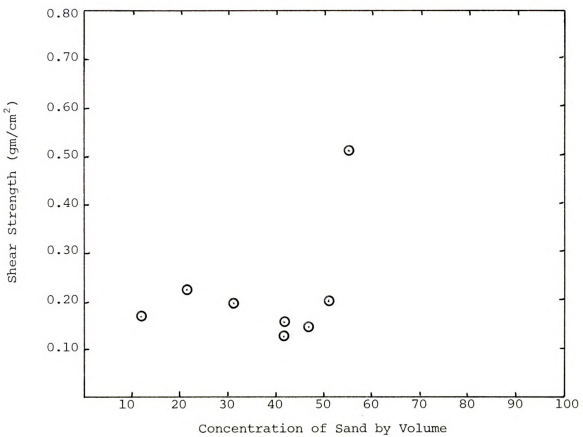

FIGURE 16f: Typical Curve, Plot of Shear Strength vs. Concentration of Sand by Volume for Cylinder No. 6.

TABLE 8. Average Values of C_u from Figures 16 a-f, for Concentrations of Sand by Volume of Less than 50 Percent.

Cylinder Number	Average Values of C_u For Concentrations < 50%
1	0.185 $\frac{gm}{cm^2}$
2	0.194 $\frac{gm}{cm^2}$
3	0.209 $\frac{gm}{cm^2}$
4	0.179 $\frac{gm}{cm^2}$
5	0.160 $\frac{gm}{cm^2}$
6	0.172 $\frac{gm}{cm^2}$

concentrations, the individual particles of sand begin to come in contact with each other, adding an additional component of friction between the grains. This accounts for the abrupt increase in c_u.

Again, variations in the measured values of c_u between cylinders is relatively minor. Table 8 shows average values of c_u for each cylinder for concentrations of sand by volume less than 50 percent. These variations can be attributed to the same flaws as cited under the clay-water mixtures.

CLAY-GLASS BEAD MIXTURES

It is felt that the clay-glass bead mixtures most nearly simulate actual mudflows in the field. As cited by Hutchinson (1970), most mudflows are composed of a semi-viscous phase, with inclusions of rock fragments and clay lumps. These fragments are relatively large when compared to the particles composing the fluid phase.

Figures 17a through f show the undrained shear strength of the soil slurry versus the concentration of beads by volume. Analysis of these figures shows a gradual linear increase in shear strength for low concentration of beads (below 50 percent), with an abrupt increase due to the additional friction component between the beads at concentrations greater than 50 percent. A linear regression analysis yielded the lines shown on these figures for concentrations less than 50 percent. This tends to support research done by other authors who have investigated the shear strength of various two-phase systems (see Table 9). These findings show that "small grain concentrations produce a linear increase in the shear strength of the fluid phase up to a value of C equal to 0.58. Beyond this value of C, there is an abrupt increase in the shear strength of the mixture as a result of the interactions between the

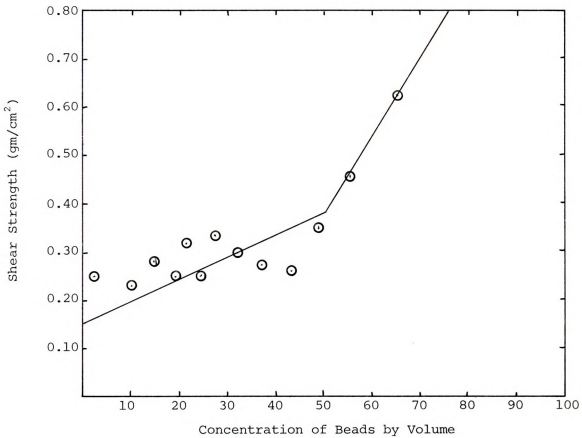

FIGURE 17a: Typical Curve, Plot of Shear Strength vs. Concentration of Beads by Volume for Cylinder No. 1.

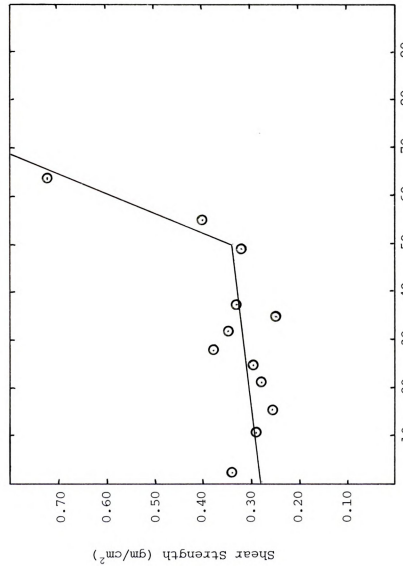

FIGURE 17b: Plot of Shear Strength vs. Concentration of Glass Beads for Cylinder No. 2.

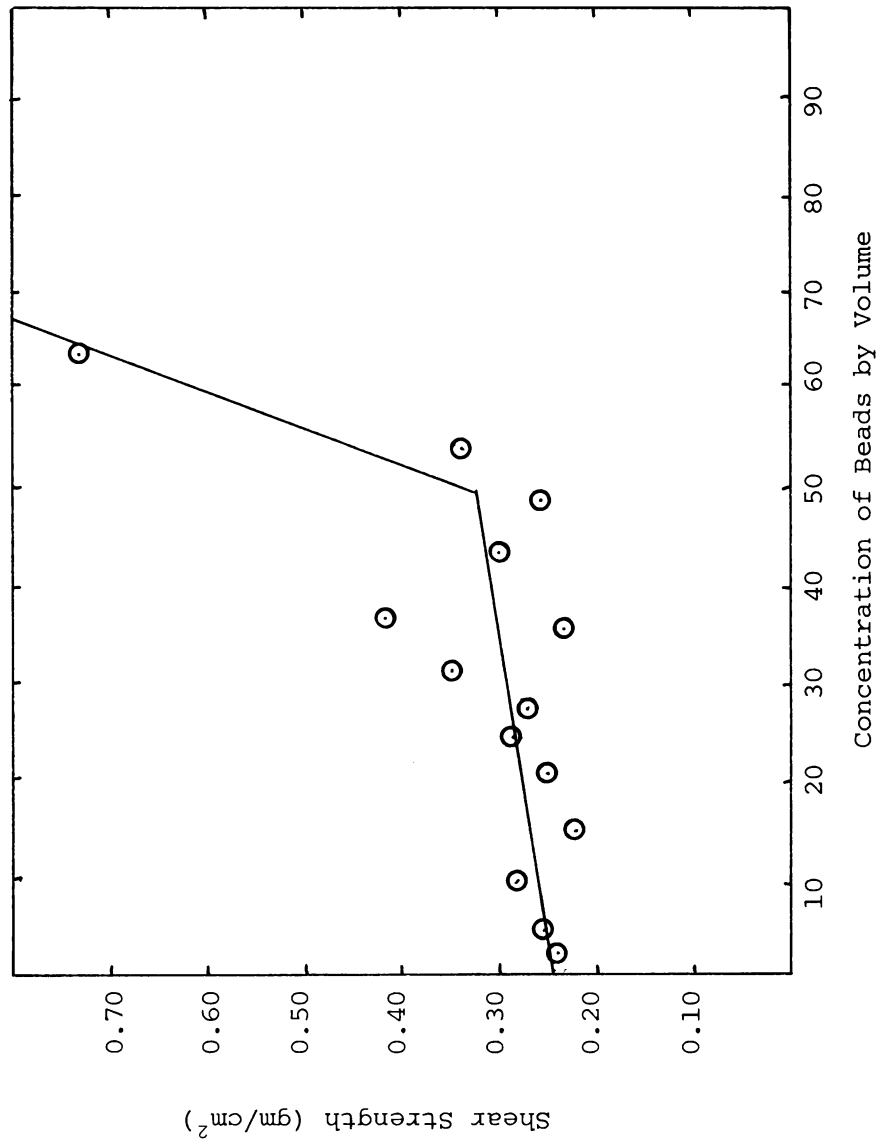

FIGURE 17c: Plot of Shear Strength vs. Concentration of Beads for Cylinder No. 3.

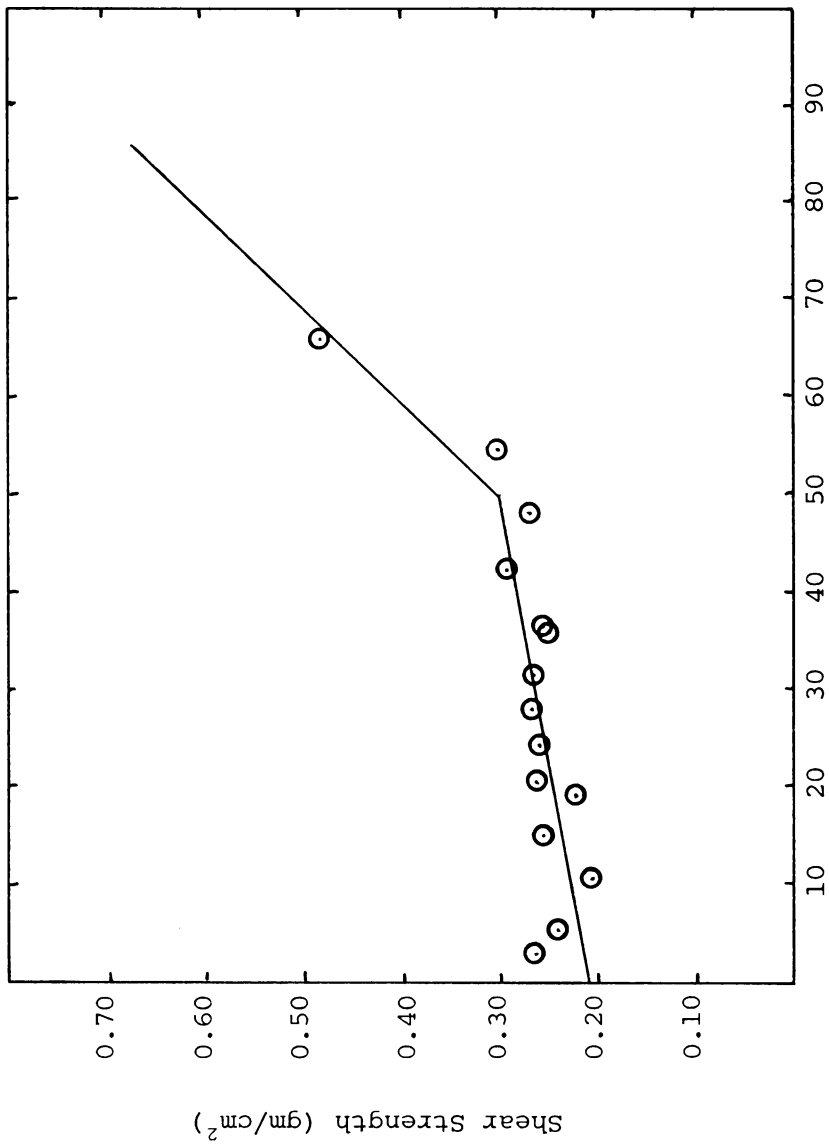

FIGURE 17d: Plot of Shear Strength vs. Concentration of Beads for Cylinder N. 4.

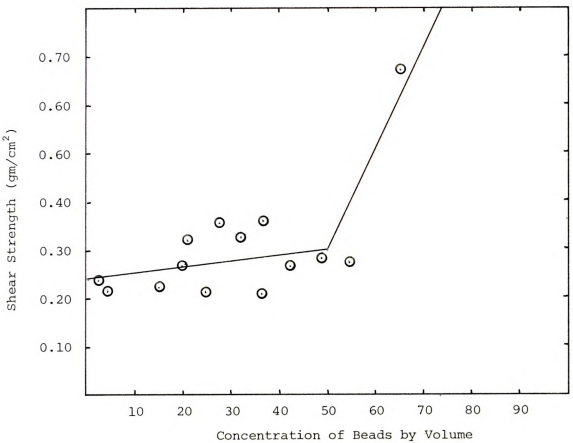

FIGURE 17e: Plot of Shear Strength vs. Concentration of Beads by Volume of Cylinder No. 5.

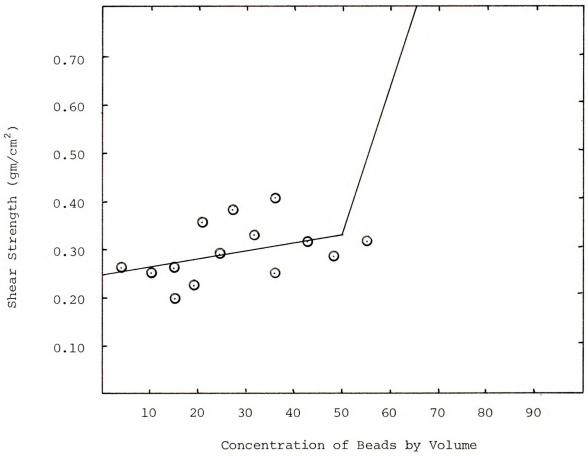

FIGURE 17f: Plot of Shear Strength vs. Concentration of Beads for Cylinder No. 6.

TABLE 9. Shear Strength as a Function of Grain Concentration Ratio, C (Vallejo, 1981b).

Mixture*	Grain Concentration Ratio C			Reference
	Mixture shear strength frictional shear resistance between grains*	Mixture shear strength ≈ Frictional plux matrix shear strength*	Mixture shear strength ≈ Matrix shear strength	
Sand-clay	>0.70	0.70 - 0.50	<0.50	Paduana (1966)
Sand-clay	>0.80	0.80 - 0.62	<0.62	Kurata and Fujishita (1960)
Sand-clay		? - 0.45	<0.45	Rodine and Johnson (1976)
Sand-ice		? - 0.42	<0.42	Goughnour and Andersland (1968)
Gravel-clay	>0.90	0.90 - 0.80	<0.80	Rico and Orozco (1975)
Average values	>0.80	0.80 - 0.56	<0.56	

* Sand or gravel = grains
Clay (kaolinite) or ice = matrix

grains of sand (in figures 17 a-f, glass beads) which introduce a frictional resistance component into the measured shear strength" (Vallejo, 1981b). The variable C here referred to is the grain concentration ratio, or the volume of the material in question (here, glass beads) divided by the total volume of the mixture.

Differences are again apparent in measured values of c_u between cylinders. Sample inhomogeneity becomes especially accute as the particle sizes become larger, as in this case. Therefore, it is felt that there is fairly good agreement between cylinders if this fact is taken into account. Cylinder No. 4 appears to give particularly consistent values of c_u.

Next the effects of the differences in lengths and diameters between the cylinders will be considered. First the differences in length. Figures 18, 19 and 20 show values of shear strengths for three cylinders versus concentrations of clay, sand and glass beads, respectively. On each figure, cylinders of the same diameter, but different lengths, are plotted. Analysis of these figures shows that there are differences of calculated shear strength between each cylinder (i.e. see Figures 18a and 18b). However, examination of Figures 19 and 20 shows that, even though there are differences, the data seems to be in fairly good agreement. In fact, some points coincide almost exactly (for example, see Figure 20b for a glass beads concentration of 48.8 percent). Figures 21, 22 and 23 show a few points which show particularly good agreement. Once again taking into account sample inhomogeneity and possible operator error, it is felt that the differences in the lengths of the cylinders produce negligible errors.

Considering the differences in diameters between the cylinders, Figures 24a, b and c show plots of cylinders with the same length,

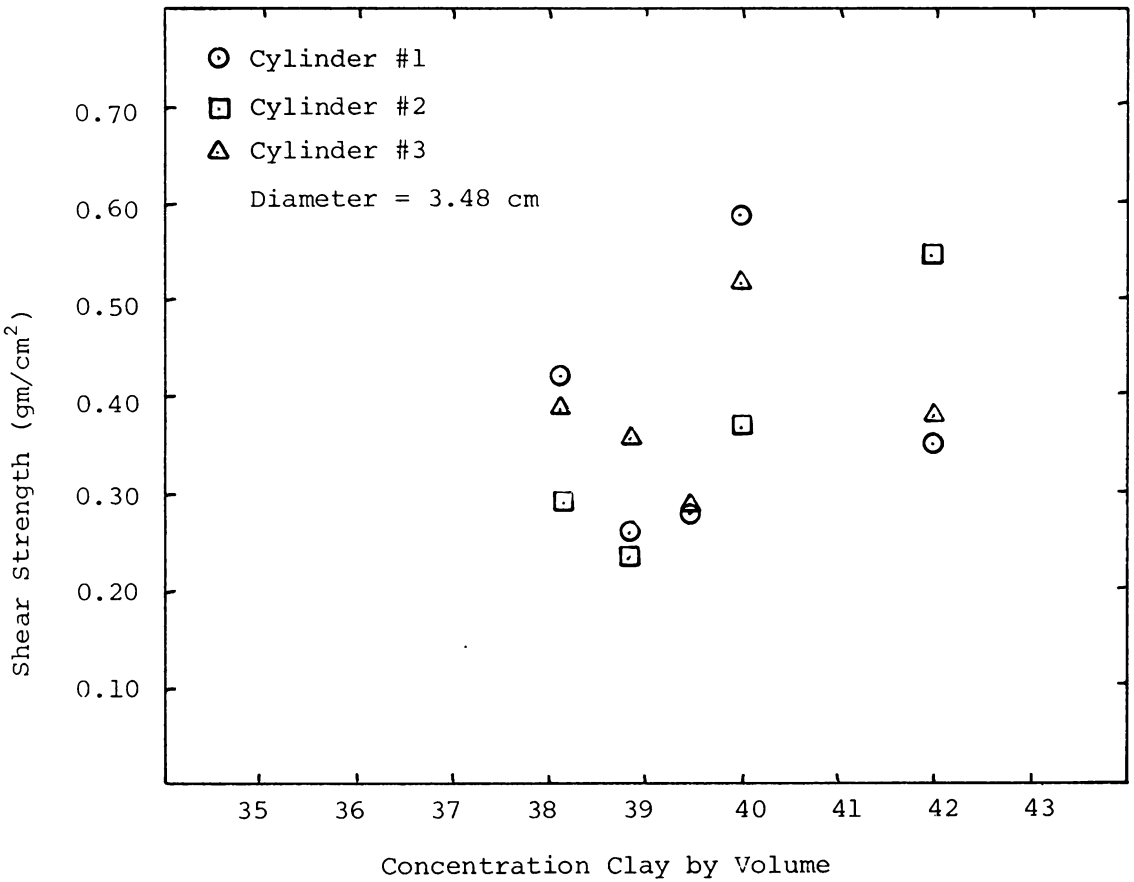

FIGURE 18a: Effect of Length for Concentration of Clay by Volume.

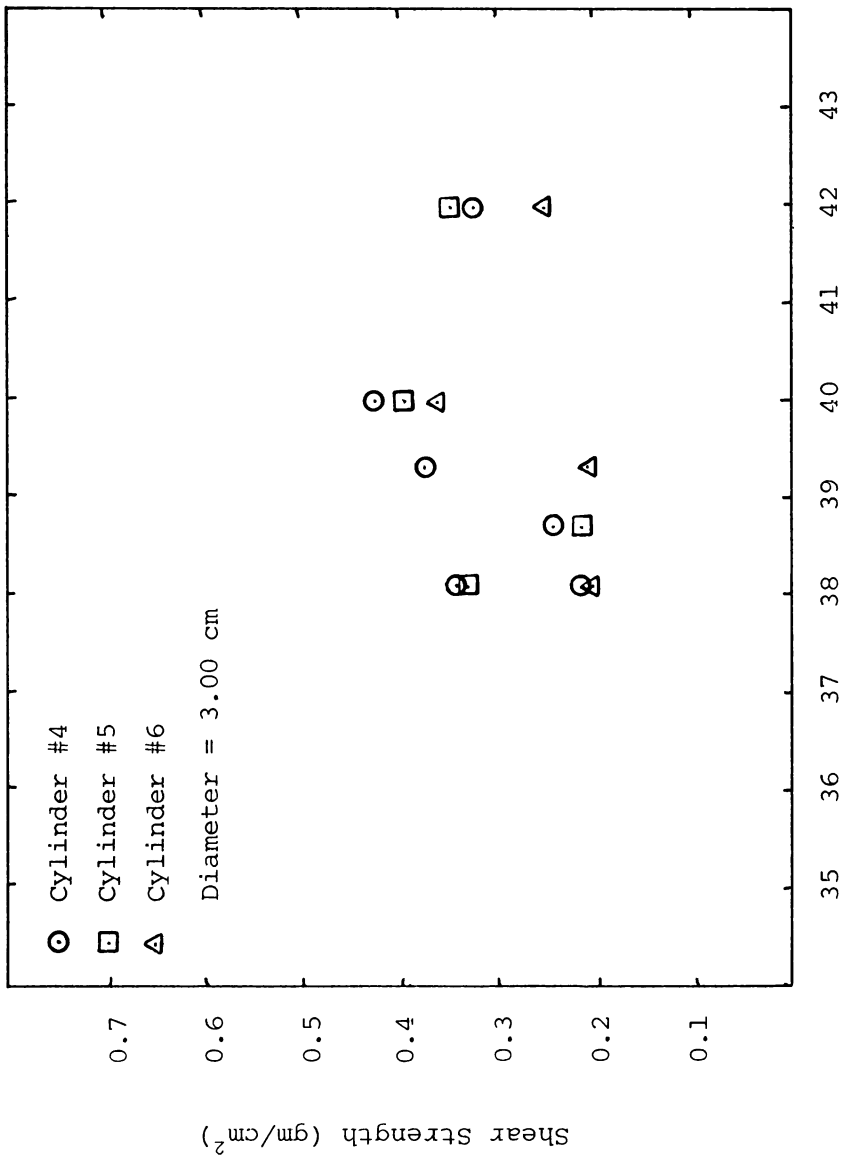

FIGURE 18b: Effect of Length for Concentration of Clay by volume.

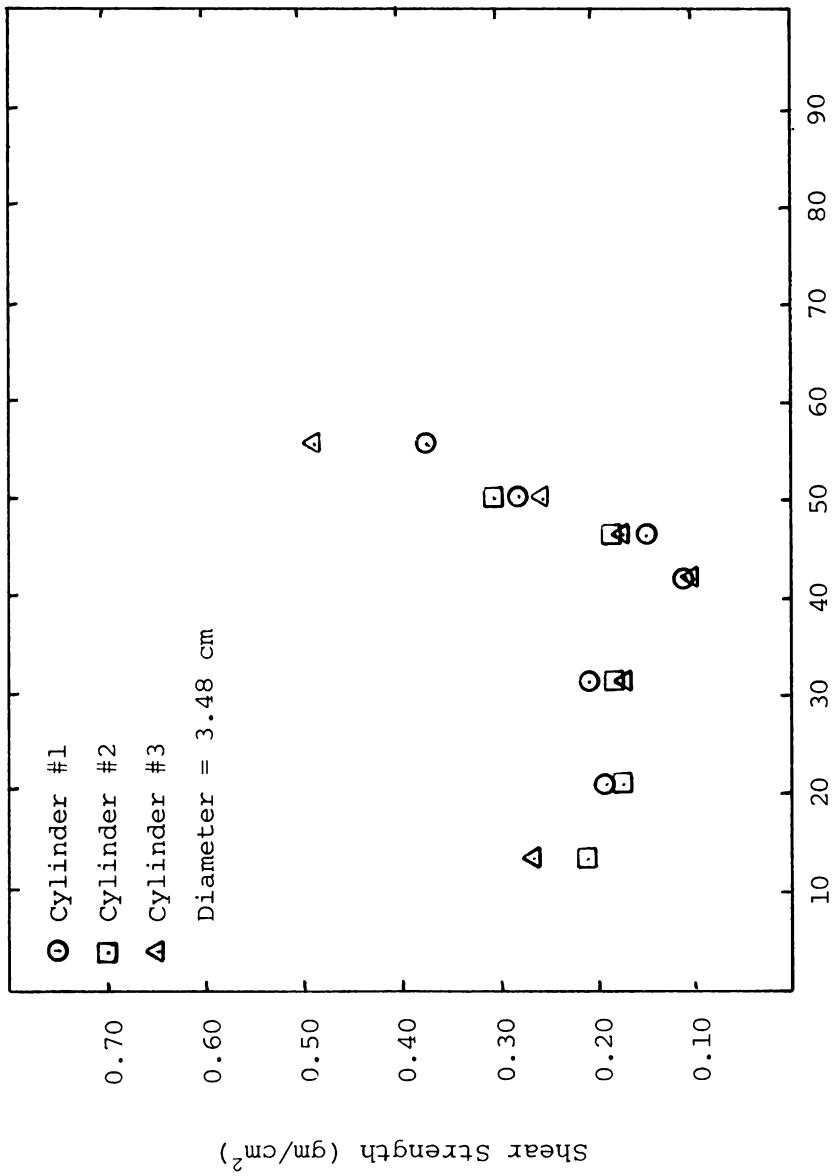

FIGURE 19a: Effect of Length for Concentration of Sand by Volume.

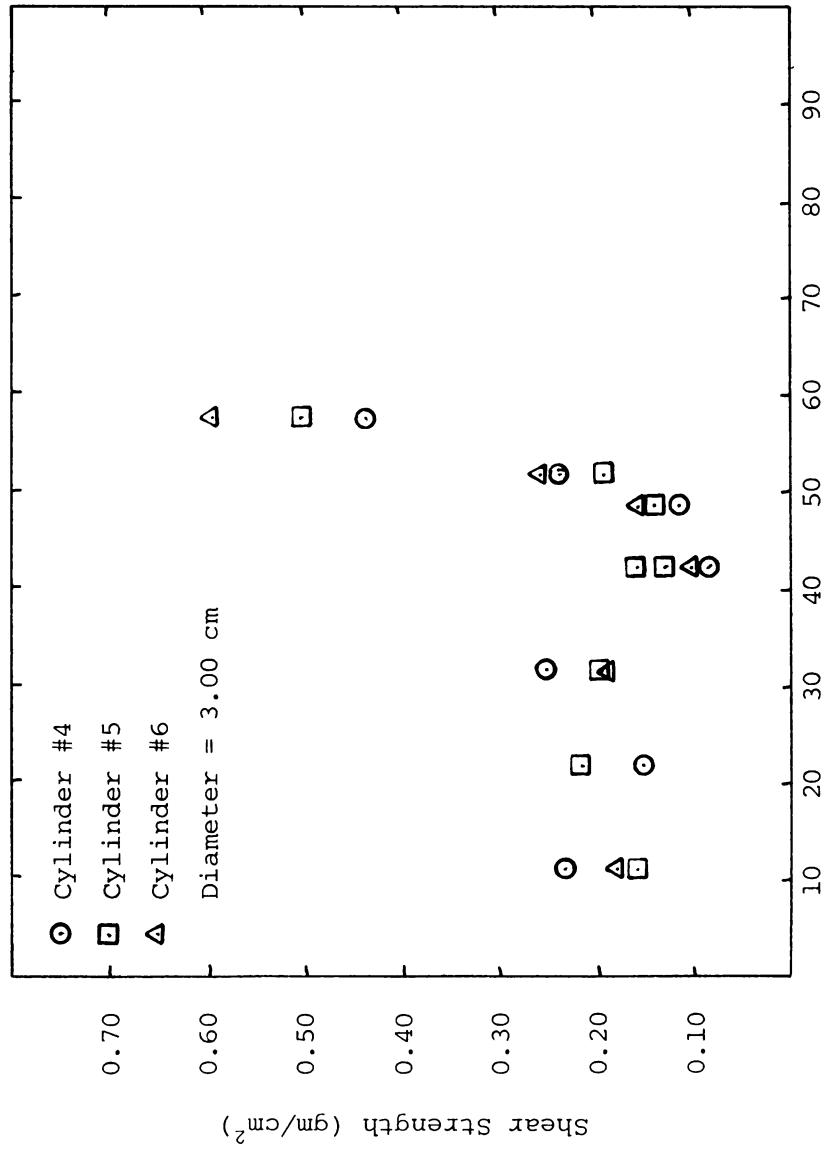

FIGURE 19b: Effect of Length for Concentration of Sand by Volume.

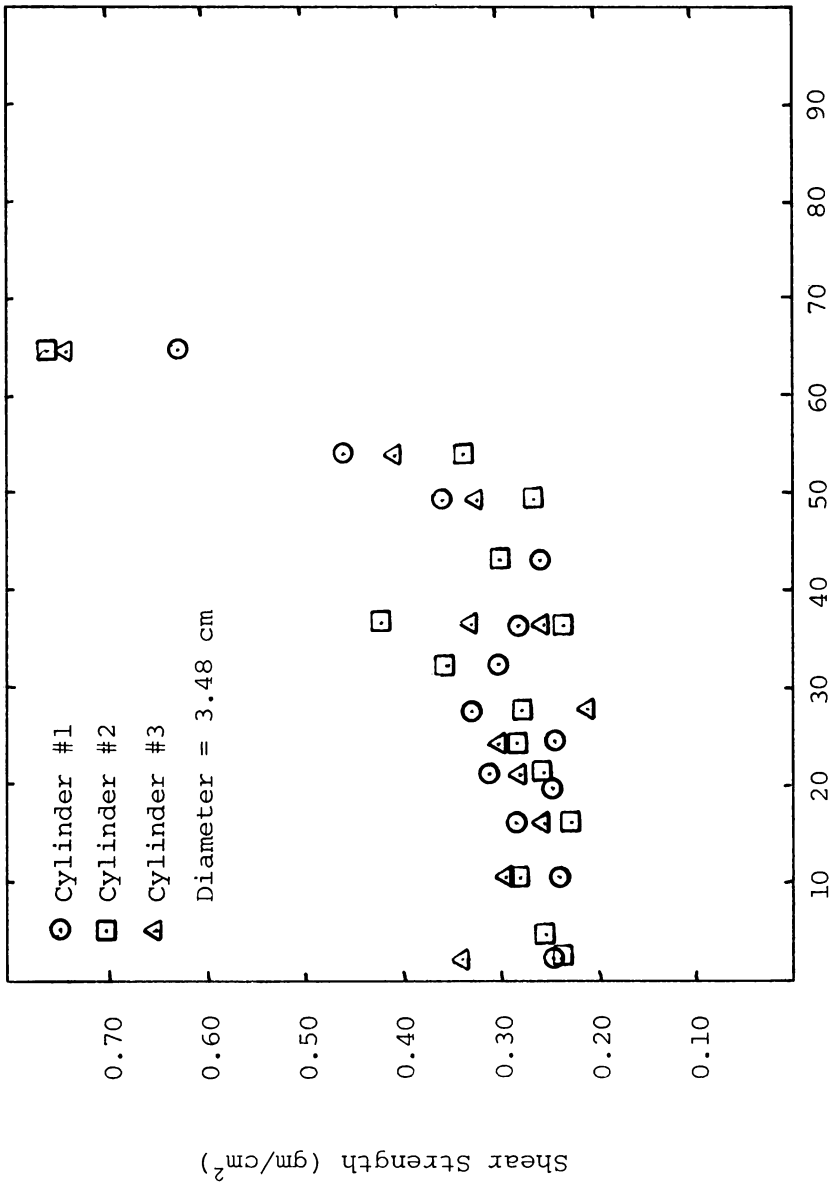

FIGURE 20a: Effect of Length for Concentration of Glass Beads by Volume.

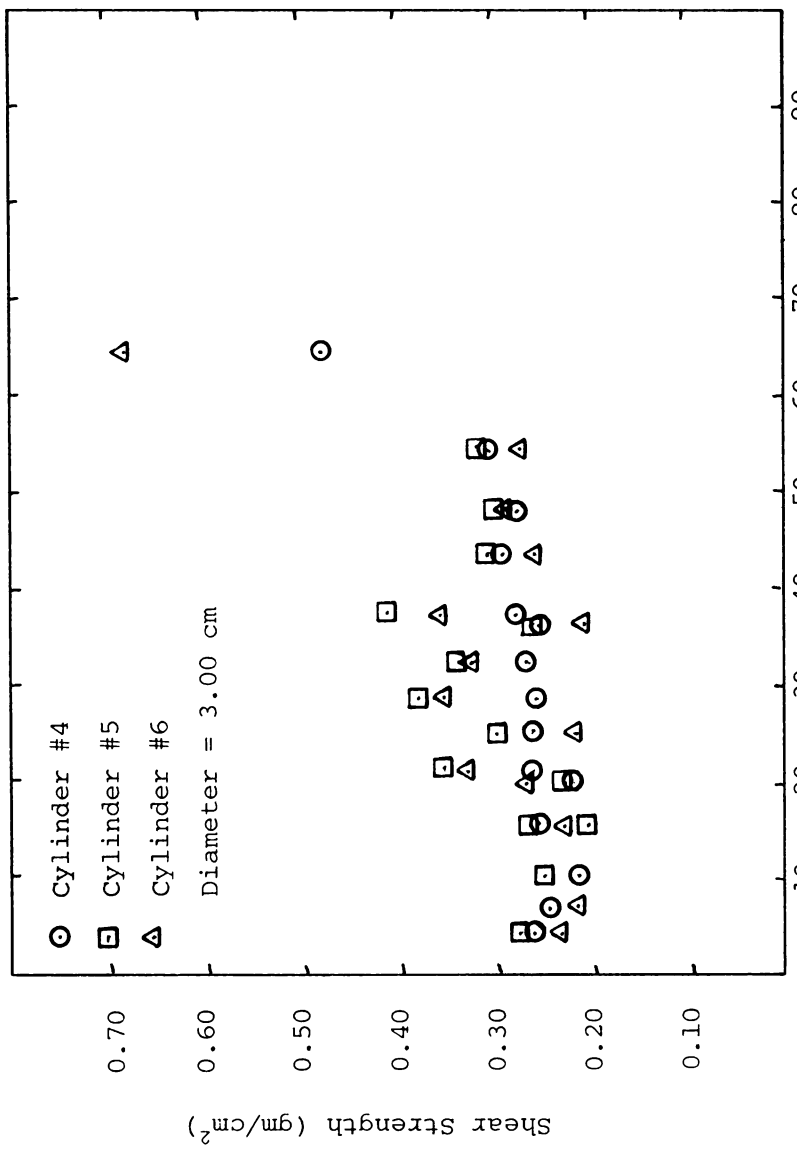

FIGURE 20b: Effect of Length for Concentration of Glass Beads by Volume.

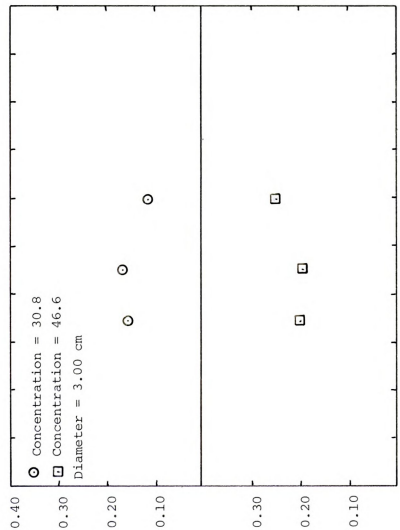

FIGURE 21: Effect of Length vs. Shear Strength, Concentration of Sand.

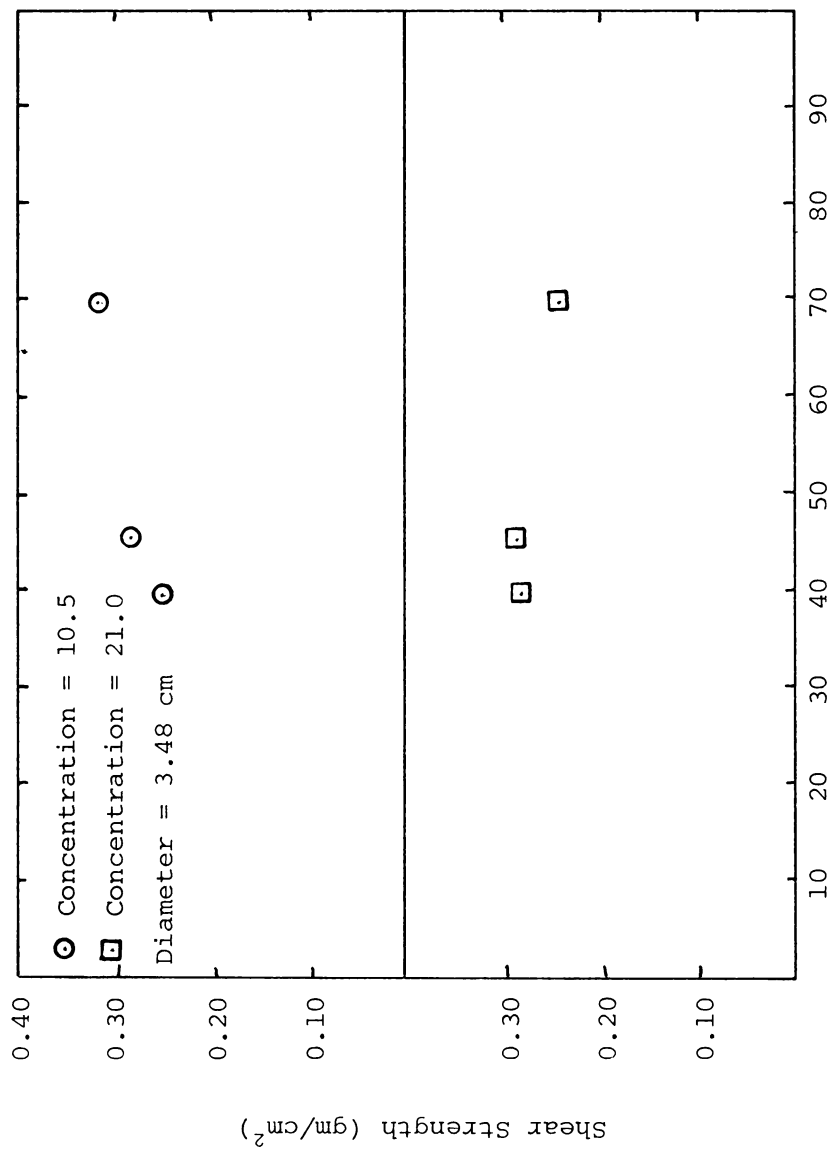

FIGURE 22: Effect of Length vs. Shear Strength, Concentration of Beads.

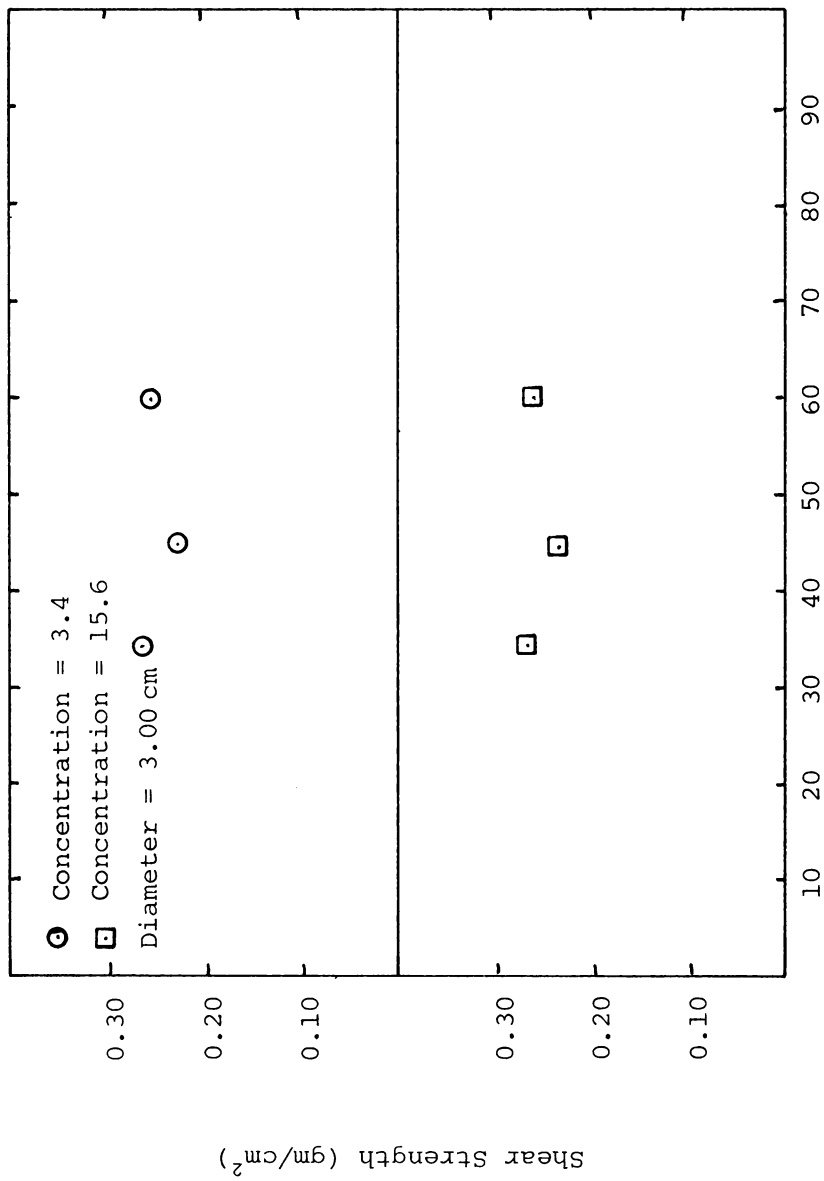

FIGURE 23: Effect of Length vs. Shear Strength, Concentration of Beads.

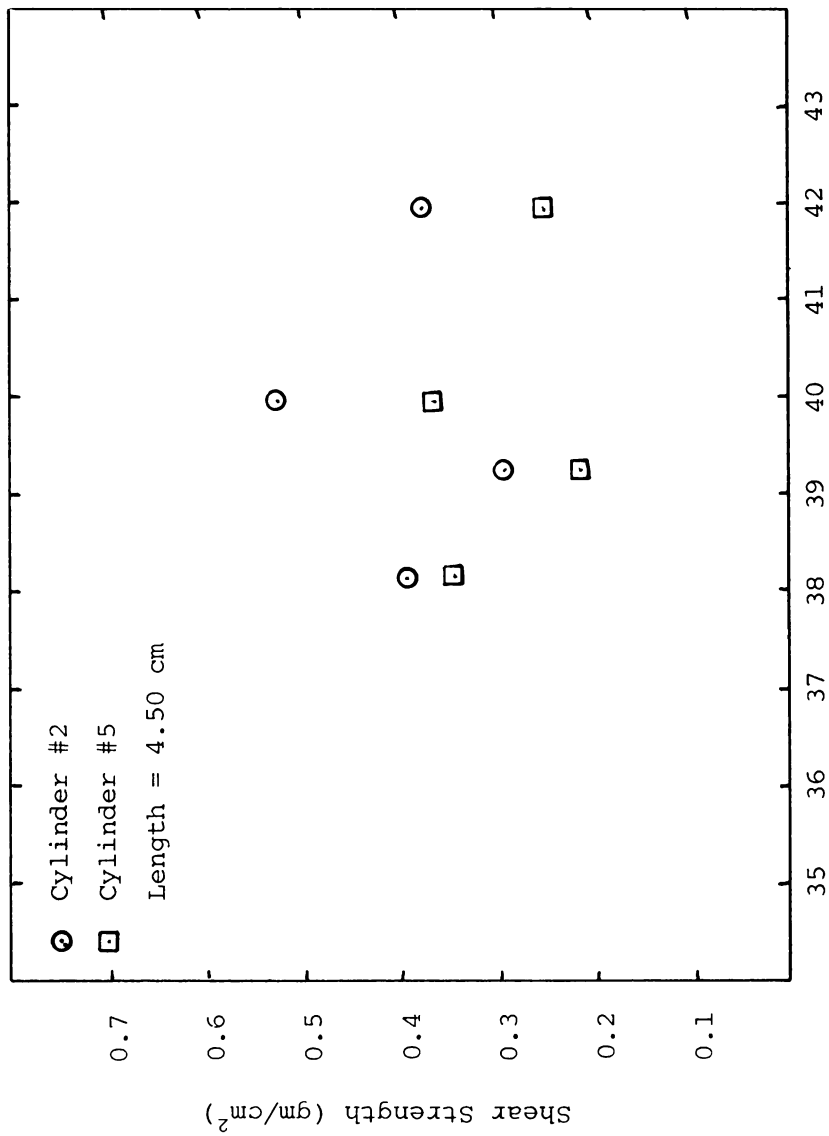

FIGURE 24a: Effect of Diameter for Concentration of Clay by Volume.

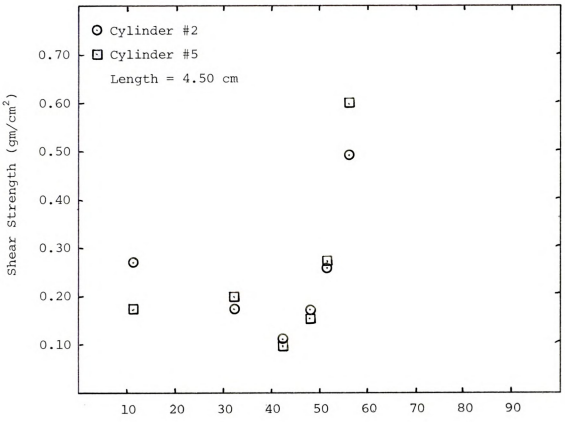

FIGURE 24b: Effect of Diameter for Concentration of Clay by Volume.

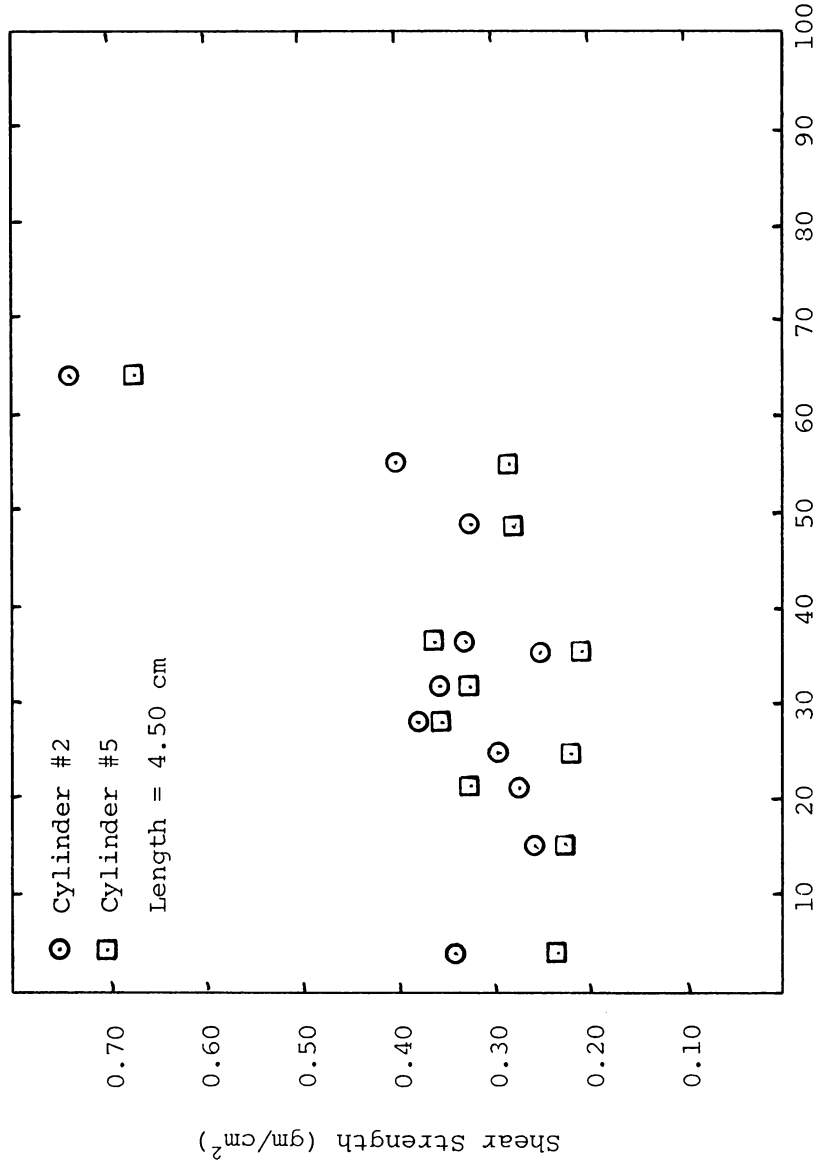

FIGURE 24c: Effect of Diameter for Concentration of Clay by Volume.

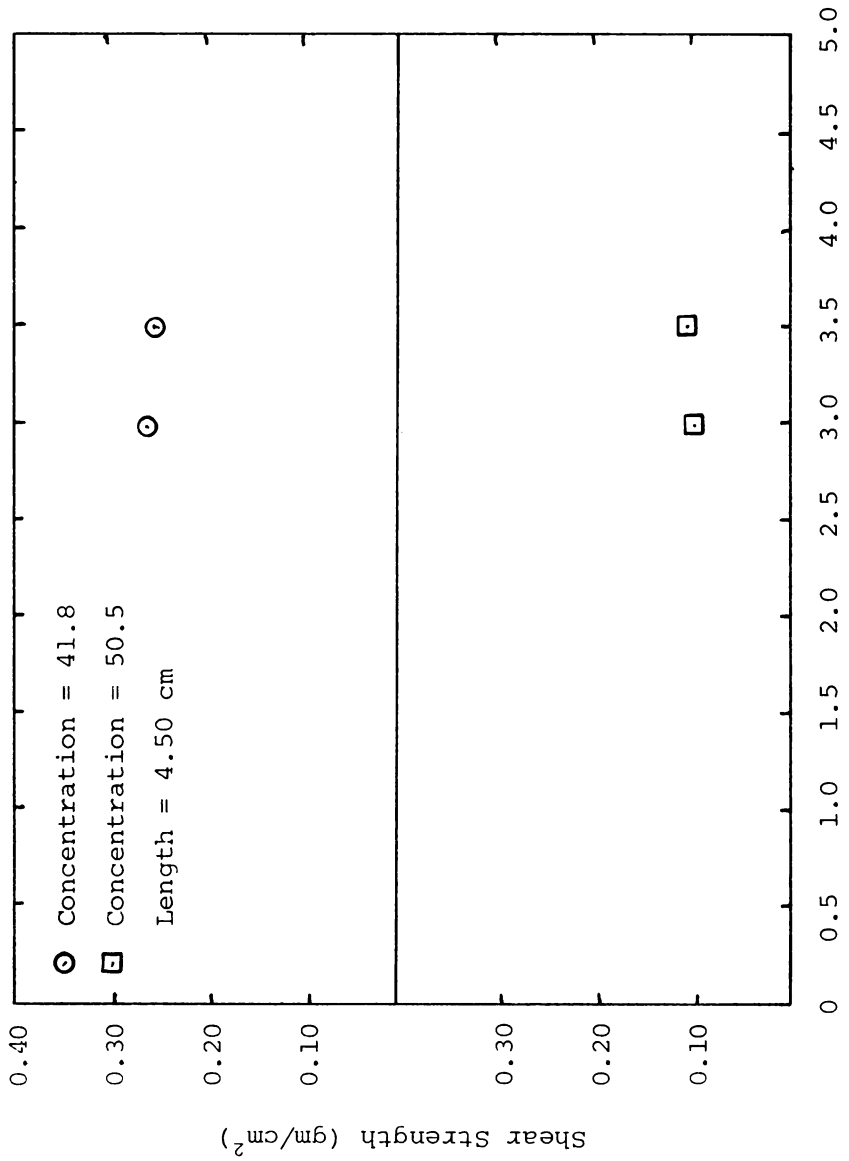

FIGURE 25: Effect of Diameter vs. Shear Strength, Concentration of Sand.

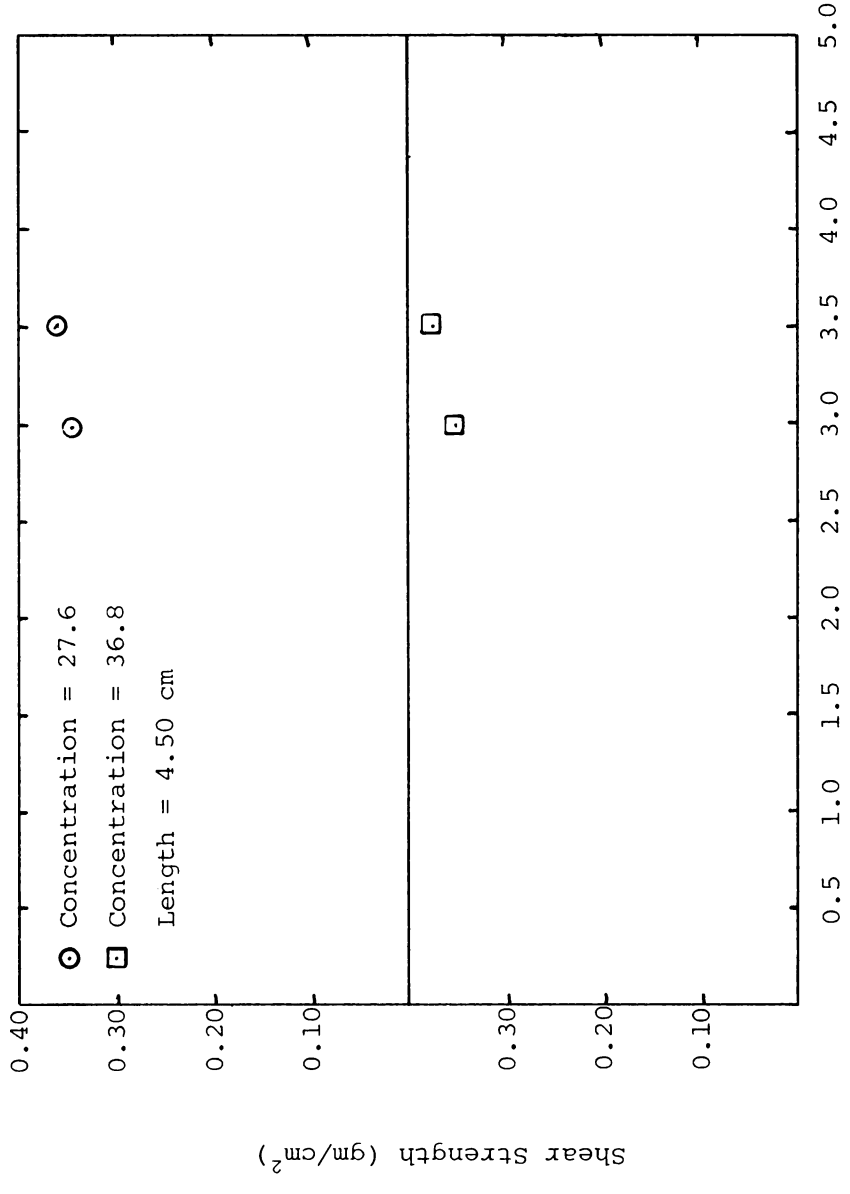

FIGURE 26: Effect of Diameter vs. Shear Strength, Concentration of Beads.

but different diameters (cylinders 2 and 5). Again, some discrepancies are readily apparent. However, these discrepancies appear relatively minor, particularly in Figures 24b and c. Figures 25 and 26 show a few points with particularly good agreement. It is once again felt that these minor discrepancies can be attributed to a non-homogeneous sample and possible operator error. Therefore, it appears that a change in length or diameter will have little, if any, effect on the calculated values for c_u. As long as the correct dimensions and unit weights are known, a cylinder of any size may be used (providing it has smooth sides and $\alpha < 90^{o}$).

VANE SHEAR COMPARISON TESTS

For comparison purposes, a vane shear test was run at the end of each test cycle. The vane used had the following dimensions: diameter - 1.27 cm and height - 2.54 cm. Using the equation developed for the vane shear in Chapter 4, the undrained shear strength was calculated for each test. The strain rate used was equal to 10 degrees per minute. Figures 27 through 29 show plots of the data obtained. It can be seen from these plots that data scatter is even more pronounced for the vane shear than it was for the cylinder strength meters. It is felt that for soils with such low shear strengths as muds the vane shear apparatus is not sensitive enough to accurately measure c_u. In other words, sample inhomogeneity will have an even greater effect on the vane shear apparatus than on the cylinder strength meters.

However, despite these reservations, Figure 29 confirms a trend which was noticed in Figures 17a-f; that is a gradual increase in c_u for low concentrations of beads, until an abrupt increase occurs at a concentration of approximately 50-55 percent. This would confirm the

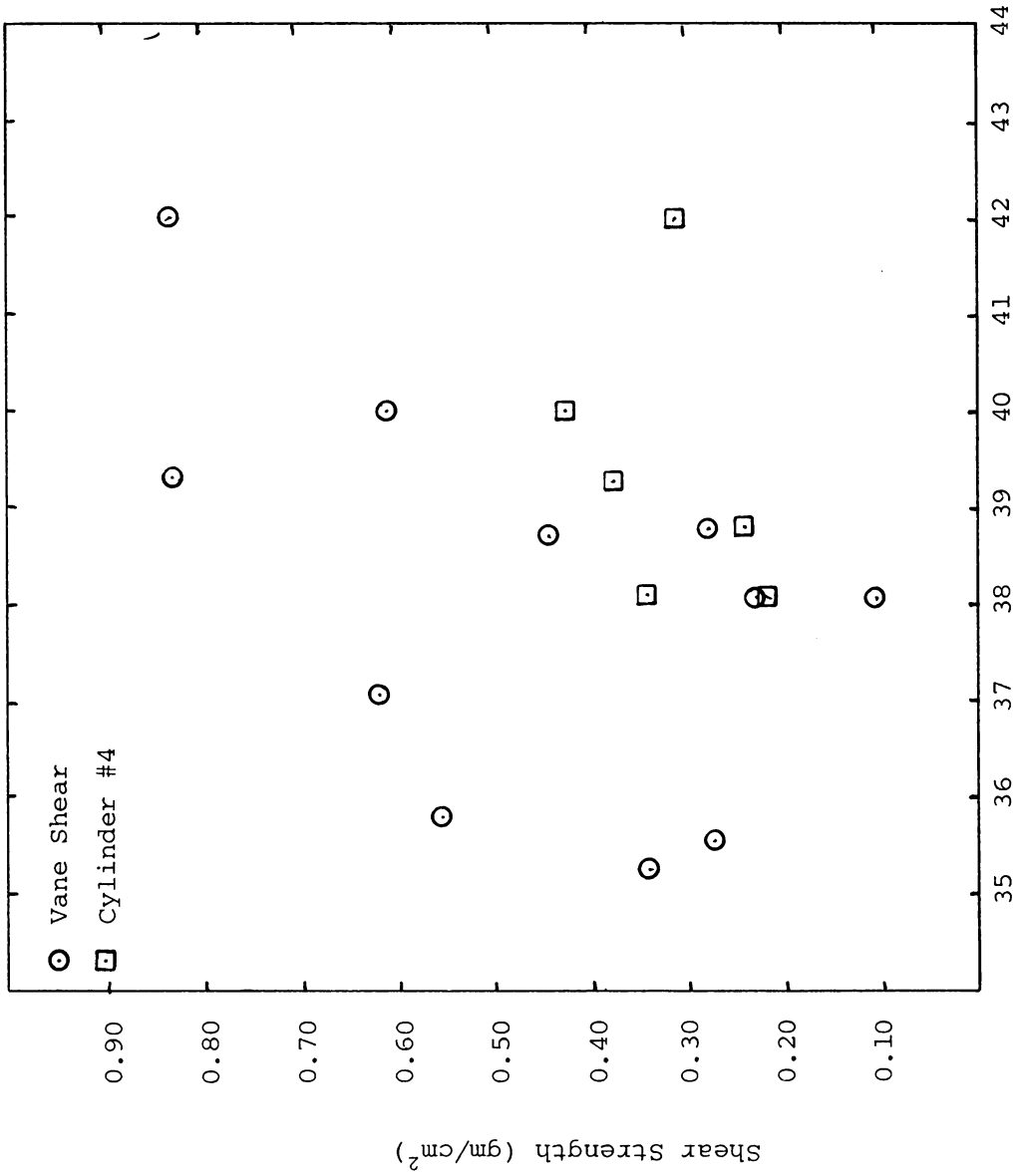

FIGURE 27: Plot of Vane Shear Data vs. Concentration of Clay by Volume

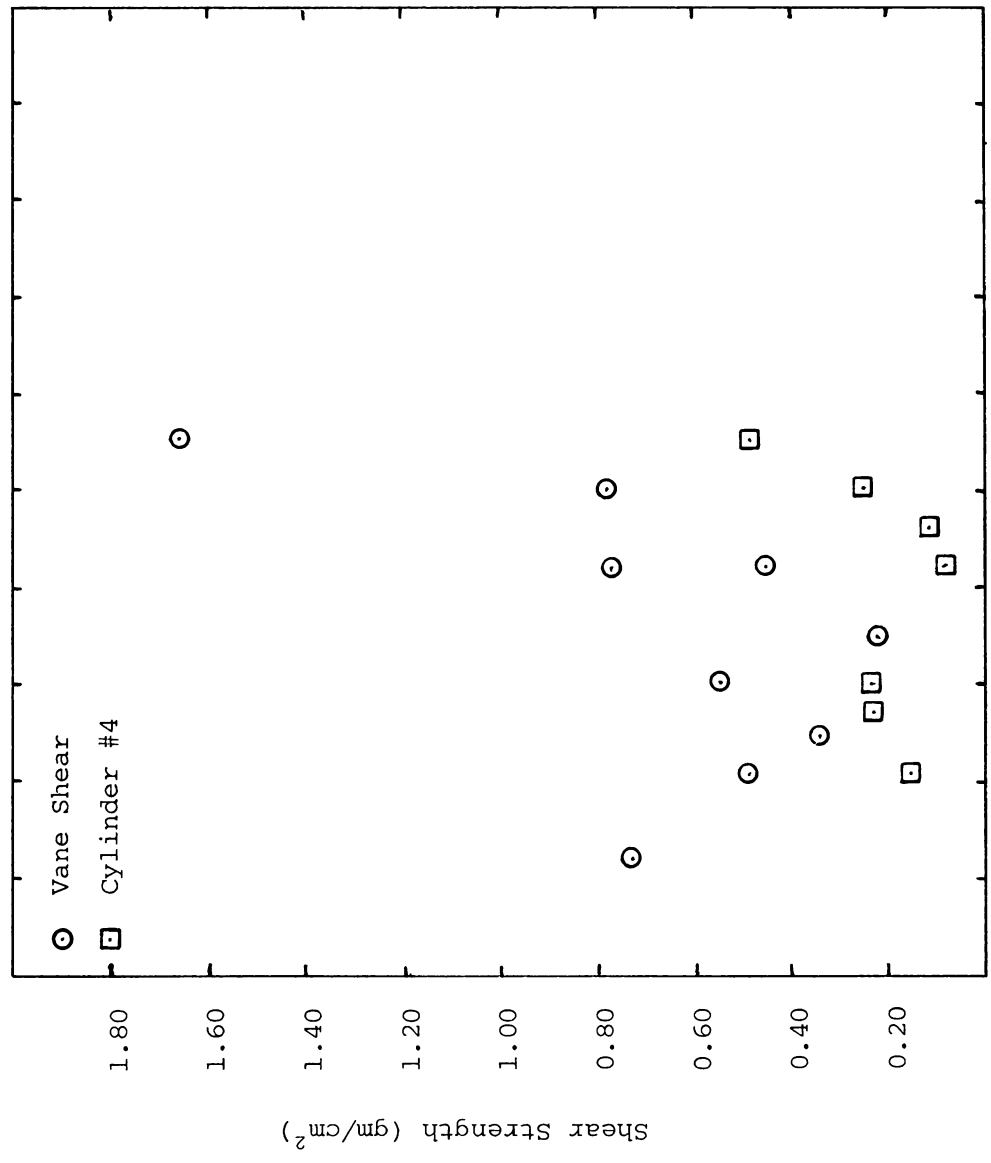

FIGURE 28: Plot of Vane Shear Data vs. Concentration of Sand by Volume.

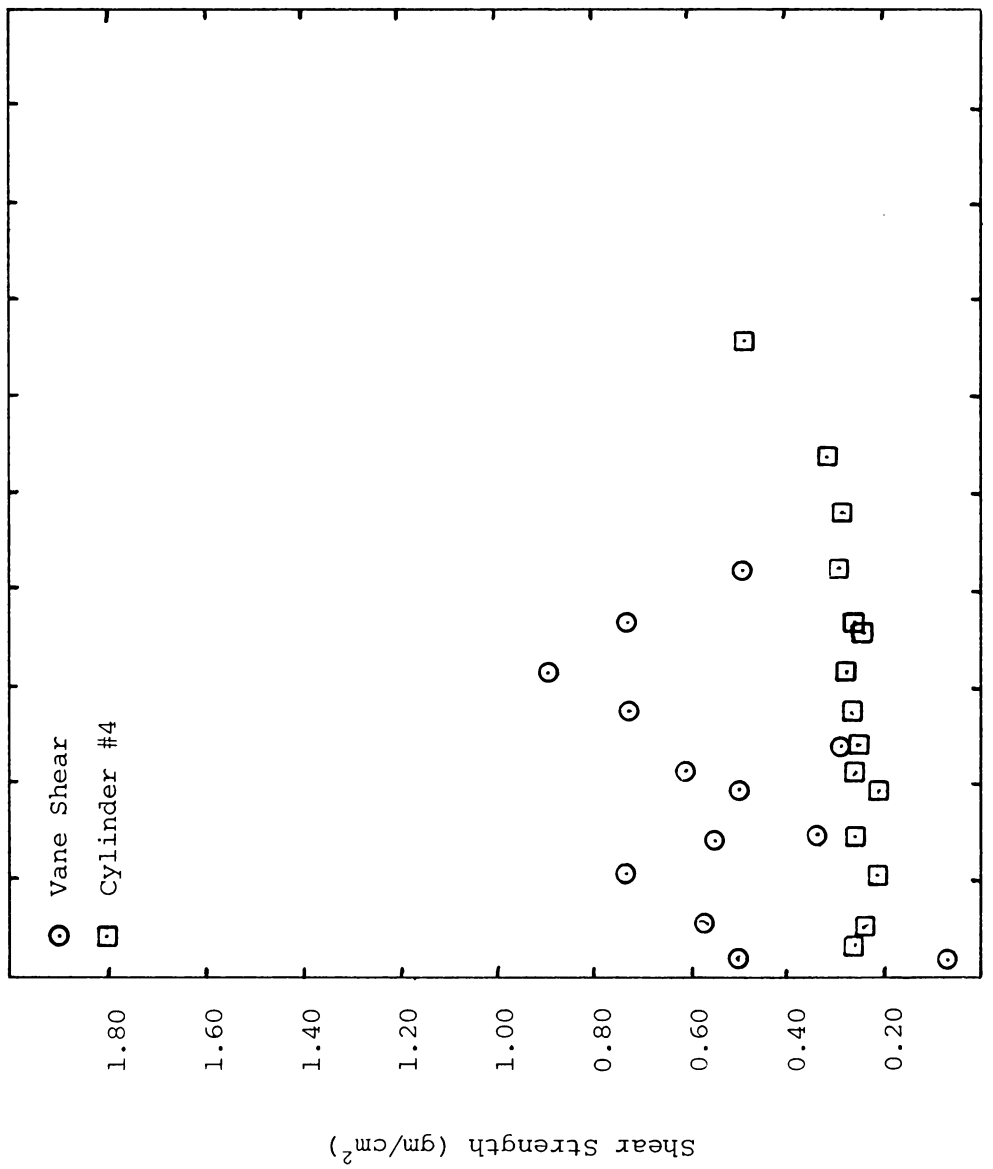

FIGURE 29: Plot of Vane Shear Data vs. Concentration of Beads by Volume.

fact that this upward trend is not peculiar to just the cylinder strength meter alone.

DESIGN CHARTS

In that it is very awkward to work with Sokolovskii's modified equation (38), a much more simple evaluation of c_u can be accomplished. A careful examination of equation (38) shows that c_u is basically a function of four distinct variables. These are γ_c, γ_f, R, and h, the unit weight of the test cylinder, the unit weight of the mud, the radius of the test cylinder, and the depth of imbedment, respectively. Taking these into account, and transforming them into dimensionless numbers, a plot of these data points roughly yields a straight line (Figure 30 shows the data plotted for cylinders one and two). A linear regression analyses on these data points, and ones for cylinders 3 through 6, also, yields the line given in Figure 31. This line is independent of the type of granular material in the mud, as this is accounted for in γ_f. So if the variables γ_c, γ_f, R and h are known or can be readily calculated, then the approximate value of c_u can be quickly found from this chart. Charts for other values of γ_c not equal to 1.19 $\frac{gm}{cm^3}$ could be easily developed by experimentation.

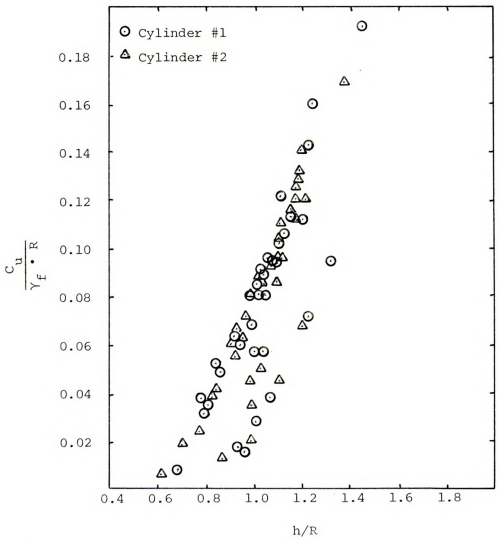

FIGURE 30: Plot of Data Reduced to Dimensionless Numbers.

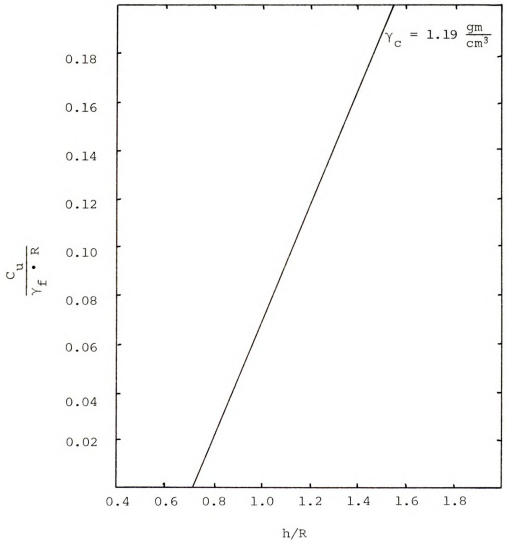

FIGURE 31: Design Chart for Finding C_u. (Linear Regression Analysis Performed on Data for Cylinders 1-6.)

VII. SUMMARY AND CONCLUSIONS

A new method to measure the undrained shear strength, C_u, of a mud based on plasticity theory is presented to hopefully alleviate the present shortcomings of the methods presently in use. The new approach uses a cylinder as a measuring device and the theory developed by Sokolovskii to calculate the indentation pressures developed in a Tresca plastic when a cylinder penetrates it. Mudflows were simulated in the laboratory using a mixture of water, kaolinite clay, and calgon (to act as a dispersing agent). Varying concentrations of sand and glass beads were added to simulate rock fragments and clay lumps present in actual mudflows. Smooth plexiglass cylinders with lengths ranging from 3.48 cm to 7.00 cm, and radii varying from 3.00 cm to 3.48 cm, were used as the measuring devices.

It was found that:

1. The value of C_u for a mud could be calculated using the smooth walled plexiglass cylinders.

2. The differences in length of the cylinders seem to have no effect in the calculation of C_u.

3. The differences in diameter of the cylinders, although small, also did not have any effect on the calculation of the undrained shear strength.

4. The comparatively small scatter in the data can be explained by the following:

   a. sample inhomogeneity;

   b. evaporation during testing;

   c. operator error.

5. Comparison of the cylinder-strength meter with the vane shear

tests show that the vane shear has an even wider scattering of the data. Statistical analyses of the data (see appendix D) shows that the variance for the "best case" test data for the vane shear is still greater than four times the "worst case" test data for the cylinder-strength meter, 0.054 vs. 0.014. This tends to support the conclusion that the cylinder-strength meter gives much more consistent results than the vane shear.

6. Design charts are developed to more easily find the value of C_u using cylinders with a unit weight equal to 1.19 $\frac{gms}{cm^3}$.

NEED FOR FUTURE RESEARCH

It is felt that with further development and refinement, this new test method could become a viable alternative to the method presently in use. Further laboratory work is necessary, though, perhaps using cylinders of different unit weights, cylinders with a larger range in diameters, a more accurate method to measure h need be developed, and an elimination or limitation on any possible operator errors should also be considered.

LIST OF REFERENCES

LIST OF REFERENCES

Agarwal, B. D., and Broutman, L. J. (1980), Analysis and Performance of Fiber Composites, New York, New York, pp. 16-20.

Bagnold, R. A. (1954), "Experiments on a Gravity-Free Dispersion of Large Solid Spheres in a Newtonian Fluid Under Shear," Proceedings of the Royal Society of London, Vol. 225A, pp. 49-63.

Bea, R. G., and Audibert, J. M. E. (1980), "Offshore Platforms and Pipelines in the Mississippi River Delta," Journal of the Geotechnical Engineering Division, American Society of Civil Engineers, Vol. 106, Number GT8, pp. 853-869.

Beck, Melinda, and Gary, Sandra (1982), "A Deluge of Deadly Weather," Newsweek, January 18, 1982.

Demars, K. R., Nacci, V. A., and Wang, W. D. (1977), "Pipeline Failure: A Need for Improved Analysis and Site Surveys," Proceedings of the Ninth Offshore Technology Conference, Houston, Texas, 1977, Paper OTC 2966, pp. 63-70. Dallas, Texas: American Institute of Mining, Metallurgical and Petroleum Engineers, Inc.

Gade, H. G. (1958), "Effects of Nonrigid, Impermeable Bottom on Plane Surface Waves in Shallow Water," Journal of Marine Research, 16 (2), pp. 61-82.

Ghazzaly, O. I., and Lim, S. J. (1975), "Experimental Investigation of Pipeline Stability in Very Soft Clay," Proceedings of the 7th Offshore Technology Conference, Houston, Texas, 1975, Paper OTC 2277, pp. 315-319.

Hampton, M. A., with Johnson (1970), "Subaqueous Debris Flow and Generation of Turbidity Currents," Ph.D. Thesis, Stanford University, Department of Geology.

Henkel, D. S. (1970), "The Role of Waves in Causing Submarine Slides," Geotechnique, Volume 20, No. 1, March, pp. 75-80.

Hirst, T. J., Richardo, A. F., and Inderbitzen, A. L. (1972), "A Static Cone Penetrometer for Ocean Sediments," Underwater Soil Sampling, Testing and Construction Control, ASTM SP No. 501, pp. 69-89.

Hutchinson, J. N. (1970), "A Coastal Mudflow in the London Clay Cliffs at Beltinge, North Kent," Geotechnique, Vol. 20, pp. 412-438.

Johnson, A. M. (1965), A Model for Debris Flow, Ph.D. Thesis, The Pennsylvania State University, Department of Geology.

Johnson, A. M. (1970), Physical Processes in Geology, Freeman, Cooper, and Co., San Francisco, p. 571.

Keulegan, G. H. (1944), "Spatially Variable Discharge Over Sloping Plane," Transactions, American Geophysical Union, pp. 956-968.

Kraft, L. M., Ahmad, N., and Focht, J. A. (1976), "Application of Remote Vane Results to Offshore Geotechnical Problems," Proceedings of the Eighth Offshore Technology Conference, Paper OTC 2626, pp. 75-96.

Krone, R. B. (1963), A Study of Rheological Properties of Esturarial Sediments, University of California at Berkeley, Hydraulic Engineering Laboratory and Sanitary Engineering Research Laboratory, SERL Report No. 63-8.

Ladd, C. C., Foot, R., Ishihara, K., Schlosser, F., and Poulos, H. G. (1977), "Stress-Deformation and Strength Characteristics," Proceedings of the Ninth International Conference on Soil Mechanics and Foundation Engineering, Tokyo, Japan, 1977, State-of-the-Art Reports, Volume 2, pp. 421-494. Tokyo, Japan: The Japanese Society of Soil Mechanics and Foundation Engineering.

Levin, E. (1955), "Indentation Pressure of Smooth Circular Punch," Quarterly Journal of Applied Mathematics, Vol. 13, pp. 133-137.

Meyerhof, G. G. (1951), "The Ultimate Bearing Capacity of Foundations," Geotechnique, Volume 2, Number 4, pp. 301-332.

Nye, J. F. (1952), "A Comparison Between the Theoretical and Measured Long Profile of the Unteraar Glacier," Journal of Glaciology, Vol. 2, No. 2, pp. 103-107.

Rodine, J. D. (1975), Analysis of the Mobilization of Debris Flows, Ph.D. Thesis, Stanford University, Department of Geology.

Schuster, Robert L. (1978), "Introduction," Landslide, Analysis and Control, Transportation Research Board Special Report 176, Washington, D.C., 1978, National Academy of Sciences, pp. 1-10.

Skempton, A. W. (1948), "The $\phi = 0$ Analysis of Stability and Its Theoretical Basis," Proceedings of the Second International Conference on Soil Mechanics, Vol. 1, pp. 72-78.

Skempton, A. W., and Golder, H. Q. (1948), "Practical Examples of the $\phi = 0$ Analysis of Stability of Clays," Proceedings of the Second International Conference on Soil Mechanics, Vol. 2, pp. 63-70.

Skempton, A. W., and Hutchinson, J. N. (1969), "Stability of Natural Slopes and Embankment Foundations," Proceedings of the Seventh International Conference on Soil Mechanics and Foundation Engineering, State-of-the-Art Volume, pp. 291-340.

Sokolovskii, V. V. (1955), Theorie Der Plastizitat, Berlin, Germany: Feb Verlag Technik Press.

Terzaghi, Karl (1936), "A Fundamental Fallacy in Earth Pressure Computations," J. Boston Civil Engineers, H. 23, S. 71-78.

Vallejo, L. E. (1979), "An Explanation for Mudflows," Geotechnique, Vol. 29, No. 3, pp. 351-354.

Vallejo, L. E. (1981a), "Stability Analysis of Mudflows on Natural Slopes," Proceedings of the Tenth International Conference on Soil Mechanics and Foundation Engineering, Stockholm, Sweden, 1981, Vol. 3, pp. 541-544.

Vallejo, L. E. (1981b), "Determination of the Shear Strength of Granulo-Viscous Materials Using the Vane Shear Apparatus and the Two-Phase Suspension Theory," Proceedings of the International Conference on the Mechanical Behaviour of Structural Media, Ottawa, Canada, 1981, Volume B, pp. 373-381.

Wright, S. G. (1976), "Analysis for Wave-Induced Sea-Floor Movements," Proceedings: Offshore Technology Conference, OTC 2427, Vol. 1, Houston, May, pp. 51-52.

Wu, T. H., and Sangray, D. A. (1978), "Strength Properties and Their Measurement," Landslides, Analysis and Control, Transportation Research Board Special Report 176, Washington, D.C., 1978, National Academy of Sciences, pp. 139-154.

APPENDIX A

APPENDIX A

SAMPLE CALCULATIONS

To determine the variables listed in Tables B1-6, the following calculations were performed:

α, the angle of imbedment with the vertical

$$\alpha = \cos^{-1}\left(\frac{R-h}{R}\right) \qquad \text{(in degrees)}$$

where R is the radius of the test cylinder, and h is the depth of imbedment of the test cylinder into the mud (see Figure 13b).

For Cylinder Number 1, Test Number 2:

$h = 1.33$

$R = 1.74$

$$\cos^{-1}\left(\frac{1.74 - 1.33}{1.74}\right) = 76.37^{\circ}$$

A, the area

The area of the end of the test cylinder which is imbedded in the mud is calculated from the equation

$$A = R^2 \ (\alpha' - \sin \alpha \cos \alpha) \qquad \text{(in square centimeters)}$$

where the parameters are the same as before, except that α' is the value of α in radians (see Figure 13b).

For Cylinder Number 1, Test Number 2:

$\alpha = 76.37^{\circ}$

$\alpha' = 1.333$ Radians

$R = 1.74$ cm

$A = (1.74)^2 (1.33 - \sin 76.37^{O} \cos 76.37^{O}) = 3.34$ cm^2

V, the volume

The volume here referred to is the volume of the test cylinder which is imbedded in the mud. This volume is simply the area, previously calculated, multiplied by the length of the test cylinder, or

$V = L * A$ (in cubic centimeters)

For Cylinder Number 1, Test Number 2:

$A = 3.34$ cm^2

$L = 7.00$ cm

$V = (7.00)(3.34) = 23.38$ cm^3

γ_f, the unit weight of the soil slurry (mud)

The unit weight of the soil slurry is determined by using the equation developed by Agarwal and Broutman (1980), which states

$$\rho_c = \frac{1}{\sum_{i=1}^{n} (W_i/\rho_i)}$$ (in grams/cubic centimeter)

where W is the weight fraction of each of the individual constituents, and ρ_i is the density of each of the individual constituents.

For Cylinder Number 1, Test Number 2:

weight of clay used = 423.2 grams

weight of calgon used = 45.5 grams

weight of water used = 242.1 grams

710.8 grams

the unit weight of clay = 2.65 gms/cm^3

the unit weight of calgon = 2.65 gms/cm^3

the unit weight of water = 1.00 gms/cm^3

then:

$$\rho_c = \frac{1}{(\frac{423.2}{710.8} / 2.65) + (\frac{45.5}{710.8} / 2.65) + (\frac{242.1}{710.8} / 1.00)} = \gamma_f$$

= 1.69 grams/cubic centimeters

P', the effective weight acting downwards

The effective downward force due to the cylinder is the weight of the cylinder minus the buoyancy force, or

$$P' = W - P_b \qquad \text{(in grams)}$$

For Cylinder Number 1, Test Number 2:

W = 79.3 grams

P_b = Volume x γ_f = 23.38 (1.69) = 39.31 grams

So that

P' = 79.3 - 39.31 = 39.9 grams

C_{KAO}, C_{SAND}, C_{BEADS}, the concentrations of materials by weight

These values are simply the weight fractions of each constituent.

For Cylinder Number 1, Test Number 2:

weight of clay used = 423.2 grams

total weight of material = 710.8 grams

$$C_{KAO} = \frac{423.2}{710.8} (100) = 59.54\%$$

C_{KAO}, C_{SAND}, C_{BEADS}, the concentrations of materials by volume

The volume fractions of each constituent are found by the equation developed by Agarwal and Broutman (1980), which states

$$V_i = \frac{\rho_c}{\rho_i} W$$

where ρ_c is the density of the total slurry

ρ_i is the density of the constituent in question, and

W_i is the weight fraction of the constituent in question.

For Cylinder Number 1, Test Number 2:

$$W_{KAO} = \frac{423.2}{710.8} = 0.5954$$

$$\rho_c = 1.69 \text{ grams/cm}^3$$

$$\rho_{KAO} = 2.65 \text{ grams/cm}^3$$

Then,

$$C_{KAO} = \frac{1.69}{2.65} (0.5954) = 0.381 \text{ or } 38.1\%$$

C_u, the calculated undrained shear strength

This is the value of the undrained shear strength using Sokolovskii's (1955) equation,

$$c_u = \frac{R [\pi \gamma_c - (\alpha - \sin \alpha \cos \alpha) \gamma_f]}{2[(\pi+2) \sin \alpha + (1 - \cos \alpha - \alpha \sin \alpha)]}$$

where the variables are as defined previously, and γ_c is the unit weight of the test cylinder.

For Cylinder Number 1, Test Number 2:

$$C_u = \frac{1.74\left[(\pi)\ (1.19) - (1.333 - \sin 76.37^{O} \cos 76.37^{O})\ (1.69)\right]}{2\left[(\pi+2)\ \sin 76.37 + (1 - \cos 76.37 - 1.333 \sin 76.37^{O})\right]}$$

$$= 0.417 \frac{\text{grams}}{\text{centimeter}^2}$$

To determine the variables listed in Table C1-6, the following calculations were performed.

h, the depth of imbedment

The h here referred to is actually the heigth of the cylinder not imbedded in the clay.

For Cylinder Number 1, Test Number 2:

$$h = 3.48 - 1.33 = 2.15 \text{ cm}$$

h/R

This value is simply the value of h divided by the radius of the test cylinder.

For Cylinder Number 1, Test Number 2:

$h = 2.15$ cm

$R = 1.74$ cm

$h/R = 1.24$

γ_f, c_u

These values are the values which were calculated in Appendix B.

$\frac{C_u}{\gamma_f L}$

This is simply the value of the undrained shear strength divided by the unit weight of the fluid and the length of the test cylinder.

This is done in order to reduce the numerous variables to one dimensionless number.

For Cylinder Number 1, Test Number 2:

$$c_u = 0.417 \frac{grms}{cm^2}$$

$$\gamma_f = 1.69 \frac{grms}{cm^3}$$

$$L = 7.00 \text{ cm}$$

$$\frac{c_u}{\gamma_f L} = 0.009$$

$$\frac{c_u}{\gamma_f R}$$

This is another reduction of the data to a workable dimensionless number. This is dependent upon the radius, rather than the length of the test cylinder, however.

For Cylinder Number 1, Test Number 2:

$$c_u = 0.417 \frac{grms}{cm^2}$$

$$\gamma_f = 1.69 \frac{grms}{cm^3}$$

$$R = 1.74 \text{ cm}$$

$$\frac{c_u}{\gamma_f R} = 0.142$$

APPENDIX B

Cylinder #1 R = 1.74 cm L = 7.00 cm

Mat'l.	Test #	α	Area	Vol.	γ_f	P'	By Weight			By Volume			Calc.	Vane
							C_{KAO}	C_{SAND}	C_{BEADS}	C_{KAO}	C_{SAND}	C_{BEADS}	C_u	C_u
Clay	1	102.95	6.10	42.70	1.62	10.33	58.29			35.6			0.017	0.277
Clay	2	76.37	3.34	23.38	1.69	39.99	59.54			38.1			0.417	0.222
Clay	3	63.00	2.10	14.70	1.76	53.63	60.03			40.0			0.593	0.610
Clay	4	88.35	4.58	32.06	1.70	25.00	60.54			38.8			0.257	0.277
Clay	5	79.40	3.65	25.55	1.80	33.51	61.77			42.0			0.347	0.832
Clay	6	85.05	4.23	29.61	1.75	27.68	59.56			39.3			0.285	0.832
Clay	7	97.60	5.55	38.85	1.70	13.46	57.09			37.1			0.139	0.610
Clay	8	101.94	6.00	42.00	1.68	8.94	60.02			38.1			0.093	0.111
Sand	9	90.24	4.79	33.53	1.81	18.81	49.27	17.91		33.7	12.0		0.193	0.721
Sand	10	88.35	4.58	32.06	1.90	18.59	42.12	29.83		30.2	21.0		0.191	0.499
Sand	11	85.39	4.27	29.89	2.00	19.72	35.05	41.60		26.5	30.8		0.203	0.555
Clay	12	98.59	5.66	39.62	1.65	14.13	57.51			35.7			0.146	0.555
Sand	13	102.28	6.03	42.21	1.90		37.62	34.59		27.0	24.3		0.000	0.333
Sand	14	94.61	5.24	36.68	2.01	5.77	30.98	46.17		23.5	34.4		0.059	0.222
Sand	15	92.96	5.07	35.49	2.09	5.33	26.48	53.99		20.9	41.8		0.055	0.444
Clay	16	106.7	6.47	45.29	1.64	5.22	56.93			35.2			0.017	0.333
Beads	17	94.28	5.21	36.47	1.69	17.87	52.81		15.01	33.7		16.4	0.184	0.333
Beads	18	89.67	4.72	33.04	1.68	23.99	50.82		18.82	32.3		19.7	0.246	0.499
Beads	19	89.67	4.72	33.04	1.68	23.99	48.25		22.34	30.6		24.2	0.246	0.277

NOTE: α in degrees; Area in cm^2; Vol. in cm^3; γ_f in $\frac{grms}{cm^3}$; P' in grams; C_u in $\frac{grams}{cm^2}$

Cylinder #1 (continued)

Mat'l.	Test #	α	Area	Vol.	γ_f	P'	By Weight			By Volume			Calc.	Vane
							C_{KAO}	C_{SAND}	C_{BEADS}	C_{KAO}	C_{SAND}	C_{BEADS}	C_u	C_u
Clay	20	100.26	5.83	40.81	1.70	10.12	60.20			38.7			0.106	0.444
Beads	21	93.62	5.14	35.98	1.72	17.61	59.81		3.04	38.8		3.4	0.181	0.499
Beads	22	88.02	4.55	31.85	1.75	23.76	61.51		2.97	40.6		3.4	0.245	0.055
Beads	23	90.99	4.86	34.02	1.74	20.31	60.29		4.91	39.6		5.5	0.208	0.555
Beads	24	88.68	4.62	32.34	1.73	23.55	57.43		9.43	37.5		10.5	0.242	0.721
Beads	25	86.05	4.34	30.38	1.72	27.25	54.50		14.04	35.4		15.6	0.280	0.555
Beads	26	83.73	4.10	28.70	1.71	30.42	51.32		19.06	33.1		21.0	0.313	0.610
Beads	27	82.74	3.99	27.93	1.70	32.02	47.39		25.26	30.4		27.6	0.330	0.721
Beads	28	85.39	4.27	29.89	1.69	28.99	44.89		29.20	28.6		31.8	0.298	0.887
Beads	29	87.04	4.44	31.08	1.68	27.29	41.89		33.94	26.6		36.8	0.280	0.721
Beads	30	90.66	4.83	33.78	1.68	22.75	41.2		33.6	26.1		36.4	0.233	
Beads	31	89.01	4.65	32.56	1.66	25.45	37.5		39.5	23.5		42.4	0.261	0.499
Beads	32	81.95	3.91	27.37	1.65	34.34	33.6		45.8	20.9		48.8	0.354	0.499
Beads	33	74.33	3.14	21.98	1.64	43.45	30.1		51.4	18.6		54.4	0.456	0.499
Beads	34	62.63	2.07	14.49	1.62	56.03	23.8		61.7	14.5		64.5	0.621	4.160
Sand	35	89.67	4.72	33.05	2.10	10.10	27.1	53.7		21.5	41.8		0.104	0.776
Sand	36	86.05	4.34	30.38	2.15	14.18	24.3	58.5		19.7	46.6		0.146	0.998
Sand	37	77.05	3.41	23.87	2.19	27.22	22.1	62.2		18.3	50.5		0.283	0.776
Sand	38	71.23	2.84	19.89	2.23	35.15	20.1	65.6		16.9	54.1		0.373	1.664

Cylinder #2 R = 1.74 L = 4.50

Mat'l.	Test #	α	Area	Vol.	γ_f	P'	By Weight			By Volume			Calc.	Vane
							C_{KAO}	C_{SAND}	C_{BEADS}	C_{KAO}	C_{SAND}	C_{BEADS}	C_u	C_u
Clay	1	110.87	6.87	30.92	1.62	0.81	58.29			35.6			0.013	0.277
Clay	2	78.06	3.51	15.80	1.69	24.20	59.54			38.1			0.391	0.222
Clay	3	67.71	2.52	11.34	1.76	30.94	60.03			40.0			0.518	0.610
Clay	4	79.74	3.68	16.56	1.70	22.75	60.54			38.8			0.366	0.277
Clay	5	77.05	3.41	15.35	1.80	23.27	61.77			42.0			0.377	0.832
Clay	6	84.39	4.17	18.77	1.75	18.05	59.56			39.3			0.289	0.832
Clay	7	98.59	5.66	25.47	1.70	7.60	57.09			37.1			0.122	0.610
Clay	8	93.62	5.14	23.13	1.68	12.04	60.02			38.1			0.192	0.111
Sand	9	84.72	4.20	18.90	1.81	16.69	49.27	17.91		33.7	12.0		0.267	0.721
Sand	10	90.99	4.86	21.87	1.90	9.35	42.12	29.83		30.2	21.0		0.149	0.499
Sand	11	87.04	4.44	19.98	2.00	10.94	35.05	41.60		26.5	30.8		0.175	0.555
Clay	12	99.93	5.79	26.06	1.65	7.01	57.51			35.7			0.113	0.555
Sand	13	98.26	5.62	25.29	1.90	2.85	37.62	34.59		27.0	24.3		0.046	0.333
Sand	14	90.33	4.79	21.56	2.01	7.56	30.98	46.17		23.5	34.4		0.121	0.222
Sand	15	91.65	4.93	22.19	2.09	4.52	26.48	53.99		20.9	41.8		0.072	0.444
Clay	16	106.36	6.44	28.98	1.64	3.37	56.93			35.2			0.055	0.333
Beads	17	94.61	5.24	23.58	1.69	11.05	52.81		15.01	33.7		16.4	0.177	0.333
Beads	18	90.33	4.79	21.56	1.68	14.68	50.82		18.82	32.3		19.7	0.234	0.499
Beads	19	85.39	4.27	19.22	1.68	18.61	48.25		22.34	30.6		24.2	0.298	0.277

Cylinder #2 (continued)

Mat'l.	Test #	α	Area	Vol.	γ_f	P'	By Weight			By Volume			Calc.	Vane
							C_{KAO}	C_{SAND}	C_{BEADS}	C_{KAO}	C_{SAND}	C_{BEADS}	c_u	c_u
Clay	20	102.95	6.10	27.45	1.70	4.24	60.20			38.7			0.068	0.444
Beads	21	94.28	5.21	23.45	1.72	10.57	59.81		3.04	38.8		3.4	0.169	0.499
Beads	22	80.74	3.79	17.06	1.75	21.05	61.51		2.97	40.6		3.4	0.338	0.055
Beads	23	92.31	5.00	22.50	1.74	11.75	60.29		4.91	39.6		5.5	0.188	0.555
Beads	24	85.05	4.23	19.04	1.73	17.96	57.43		9.43	37.5		10.5	0.287	0.721
Beads	25	87.69	4.51	20.30	1.72	15.98	54.50		14.04	35.4		15.6	0.255	0.555
Beads	26	86.38	4.37	19.67	1.71	17.26	51.32		19.06	33.1		21.0	0.276	0.610
Beads	27	79.07	3.61	16.25	1.70	23.28	47.39		25.26	30.4		27.6	0.375	0.721
Beads	28	81.07	3.82	17.19	1.69	21.85	44.89		29.20	28.6		31.8	0.351	0.887
Beads	29	82.40	3.96	17.82	1.68	20.96	41.89		33.94	26.6		36.8	0.336	0.721
Beads	30	89.01	4.65	20.93	1.68	15.74	41.2		33.6	26.1		36.4	0.251	
Beads	31	93.29	5.10	22.96	1.66	12.79	37.5		39.5	23.5		42.4	0.204	0.499
Beads	32	84.72	4.20	18.90	1.65	19.72	33.6		45.8	20.9		48.8	0.316	0.499
Beads	33	78.40	3.55	15.98	1.64	24.69	30.1		51.4	18.6		54.4	0.399	0.499
Beads	34	55.72	1.54	6.91	1.62	39.71	23.8		61.7	14.5		64.5	0.721	4.160
Sand	35	89.67	4.72	21.24	2.10	6.30	27.1	53.7		21.5	41.8		0.101	0.776
Sand	36	84.39	4.16	18.74	2.15	10.61	24.3	58.5		19.7	46.6		0.170	0.998
Sand	37	78.40	3.55	15.96	2.19	15.95	22.1	62.2		18.3	50.5		0.258	0.776
Sand	38	64.10	2.20	9.89	2.23	28.85	20.1	65.6		16.9	54.1		0.493	1.664

Cylinder #3 R = 1.74 L = 4.00

Mat'l.	Test #	α	Area	Vol.	γ_f	P'	By Weight			By Volume			Calc.	Vane
							C_{KAO}	C_{SAND}	C_{BEADS}	C_{KAO}	C_{SAND}	C_{BEADS}	C_u	C_u
Clay	1	107.04	6.50	26.00	1.62	3.08	58.29			35.6			0.056	0.277
Clay	2	85.39	4.27	17.08	1.69	16.33	59.54			38.1			0.294	0.222
Clay	3	78.40	3.55	14.20	1.76	20.21	60.03			40.0			0.367	0.610
Clay	4	89.67	4.72	18.88	1.70	13.10	60.54			38.8			0.235	0.277
Clay	5	65.56	2.32	9.28	1.80	28.50	61.77			42.0			0.543	0.832
Clay	6	92.96	5.07	20.28	1.75	9.71	59.56			39.3			0.175	0.832
Clay	7	98.59	5.66	22.64	1.70	6.71	57.09			37.1			0.121	0.610
Clay	8	100.26	5.83	23.32	1.68	6.02	60.02			38.1			0.109	0.111
Sand	9	89.01	4.65	18.60	1.81	11.53	49.27	17.91		33.7	12.0		0.207	0.721
Sand	10	89.34	4.69	18.76	1.90	9.56	42.12	29.83		30.2	21.0		0.172	0.499
Sand	11	86.38	4.37	17.48	2.00	10.24	35.05	41.60		26.5	30.8		0.184	0.555
Clay	12	104.99	6.30	25.20	1.65	3.62	57.51			35.7			0.066	0.555
Sand	13	97.93	5.59	22.36	1.90	2.72	37.62	34.59		27.0	24.3		0.049	0.333
Sand	14	91.65	4.93	19.72	2.01	5.56	30.98	46.17		23.5	34.4		0.100	0.222
Sand	15	93.29	5.10	20.40	2.09	2.56	26.48	53.99		20.9	41.8		0.046	0.444
Clay	16	106.36	6.44	25.76	1.64	2.95	56.93			35.2			0.054	0.333
Beads	17	93.29	5.10	20.40	1.69	10.72	52.81		15.01	33.7		16.4	0.193	0.333
Beads	18	91.65	4.93	19.72	1.68	12.07	50.82		18.82	32.3		19.7	0.217	0.499
Beads	19	86.05	4.34	17.36	1.68	16.03	48.25		22.34	30.6		24.2	0.288	0.277

Cylinder #3 (continued)

Mat'l.	Test #	α	Area	Vol.	γ_f	P'	By Weight			By Volume			Calc.	Vane
							C_{KAO}	C_{SAND}	C_{BEADS}	C_{KAO}	C_{SAND}	C_{BEADS}	C_u	C_u
Clay	20	106.36	6.44	25.76	1.70	1.41	60.20			38.7			0.026	0.444
Beads	21	94.95	5.28	21.12	1.72	8.87	59.81		3.04	38.8		3.4	0.160	0.499
Beads	22	88.02	4.55	18.20	1.75	13.35	61.51		2.97	40.6		3.4	0.240	0.055
Beads	23	87.36	4.48	17.92	1.74	14.02	60.29		4.91	39.6		5.5	0.252	0.555
Beads	24	85.39	4.27	17.08	1.73	15.65	51.43		9.43	37.5		10.5	0.282	0.721
Beads	25	90.00	4.76	19.04	1.72	12.45	54.50		14.04	35.4		15.6	0.224	0.555
Beads	26	88.02	4.55	18.20	1.71	14.08	51.32		19.06	33.1		21.0	0.253	0.610
Beads	27	86.38	4.37	17.48	1.70	15.48	47.39		25.26	30.4		27.6	0.278	0.721
Beads	28	80.74	3.79	15.16	1.69	19.58	44.89		29.20	28.6		31.8	0.354	0.887
Beads	29	76.37	3.34	13.36	1.68	22.76	41.89		33.94	26.6		36.8	0.416	0.721
Beads	30	90.0	4.76	19.02	1.68	13.25	41.2		33.6	26.1		36.4	0.238	
Beads	31	85.72	4.30	17.22	1.66	16.61	37.5		39.5	23.5		42.4	0.299	0.499
Beads	32	88.35	4.58	18.33	1.65	14.96	33.6		45.8	20.9		48.8	0.269	0.499
Beads	33	83.07	4.03	16.11	1.64	18.78	30.1		51.4	18.6		54.4	0.339	0.499
Beads	34	55.32	1.51	6.03	1.62	35.43	23.8		61.7	14.5		64.5	0.727	4.160
Sand	35	90.34	4.79	19.17	2.10	4.94	27.1	53.7		21.5	41.8		0.089	0.776
Sand	36	83.73	4.10	16.38	2.15	9.98	24.3	58.5		19.7	46.6		0.180	0.998
Sand	37	75.69	3.27	13.10	2.19	16.51	22.1	62.2		18.3	50.5		0.302	0.776
Sand	38	51.21	1.23	4.91	2.23	34.25	20.1	65.6		16.9	54.1		0.732	1.664

Cylinder #4 R = 1.50 L = 5.99

Mat'l.	Test #	α	Area	Vol.	γ_f	P'	By Weight			By Volume			Calc.	Vane
							C_{KAO}	C_{SAND}	C_{BEADS}	C_{KAO}	C_{SAND}	C_{BEADS}	C_u	C_u
Clay	1	98.43	4.19	25.10	1.62	9.64	58.29			35.6			0.135	0.277
Clay	2	77.68	2.58	15.45	1.69	24.19	59.54			38.1			0.341	0.222
Clay	3	69.31	1.98	11.86	1.76	29.43	60.03			40.0			0.426	0.610
Clay	4	86.18	3.23	19.35	1.70	17.41	60.54			38.8			0.242	0.277
Clay	5	77.29	2.55	15.27	1.80	22.81	61.77			42.0			0.322	0.832
Clay	6	73.74	2.29	13.72	1.75	26.29	59.56			39.3			0.375	0.832
Clay	7	98.43	4.19	25.10	1.70	7.63	57.09			37.1			0.107	0.610
Clay	8	89.62	3.50	20.97	1.68	15.07	60.02			38.1			0.210	0.111
Sand	9	84.26	3.09	18.51	1.81	16.80	49.27	17.91		33.7	12.0		0.234	0.721
Sand	10	88.85	3.44	20.61	1.90	11.14	42.12	29.83		30.2	21.0		0.155	0.499
Sand	11	79.63	2.73	16.35	2.00	17.60	35.05	41.60		26.5	30.8		0.247	0.555
Clay	12	101.93	4.46	26.72	1.65	6.21	57.51			35.7			0.087	0.555
Sand	13	96.89	4.07	23.96	1.90	4.78	37.62	34.59		27.0	24.3		0.067	0.333
Sand	14	90.38	3.56	21.32	2.01	7.45	30.98	46.17		23.5	34.4		0.104	0.222
Sand	15	91.53	3.65	21.86	2.09	4.61	26.48	53.99		20.9	41.8		0.064	0.444
Clay	16	105.47	4.72	28.72	1.64	3.20	56.93			35.2			0.045	0.333
Beads	17	90.76	3.59	21.50	1.69	13.97	52.81		15.01	33.7		16.4	0.194	0.333
Beads	18	88.85	3.44	20.61	1.68	15.68	50.82		18.82	32.3		19.7	0.218	0.499
Beads	19	85.41	3.17	18.99	1.68	18.40	48.25		22.34	30.6		24.2	0.256	0.277

Cylinder #4 (continued)

Mat'l.	Test #	α	Area	Vol.	γ_f	P'	By Weight			By Volume			Calc.	Vane
							C_{KAO}	C_{SAND}	C_{BEADS}	C_{KAO}	C_{SAND}	C_{BEADS}	C_u	C_u
Clay	20	100.37	4.44	26.60	1.70	5.08	60.20			38.7			0.071	0.444
Beads	21	96.89	4.07	24.38	1.72	8.37	59.81		3.04	38.8		3.4	0.117	0.499
Beads	22	83.49	3.03	18.15	1.75	18.54	61.51		2.97	40.6		3.4	0.259	0.055
Beads	23	85.03	3.14	18.81	1.74	17.57	60.29		4.91	39.6		5.5	0.245	0.555
Beads	24	88.47	3.41	20.43	1.73	14.96	57.43		9.43	37.5		10.5	0.208	0.721
Beads	25	84.64	3.11	18.63	1.72	18.26	54.50		14.04	35.4		15.6	0.255	0.555
Beads	26	84.64	3.11	18.63	1.71	18.44	51.32		19.06	33.1		21.0	0.257	0.610
Beads	27	84.64	3.11	18.63	1.70	18.63	47.39		25.26	30.4		27.6	0.260	0.721
Beads	28	84.26	3.09	18.51	1.69	19.02	44.89		29.20	28.6		31.8	0.265	0.887
Beads	29	85.03	3.14	18.81	1.68	18.70	41.89		33.94	26.6		36.8	0.261	0.721
Beads	30	86.18	3.23	19.38	1.68	17.74	41.2		33.6	26.1		36.4	0.247	
Beads	31	82.34	2.94	17.59	1.66	21.10	37.5		39.5	23.5		42.4	0.295	0.499
Beads	32	83.88	3.06	18.30	1.65	20.11	33.6		45.8	20.9		48.8	0.281	0.499
Beads	33	81.95	2.91	17.41	1.64	21.75	30.1		51.4	18.6		54.4	0.304	0.499
Beads	34	66.42	1.78	10.68	1.62	33.00	23.8		61.7	14.5		64.5	0.485	4.160
Sand	35	88.47	3.53	21.17	2.10	5.84	27.1	53.7		21.5	41.8		0.081	0.776
Sand	36	86.56	3.26	19.55	2.15	8.27	24.3	58.5		19.7	46.6		0.115	0.998
Sand	37	76.90	2.51	15.11	2.19	17.21	22.1	62.2		18.3	50.5		0.243	0.776
Sand	38	63.04	1.57	9.38	2.23	29.38	20.1	65.6		16.9	54.1		0.440	1.664

Cylinder # 5 R = 1.50 L = 4.50

Mat'l.	Test #	α	Area	Vol.	γ_f	P'	By Weight			By Volume			Calc.	Vane
							C_{KAO}	C_{SAND}	C_{BEADS}	C_{KAO}	C_{SAND}	C_{BEADS}	C_u	C_u
Clay	1	108.66	4.95	22.28	1.62	1.71	58.29			35.6			0.032	0.277
Clay	2	77.68	2.58	11.61	1.69	18.18	59.54			38.1			0.341	0.222
Clay	3	74.53	2.35	10.58	1.76	19.18	60.03			40.0			0.363	0.610
Clay	4	91.53	3.65	16.43	1.70	9.87	60.54			38.8			0.183	0.277
Clay	5	82.74	2.97	13.37	1.80	13.73	61.77			42.0			0.255	0.832
Clay	6	88.09	3.38	15.21	1.75	11.18	59.56			39.3			0.207	0.832
Clay	7	98.43	4.19	18.86	1.70	5.74	57.09			37.1			0.107	0.610
Clay	8	90.0	3.54	15.93	1.68	11.04	60.02			38.1			0.204	0.111
Sand	9	88.85	3.44	15.48	1.81	9.78	49.27	17.91		33.7	12.0		0.181	0.721
Sand	10	91.91	3.68	16.56	1.90	6.34	42.12	29.83		30.2	21.0		0.117	0.499
Sand	11	83.49	3.03	13.64	2.00	10.52	35.05	41.60		26.5	30.8		0.195	0.555
Clay	12	103.49	4.57	20.57	1.65	3.86	57.51			35.7			0.072	0.555
Sand	13	84.64	3.95	17.78	1.90	4.02	37.62	34.59		27.0	24.3		0.075	0.333
Sand	14	95.36	3.71	16.70	2.01	4.23	30.98	46.17		23.5	34.4		0.078	0.222
Sand	15	90.76	3.59	16.16	2.09	4.03	26.48	53.99		20.9	41.1		0.075	0.444
Clay	16	102.32	4.49	20.21	1.64	4.66	56.93			35.2			0.087	0.333
Beads	17	91.15	3.62	16.29	1.69	10.27	52.81		15.01	33.7		16.4	0.190	0.333
Beads	18	84.26	3.09	13.91	1.68	14.43	50.82		18.82	32.3		19.7	0.268	0.499
Beads	19	89.24	3.47	15.62	1.68	11.56	48.25		22.34	30.6		24.2	0.214	0.277

Cylinder #5 (continued)

Mat'l.	Test #	α	Area	Vol.	γ_f	P'	By Weight			By Volume			Calc.	Vane
							C_{KAO}	C_{SAND}	C_{BEADS}	C_{KAO}	C_{SAND}	C_{BEADS}	C_u	C_u
Clay	20	98.82	4.22	18.99	1.70	5.52	60.20			38.7			0.103	0.444
Beads	21	91.53	3.65	16.43	1.72	9.54	59.81		3.04	38.8		3.4	0.177	0.499
Beads	22	85.41	3.17	14.27	1.75	12.83	61.51		2.97	40.6		3.4	0.238	0.055
Beads	23	87.33	3.32	14.94	1.74	11.80	60.29		4.91	39.6		5.5	0.219	0.555
Beads	24	91.53	3.65	16.43	1.73	9.38	51.43		9.43	37.5		10.5	0.174	0.721
Beads	25	87.33	3.32	14.94	1.72	12.10	54.50		14.04	35.4		15.6	0.225	0.555
Beads	26	78.85	2.67	12.02	1.71	17.25	51.32		19.06	33.1		21.0	0.323	0.610
Beads	27	76.51	2.49	11.21	1.70	18.74	47.39		25.26	30.4		27.6	0.353	0.721
Beads	28	79.24	2.70	12.15	1.69	17.27	44.89		29.20	28.6		31.8	0.323	0.887
Beads	29	76.51	2.49	11.21	1.68	18.97	41.89		33.94	26.6		36.8	0.357	0.721
Beads	30	90.0	3.53	15.90	1.68	11.09	41.2		33.6	26.1		36.4	0.205	
Beads	31	85.41	3.17	14.29	1.66	14.08	37.5		39.5	23.5		42.4	0.261	0.499
Beads	32	83.49	3.03	13.61	1.65	15.34	33.6		45.8	20.9		48.8	0.285	0.499
Beads	33	84.64	3.11	14.00	1.64	14.84	30.1		51.4	18.6		54.4	0.275	0.499
Beads	34	52.17	0.96	4.31	1.62	30.82	23.8		61.7	14.5		64.5	0.672	4.160
Sand	35	88.85	3.44	15.50	2.10	5.25	27.1	53.7		21.5	41.8		0.097	0.776
Sand	36	83.88	3.06	13.75	2.15	8.24	24.3	58.5		19.7	46.6		0.153	0.998
Sand	37	75.72	2.44	10.96	2.19	13.80	22.1	62.2		18.3	50.5		0.260	0.776
Sand	38	53.13	1.01	4.53	2.23	27.70	20.1	65.6		16.9	54.1		0.598	1.664

Cylinder #6 R = 1.50 L = 3.48

Mat'l.	Test #	α	Area	Vol.	γ_f	P'	By Weight			By Volume			Calc.	Vane
							C_{KAO}	C_{SAND}	C_{BEADS}	C_{KAO}	C_{SAND}	C_{BEADS}	C_u	C_u
Clay	1	105.86	4.75	16.53	1.62	2.52	58.29			35.6			0.061	0.277
Clay	2	78.46	2.64	9.19	1.69	13.77	59.54			38.1			0.334	0.222
Clay	3	72.54	2.20	7.66	1.76	15.82	60.03			40.0			0.390	0.610
Clay	4	89.24	3.47	12.08	1.70	8.76	60.54			38.8			0.210	0.277
Clay	5	75.72	2.44	8.49	1.80	14.02	61.77			42.0			0.342	0.832
Clay	6	90.38	3.56	12.39	1.75	7.62	59.56			39.3			0.182	0.832
Clay	7	100.76	4.37	15.21	1.70	3.44	57.09			37.1			0.083	0.610
Clay	8	92.29	3.71	12.91	1.68	7.61	60.02			38.1			0.182	0.111
Sand	9	90.0	3.54	12.32	1.81	7.00	49.27	17.91		33.7	12.0		0.168	0.721
Sand	10	84.26	3.09	10.75	1.90	8.88	42.12	29.83		30.2	21.0		0.213	0.499
Sand	11	83.49	3.03	10.54	2.00	8.22	35.05	41.60		26.5	30.8		0.198	0.555
Clay	12	103.89	4.60	16.01	1.65	2.88	57.51			35.7			0.070	0.555
Sand	13	93.06	3.77	13.12	1.90	4.37	37.62	34.59		27.0	24.3		0.105	0.333
Sand	14	91.53	3.65	12.70	2.01	3.77	30.98	46.17		23.5	34.4		0.090	0.222
Sand	15	85.02	3.14	10.93	2.09	6.46	26.48	53.99		20.9	41.8		0.155	0.444
Clay	16	100.76	4.37	15.21	1.64	4.36	56.93			35.2			0.105	0.333
Beads	17	90.0	3.54	12.32	1.69	8.48	52.81		15.01	33.7		16.4	0.203	0.333
Beads	18	88.09	3.38	11.76	1.68	9.54	50.82		18.82	32.3		19.7	0.229	0.499
Beads	19	82.34	2.94	10.23	1.68	12.11	48.25		22.34	30.6		24.2	0.291	0.277

Cylinder #6 (continued)

Mat'l.	Test #	α	Area	Vol.	γ_f	P'	By Weight			By Volume			Calc.	Vane
							C_{KAO}	C_{SAND}	C_{BEADS}	C_{KAO}	C_{SAND}	C_{BEADS}	C_u	C_u
Clay	20	99.59	4.28	14.89	1.79	3.99	60.20			38.7			0.096	0.444
Beads	21	96.89	4.07	14.16	1.72	4.94	59.81		3.04	38.8		3.4	0.119	0.499
Beads	22	83.11	3.00	10.44	1.75	11.03	61.51		2.97	40.6		3.4	0.265	0.055
Beads	23	90.76	3.59	12.49	1.74	7.57	60.29		4.91	39.6		5.5	0.181	0.555
Beads	24	85.03	3.14	10.93	1.73	10.39	57.43		9.43	37.5		10.5	0.249	0.721
Beads	25	84.26	3.09	10.75	1.72	10.81	54.50		14.04	35.4		15.6	0.260	0.555
Beads	26	76.51	2.49	8.67	1.71	14.47	51.32		19.06	33.1		21.0	0.352	0.610
Beads	27	74.53	2.35	8.18	1.70	15.39	47.39		25.26	30.4		27.6	0.377	0.721
Beads	28	78.46	2.64	9.19	1.69	13.77	44.89		29.20	28.6		31.8	0.334	0.887
Beads	29	72.14	2.18	7.59	1.68	16.55	41.89		33.94	26.6		36.8	0.408	0.721
Beads	30	86.18	3.23	11.26	1.68	10.38	41.2		33.6	26.1		36.4	0.249	
Beads	31	81.18	2.85	9.91	1.66	12.85	37.5		39.5	23.5		42.4	0.310	0.499
Beads	32	83.11	3.00	10.43	1.65	12.09	33.6		45.8	20.9		48.8	0.291	0.449
Beads	33	81.57	2.88	10.01	1.64	12.88	30.1		51.4	18.6		54.4	0.310	0.499
Beads	34	38.74	0.42	1.47	1.62	26.92	23.8		61.7	14.5		64.5	0.917	4.160
Sand	35	86.56	3.26	11.36	2.10	5.44	27.1	53.7		21.5	41.8		0.130	0.776
Sand	36	84.64	3.11	10.84	2.15	5.99	25.3	58.5		19.7	46.6		0.144	0.998
Sand	37	80.41	2.79	9.70	2.19	8.06	22.1	62.2		18.3	50.5		0.195	0.776
Sand	38	59.11	1.33	4.63	2.23	18.98	20.1	65.6		16.9	54.1		0.503	1.664

APPENDIX C

Cylinder #1 L = 7.00 cm R = 1.74 cm

Mat'l.	Test #	h	h/R	γ_f	C_u	$\frac{C_u}{\gamma_f \cdot L}$	$\frac{C_u}{\gamma_f \cdot R}$
Clay	1	1.35	0.78	1.62	0.107	0.009	0.038
Clay	2	2.15	1.24	1.69	0.417	0.035	0.142
Clay	3	2.53	1.45	1.76	0.593	0.048	0.194
Clay	4	1.79	1.03	1.70	0.257	0.022	0.087
Clay	5	2.06	1.18	1.80	0.347	0.028	0.111
Clay	6	1.89	1.09	1.75	0.285	0.023	0.094
Clay	7	1.51	0.87	1.70	0.139	0.012	0.047
Clay	8	1.38	0.79	1.68	0.093	0.008	0.032
Sand	9	1.73	0.99	1.81	0.193	0.015	0.061
Sand	10	1.79	1.03	1.90	0.191	0.014	0.058
Sand	11	1.88	1.08	2.00	0.203	0.015	0.058
Clay	12	1.48	0.85	1.65	0.146	0.013	0.051
Sand	13	1.37	0.79	1.90			
Sand	14	1.60	0.92	2.01	0.059	0.004	0.017
Sand	15	1.65	0.95	2.09	0.055	0.004	0.015
Clay	16	1.24	0.71	1.64	0.017	0.001	0.006
Beads	17	1.61	0.93	1.69	0.184	0.016	0.063
Beads	18	1.75	1.01	1.68	0.246	0.021	0.084
Beads	19	1.75	1.01	1.68	0.246	0.021	0.084
Clay	20	1.43	0.82	1.70	0.105	0.009	0.035
Beads	21	1.63	0.94	1.72	0.181	0.015	0.060
Beads	22	1.80	1.03	1.75	0.245	0.020	0.080
Beads	23	1.71	0.98	1.74	0.208	0.017	0.069
Beads	24	1.78	1.02	1.73	0.242	0.020	0.080
Beads	25	1.86	1.07	1.72	0.280	0.023	0.094
Beads	26	1.93	1.11	1.71	0.313	0.026	0.105
Beads	27	1.96	1.13	1.70	0.330	0.028	0.112
Beads	28	1.88	1.08	1.69	0.298	0.025	0.101
Beads	29	1.83	1.05	1.68	0.280	0.024	0.096
Beads	30	1.72	0.99	1.68	0.233	0.020	0.080
Beads	31	1.77	1.02	1.66	0.261	0.022	0.090

NOTE: h in cm; γ_f in $\frac{\text{grms}}{\text{cm}^3}$; c_u in $\frac{\text{grms}}{\text{cm}^2}$

Cylinder #1 (continued)

Mat'l.	Test #	h	h/R	γ_f	C_u	$\frac{C_u}{\gamma_f \cdot L}$	$\frac{C_u}{\gamma_f \cdot R}$
Beads	32	1.88	1.08	1.65	0.354	0.031	0.123
Beads	33	2.21	1.27	1.64	0.456	0.040	0.160
Beads	34	2.54	1.46	1.62	0.621	0.055	0.220
Sand	35	1.75	1.01	2.10	0.104	0.007	0.028
Sand	36	1.86	1.07	2.15	0.146	0.010	0.039
Sand	37	2.13	1.22	2.19	0.283	0.018	0.074
Sand	38	2.30	1.32	2.23	0.373	0.024	0.096

Cylinder #2 L = 4.50 cm R = 1.74 cm

Mat'l.	Test #	h	h/R	γ_f	C_u	$\frac{C_u}{\gamma_f \cdot L}$	$\frac{C_u}{\gamma_f \cdot R}$
Clay	1	1.12	0.64	1.62	0.013	0.002	0.005
Clay	2	2.10	1.21	1.69	0.391	0.051	0.133
Clay	3	2.40	1.38	1.76	0.518	0.065	0.169
Clay	4	2.05	1.18	1.70	0.366	0.048	0.124
Clay	5	2.13	1.22	1.80	0.377	0.047	0.120
Clay	6	1.91	1.10	1.75	0.289	0.037	0.095
Clay	7	1.48	0.85	1.70	0.122	0.016	0.041
Clay	8	1.63	0.94	1.68	0.192	0.025	0.066
Sand	9	1.90	1.09	1.81	0.267	0.033	0.085
Sand	10	1.71	0.98	1.90	0.149	0.017	0.045
Sand	11	1.83	1.05	2.00	0.175	0.019	0.050
Clay	12	1.44	0.83	1.65	0.113	0.015	0.039
Sand	13	1.49	0.86	1.90	0.046	0.005	0.014
Sand	14	1.73	0.99	2.01	0.121	0.013	0.035
Sand	15	1.69	0.97	2.09	0.072	0.008	0.020
Clay	16	1.25	0.72	1.64	0.055	0.007	0.019
Beads	17	1.60	0.92	1.69	0.177	0.023	0.060
Beads	18	1.73	0.99	1.68	0.234	0.031	0.080
Beads	19	1.88	1.08	1.68	0.298	0.039	0.102
Clay	20	1.35	0.78	1.70	0.068	0.009	0.023
Beads	21	1.61	0.93	1.72	0.169	0.022	0.056
Beads	22	2.02	1.16	1.75	0.338	0.043	0.111
Beads	23	1.67	0.96	1.74	0.188	0.024	0.062
Beads	24	1.89	1.09	1.73	0.287	0.037	0.095
Beads	25	1.81	1.04	1.72	0.255	0.033	0.085
Beads	26	1.85	1.06	1.71	0.275	0.036	0.093
Beads	27	2.07	1.19	1.70	0.375	0.049	0.127
Beads	28	2.01	1.16	1.69	0.351	0.046	0.119
Beads	29	1.97	1.13	1.68	0.336	0.044	0.115
Beads	30	1.77	1.02	1.68	0.251	0.033	0.086
Beads	31	1.64	0.94	1.66	0.204	0.027	0.071

Cylinder #2 (continued)

Mat'l.	Test #	h	h/R	γ_f	C_u	$\frac{C_u}{\gamma_f \cdot L}$	$\frac{C_u}{\gamma_f \cdot R}$
Beads	32	1.90	1.09	1.65	0.316	0.043	0.110
Beads	33	2.09	1.20	1.64	0.399	0.054	0.140
Beads	34	2.72	1.56	1.62	0.721	0.099	0.256
Sand	35	1.75	1.01	2.10	0.101	0.011	0.028
Sand	36	1.91	1.10	2.15	0.170	0.018	0.045
Sand	37	2.09	1.20	2.19	0.258	0.026	0.068
Sand	38	2.50	1.44	2.23	0.493	0.049	0.127

Cylinder #3 L = 4.00 cm R = 1.74 cm

Mat'l.	Test #	h	h/R	γ_f	C_u	$\frac{C_u}{\gamma_f \cdot L}$	$\frac{C_u}{\gamma_f \cdot R}$
Clay	1	1.23	0.71	1.62	0.056	0.009	0.020
Clay	2	1.88	1.08	1.69	0.294	0.043	0.100
Clay	3	2.09	1.20	1.76	0.367	0.052	0.120
Clay	4	1.75	1.01	1.70	0.235	0.035	0.079
Clay	5	2.46	1.41	1.80	0.543	0.075	0.173
Clay	6	1.65	0.95	1.75	0.175	0.025	0.057
Clay	7	1.48	0.85	1.70	0.121	0.018	0.041
Clay	8	1.43	0.82	1.68	0.109	0.016	0.037
Sand	9	1.77	1.02	1.81	0.207	0.029	0.066
Sand	10	1.76	1.01	1.90	0.172	0.023	0.052
Sand	11	1.85	1.06	2.00	0.184	0.023	0.053
Clay	12	1.29	0.74	1.65	0.066	0.010	0.023
Sand	13	1.50	0.86	1.90	0.049	0.006	0.015
Sand	14	1.69	0.97	2.01	0.100	0.012	0.029
Sand	15	1.64	0.94	2.09	0.046	0.006	0.013
Clay	16	1.25	0.72	1.64	0.054	0.008	0.019
Beads	17	1.64	0.94	1.69	0.193	0.029	0.066
Beads	18	1.69	0.97	1.68	0.217	0.032	0.074
Beads	19	1.86	1.07	1.68	0.288	0.043	0.099
Clay	20	1.25	0.72	1.70	0.026	0.004	0.009
Beads	21	1.59	0.91	1.72	0.160	0.023	0.053
Beads	22	1.80	1.03	1.75	0.240	0.034	0.079
Beads	23	1.82	1.05	1.74	0.252	0.036	0.083
Beads	24	1.88	1.08	1.73	0.282	0.041	0.094
Beads	25	1.74	1.00	1.72	0.224	0.033	0.075
Beads	26	1.80	1.03	1.71	0.253	0.037	0.085
Beads	27	1.85	1.06	1.70	0.278	0.041	0.094
Beads	28	2.02	1.16	1.69	0.354	0.052	0.120
Beads	29	2.15	1.25	1.68	0.416	0.062	0.142
Beads	30	1.74	1.00	1.68	0.238	0.035	0.081
Beads	31	1.87	1.07	1.66	0.299	0.045	0.104

Cylinder #3 (continued)

Mat'l.	Test #	h	h/R	γ_f	C_u	$\frac{C_u}{\gamma_f \cdot L}$	$\frac{C_u}{\gamma_f \cdot R}$
Beads	32	1.79	1.03	1.65	0.269	0.041	0.094
Beads	33	1.95	1.12	1.64	0.339	0.052	0.119
Beads	34	2.73	1.57	1.62	0.727	0.112	0.258
Sand	35	1.73	0.99	2.10	0.089	0.011	0.024
Sand	36	1.93	1.11	2.15	0.180	0.021	0.048
Sand	37	2.17	1.25	2.19	0.302	0.034	0.079
Sand	38	2.83	1.63	2.23	0.732	0.082	0.189

Cylinder #4 L = 5.99 cm R = 1.50 cm

Mat'l.	Test #	h	h/R	γ_f	C_u	$\frac{C_u}{\gamma_f \cdot L}$	$\frac{C_u}{\gamma_f \cdot R}$
Clay	1	1.28	0.85	1.62	0.135	0.014	0.056
Clay	2	1.82	1.21	1.69	0.341	0.034	0.135
Clay	3	2.03	1.35	1.76	0.426	0.040	0.161
Clay	4	1.60	1.07	1.70	0.242	0.024	0.095
Clay	5	1.83	1.22	1.80	0.322	0.030	0.119
Clay	6	1.92	1.28	1.75	0.375	0.036	0.143
Clay	7	1.28	0.85	1.70	0.107	0.011	0.042
Clay	8	1.51	1.01	1.68	0.210	0.021	0.083
Sand	9	1.65	1.10	1.81	0.234	0.022	0.086
Sand	10	1.53	1.02	1.90	0.155	0.014	0.054
Sand	11	1.77	1.18	2.00	0.247	0.021	0.082
Clay	12	1.19	0.79	1.65	0.087	0.009	0.035
Sand	13	1.38	0.92	1.90	0.067	0.006	0.024
Sand	14	1.49	0.99	2.01	0.104	0.009	0.034
Sand	15	1.46	0.97	2.09	0.064	0.005	0.020
Clay	16	1.10	0.73	1.64	0.046	0.005	0.018
Beads	17	1.48	0.99	1.69	0.194	0.019	0.077
Beads	18	1.53	1.02	1.68	0.218	0.022	0.087
Beads	19	1.62	1.08	1.68	0.256	0.025	0.102
Clay	20	1.23	0.82	1.70	0.071	0.007	0.028
Beads	21	1.38	0.92	1.72	0.117	0.011	0.045
Beads	22	1.67	1.11	1.75	0.259	0.025	0.099
Beads	23	1.63	1.09	1.74	0.246	0.024	0.094
Beads	24	1.54	1.03	1.73	0.208	0.020	0.080
Beads	25	1.64	1.09	1.72	0.255	0.025	0.099
Beads	26	1.64	1.09	1.71	0.257	0.025	0.100
Beads	27	1.64	1.09	1.70	0.260	0.026	0.102
Beads	28	1.65	1.10	1.69	0.265	0.026	0.105
Beads	29	1.63	1.09	1.68	0.261	0.026	0.104
Beads	30	1.60	1.07	1.68	0.247	0.025	0.098
Beads	31	1.70	1.13	1.66	0.295	0.030	0.118

Cylinder #4 (continued)

Mat'l.	Test #	h	h/R	γ_f	C_u	$\frac{C_u}{\gamma_f \cdot L}$	$\frac{C_u}{\gamma_f \cdot R}$
Beads	34	2.10	1.40	1.62	0.485	0.050	0.200
Sand	35	1.54	1.03	2.10	0.081	0.006	0.026
Sand	36	1.59	1.06	2.15	0.115	0.009	0.036
Sand	37	1.84	1.23	2.19	0.243	0.019	0.074
Sand	38	2.18	1.45	2.23	0.440	0.033	0.132

Cylinder #5 L = 4.50 cm R = 1.50 cm

Mat'l.	Test #	h	h/R	γ_f	C_u	$\frac{C_u}{\gamma_f \cdot L}$	$\frac{C_u}{\gamma_f \cdot R}$
Clay	1	1.02	0.68	1.62	0.032	0.004	0.013
Clay	2	1.82	1.21	1.69	0.341	0.045	0.135
Clay	3	1.90	1.27	1.76	0.363	0.046	0.138
Clay	4	1.46	0.96	1.70	0.183	0.024	0.072
Clay	5	1.72	1.15	1.80	0.255	0.031	0.094
Clay	6	1.55	1.03	1.75	0.207	0.026	0.079
Clay	7	1.28	0.85	1.70	0.107	0.014	0.042
Clay	8	1.50	1.00	1.68	0.204	0.027	0.081
Sand	9	1.53	1.02	1.81	0.181	0.022	0.067
Sand	10	1.45	0.97	1.90	0.117	0.014	0.041
Sand	11	1.67	1.11	2.00	0.195	0.022	0.065
Clay	12	1.15	0.77	1.65	0.072	0.010	0.029
Sand	13	1.36	0.91	1.90	0.075	0.009	0.026
Sand	14	1.44	0.96	2.01	0.078	0.009	0.026
Sand	15	1.48	0.99	2.09	0.075	0.008	0.024
Clay	16	1.18	0.79	1.64	0.087	0.012	0.035
Beads	17	1.47	0.98	1.69	0.190	0.025	0.075
Beads	18	1.65	1.10	1.68	0.268	0.035	0.106
Beads	19	1.52	1.01	1.68	0.214	0.028	0.085
Clay	20	1.27	0.85	1.70	0.103	0.013	0.040
Beads	21	1.46	0.97	1.72	0.177	0.023	0.069
Beads	22	1.62	1.08	1.75	0.238	0.030	0.091
Beads	23	1.57	1.05	1.74	0.219	0.028	0.084
Beads	24	1.46	0.97	1.73	0.174	0.022	0.067
Beads	25	1.57	1.05	1.72	0.225	0.029	0.087
Beads	26	1.79	1.19	1.71	0.323	0.042	0.126
Beads	27	1.85	1.23	1.70	0.353	0.046	0.138
Beads	28	1.78	1.19	1.69	0.323	0.042	0.127
Beads	29	1.85	1.23	1.68	0.357	0.047	0.142
Beads	30	1.50	1.00	1.68	0.205	0.027	0.081
Beads	31	1.62	1.08	1.66	0.261	0.035	0.105

Cylinder #5 (continued)

Mat'l.	Test #	h	h/R	γ_f	C_u	$\frac{C_u}{\gamma_f \cdot L}$	$\frac{C_u}{\gamma_f \cdot R}$
Beads	32	1.67	1.11	1.65	0.285	0.038	0.115
Beads	33	1.64	1.09	1.64	0.275	0.037	0.112
Beads	34	2.42	1.61	1.62	0.672	0.092	0.277
Sand	35	1.53	1.02	2.10	0.097	0.010	0.031
Sand	36	1.66	1.11	2.15	0.153	0.016	0.047
Sand	37	1.87	1.25	2.19	0.260	0.026	0.079
Sand	38	2.40	1.60	2.23	0.598	0.060	0.179

Cylinder #6 L = 3.48 cm R = 1.50 cm

Mat'l.	Test #	h	h/R	γ_f	C_u	$\frac{C_u}{\gamma_f \cdot L}$	$\frac{C_u}{\gamma_f \cdot R}$
Clay	1	1.09	0.72	1.62	0.061	0.011	0.025
Clay	2	1.80	1.20	1.69	0.334	0.057	0.132
Clay	3	1.95	1.30	1.76	0.390	0.064	0.148
Clay	4	1.52	1.01	1.70	0.210	0.035	0.082
Clay	5	1.87	1.25	1.80	0.342	0.055	0.127
Clay	6	1.49	0.99	1.75	0.182	0.030	0.069
Clay	7	1.22	0.81	1.70	0.083	0.014	0.033
Clay	8	1.44	0.96	1.68	0.182	0.031	0.072
Sand	9	1.50	1.00	1.81	0.168	0.027	0.062
Sand	10	1.65	1.10	1.90	0.213	0.032	0.075
Sand	11	1.67	1.11	2.00	0.198	0.028	0.066
Clay	12	1.14	0.76	1.65	0.070	0.012	0.028
Sand	13	1.42	0.95	1.90	0.105	0.016	0.037
Sand	14	1.46	0.97	2.01	0.090	0.013	0.030
Sand	15	1.63	1.09	2.09	0.155	0.021	0.049
Clay	16	1.22	0.81	1.64	0.105	0.018	0.043
Beads	17	1.50	1.00	1.69	0.203	0.035	0.080
Beads	18	1.55	1.03	1.68	0.229	0.039	0.091
Beads	19	1.70	1.13	1.68	0.291	0.050	0.115
Clay	20	1.25	0.83	1.70	0.096	0.016	0.038
Beads	21	1.32	0.88	1.72	0.119	0.020	0.046
Beads	22	1.68	1.12	1.75	0.264	0.044	0.101
Beads	23	1.48	0.99	1.74	0.181	0.030	0.069
Beads	24	1.63	1.09	1.73	0.249	0.041	0.096
Beads	25	1.65	1.10	1.72	0.260	0.043	0.101
Beads	26	1.85	1.23	1.71	0.352	0.059	0.137
Beads	27	1.90	1.27	1.70	0.377	0.064	0.148
Beads	28	1.80	1.20	1.69	0.334	0.057	0.132
Beads	29	1.96	1.31	1.68	0.408	0.070	0.162
Beads	30	1.60	1.07	1.68	0.249	0.043	0.099
Beads	31	1.73	1.15	1.66	0.310	0.054	0.124

Cylinder #6 (continued)

Mat'l.	Test #	h	h/R	γ_f	C_u	$\frac{C_u}{\gamma_f \cdot L}$	$\frac{C_u}{\gamma_f \cdot R}$
Beads	32	1.68	1.12	1.65	0.291	0.051	0.118
Beads	33	1.72	1.15	1.64	0.310	0.054	0.126
Beads	34	2.67	1.78	1.62	0.917	0.163	0.377
Sand	35	1.59	1.06	2.10	0.130	0.018	0.041
Sand	36	1.64	1.09	2.15	0.144	0.019	0.045
Sand	37	1.75	1.17	2.19	0.195	0.026	0.059
Sand	38	2.27	1.51	2.23	0.503	0.065	0.150

APPENDIX D

APPENDIX D

A statistical anslysis was performed on the data for cylinders 1 through 6, along with the data for the vane shear device for comparison purposes. (See accompanying table.) In this analysis, the mean, $\bar{y}$, the standard deviation, $\bar{\sigma}$, and the variance, $\bar{\sigma}^2$, was calculated for the various data. For the cases of the clay-sand and clay-beads mixtures, only concentrations by volume of less than 55 percent were used, since at higher concentrations, the material tends to act more as a solid rather than a viscous mud.

		Cylinder No. 1	Cylinder No. 2	Cylinder No. 3	Cylinder No. 4	Cylinder No. 5	Cylinder No. 6	Vane Shear
Clay-Water	$\bar{y}$	0.380	0.388	0.360	0.341	0.292	0.319	0.464
	$\bar{\sigma}$	0.134	0.083	0.134	0.068	0.073	0.077	0.243
	$\bar{\sigma}^2$	0.014	0.005	0.013	0.004	0.004	0.004	0.054
Clay-Sand	$\bar{y}$	0.185	0.194	0.209	0.179	0.160	0.172	0.592
	$\bar{\sigma}$	0.067	0.069	0.054	0.072	0.068	0.031	0.246
	$\bar{\sigma}^2$	0.004	0.004	0.002	0.004	0.004	0.001	0.054
Clay-Beads	$\bar{y}$	0.289	0.317	0.287	0.258	0.273	0.295	0.525
	$\bar{\sigma}$	0.064	0.048	0.054	0.026	0.053	0.058	0.204
	$\bar{\sigma}^2$	0.004	0.002	0.003	0.001	0.003	0.003	0.039

NOTE: $\bar{y}$ = mean $(\frac{gms}{cm^2})$; $\bar{\sigma}$ = standard deviation; $\bar{\sigma}^2$ = variance.